
Electronic Thesis and Dissertation Repository

8-5-2016 12:00 AM

Efficient and Virtualized Scheduling for OFDM-Based High Mobility Wireless Communications Objects

Mohamed Hussein Abdelwahab Ahmed, *The University of Western Ontario*

Supervisor: Dr. Abdallah Shami, *The University of Western Ontario*

Joint Supervisor: Dr. Serguei Primak, *The University of Western Ontario*

A thesis submitted in partial fulfillment of the requirements for the Doctor of Philosophy degree in Electrical and Computer Engineering

© Mohamed Hussein Abdelwahab Ahmed 2016

Follow this and additional works at: <https://ir.lib.uwo.ca/etd>



Part of the [Systems and Communications Commons](#)

Recommended Citation

Hussein Abdelwahab Ahmed, Mohamed, "Efficient and Virtualized Scheduling for OFDM-Based High Mobility Wireless Communications Objects" (2016). *Electronic Thesis and Dissertation Repository*. 3928. <https://ir.lib.uwo.ca/etd/3928>

This Dissertation/Thesis is brought to you for free and open access by Scholarship@Western. It has been accepted for inclusion in Electronic Thesis and Dissertation Repository by an authorized administrator of Scholarship@Western. For more information, please contact wlsadmin@uwo.ca.

Abstract

Services providers (SPs) in the radio platform technology standard long term evolution (LTE) systems are enduring many challenges in order to accommodate the rapid expansion of mobile data usage. The modern technologies demonstrate new challenges to SPs, for example, reducing the cost of the capital and operating expenditures while supporting high data throughput per customer, extending battery life-per-charge of the cell phone devices, and supporting high mobility communications with fast and seamless handover (HO) networking architecture. In this thesis, a variety of optimized techniques aimed at providing innovative solutions for such challenges are explored.

The thesis is divided into three parts. The first part outlines the benefits and challenges of deploying virtualized resource sharing concept. Wherein, SPs achieving a different schedulers policy are sharing evolved network B, allowing SPs to customize their efforts and provide service requirements; as a promising solution for reducing operational and capital expenditures, leading to potential energy savings, and supporting higher peak rates. The second part, formulates the optimized power allocation problem in a virtualized scheme in LTE uplink systems, aiming to extend the mobile devices' battery utilization time per charge. While, the third part extrapolates a proposed hybrid-HO (HY-HO) technique, that can enhance the system performance in terms of latency and HO reliability at cell boundary for high mobility objects (up to 350 km/hr; wherein, HO will occur more frequent).

The main contributions of this thesis are in designing optimal binary integer programming-based and suboptimal heuristic (with complexity reduction) scheduling algorithms subject to exclusive and contiguous allocation, maximum transmission power, and rate constraints. Moreover, designing the HY-HO based on the combination of soft and hard HO was able to enhance the system performance in term of latency, interruption time and reliability during HO. The results prove that the proposed solutions effectively contribute in addressing the challenges caused by the demand for high data rates and power transmission in mobile networks especially in virtualized resources sharing scenarios that can support high data rates with improving quality of services (QoS).

Keywords: LTE, Virtualization, QoSs, SPs Schedulers' Policy, Resources Sharing, LTE UL Scheduling, Efficient Power Allocation, Mobility, Handover.

Acknowledgements

All praise goes to ALLAH for the blessing of completing this thesis. Pursuing doctoral degree in The University of Western Ontario is a memorable experience for me. It is with pleasure that I write this page to express my joy and to acknowledge all those who have supported me in successfully completing this thesis. I have no doubt that I could not have been able to do it without the love, and support of my family, friends, and colleagues.

First and foremost, I would like to express my deepest gratitude and graciously appreciation to my supervisors; Professor Abdallah Shami and Professor Serguei Primak for all their encouragement, fruitful cooperation, precious guidance, and philosophy that I have received and learned from them at every stage of the research. The valuable discussions we had were always a source of inspiration to me.

It is a wonderful feeling to express my thanks to my colleagues for their help in conducting the research. I am grateful for their valuable advice which I implemented in my experiments. I am also glad to extend my thanks to the Department of Electrical and Computer Engineering at Western University for their assistance while conducting my studies in the lab.

I owe a special word of indebtedness to my mother, father, and brothers. Although, they are thousands of miles away from me during the days I studied in Canada, I can always get the strongest support from them. There are no words sufficient enough to express my full gratitude to my parents.

My heartfelt thanks go out to my beloved wife for her constant inspiration, encouragement, sacrifice, and tolerance during my research work; I am extremely thankful to her for taking care of our sweet sons during this journey. My family and wives prayers during this period have helped tremendously in completing the research work successfully.

Thank you,

Mohamed Hussein Abdelwahab Ahmed

Contents

Certificate of Examination	ii
Abstract	iii
Acknowledgements	iv
List of Figures	ix
List of Tables	xii
Acronyms	xiii
1 Introduction	1
1.1 Thesis Contributions	2
1.2 Thesis Organization	3
2 Background and Literature Review	5
2.1 Multicarrier Systems	5
2.1.1 OFDM and OFDMA	6
2.1.2 Key Challenges	9
2.2 Background of LTE Systems	10
2.2.1 LTE Objectives	10
2.2.2 eNBs Main Functions	11
2.2.3 LTE Performance of Demands	11
2.2.4 LTE Performance with Respect to Mobility	12
2.2.5 LTE Traffic Quality of Services	12
2.2.6 LTE Spectrum Flexibility	13
2.2.7 LTE Frame Structure	15

2.2.8	UL/DL Information Exchange	19
2.3	Chapter Summary	24
3	Sharing Resources in 3GPP-LTE Systems Framework	25
3.1	Introduction	25
3.2	Related Work	26
3.3	System Modeling Framework	28
3.3.1	Data Transmission Sequence	28
3.3.2	LTE Traffic Classes	30
3.3.3	Transmission Block Size and MCSs	33
3.3.4	LTE Frame work Scenario	34
3.4	The Considered Scheduling Algorithms	35
3.4.1	The Strict Priority Scheduling Algorithm	37
3.4.2	The LWDF Scheduling Algorithm	37
3.4.3	The UE's Internal Scheduler	41
3.5	Sharing Radio Resources Strategy	41
3.6	Simulation Results	46
3.6.1	Case Study and Results Analysis	48
3.6.2	Larger Scale Scenario	54
3.7	Virtualization and Resources Sharing in Two-Tier Cellular Networks	54
3.7.1	Recent Relevant Research Work	56
3.7.2	System Model	57
Semi-Soft Allocation Technique	58	
Non-sharing Allocation Scenario	60	
Virtualized Sharing Allocation	61	
3.7.3	Simulation Results	61
3.8	Chapter Summary	64
4	Efficient Power Allocation in Virtualized 3GPP-LTE Systems	65
4.1	Introduction	66
4.2	Recent Relevant Research Work	68
4.3	System Model	70
4.3.1	Exclusive and Contiguous Allocation	71

4.3.2	Transmission Block Size	72
4.3.3	Transmission Power Calculation	72
4.4	Problem Formulation	73
4.4.1	Static Sharing Allocation Problem	74
4.4.2	Dynamic Sharing Allocation Problem	76
4.5	Scheduling Framework	77
4.5.1	The BIP-based Resource Allocation Algorithm	77
	BIP Complexity	79
4.5.2	The Heuristic Allocation Algorithm	79
	Static Sharing Scenario	82
	Dynamic Sharing Scenario	82
	Heuristic Complexity	82
4.6	Simulation results	83
4.7	Chapter Summary and Conclusion	90
5	Intra-MME/S-GW Handover in Virtualized 3GPP-LTE Systems	92
5.1	Introduction	93
5.2	Recent Relevant Research Work	94
5.3	Users Mobility	95
5.4	Handover in Wireless Systems	98
5.4.1	Handover Algorithm and Message Sequence	98
5.4.2	Hard Handover Technique	102
5.4.3	Soft Handover Technique	102
	Macro Diversity Handover	102
	Fast Base Station Switching	103
5.5	System Model	104
5.5.1	Transmission Block Size	104
5.5.2	LTE RSRP Measurement Report	106
5.5.3	Traffic in Wireless System	109
5.6	Hybrid-Handover Technique	109
5.7	The Allocation Scheduling Algorithms	111
5.7.1	Proportional Fair Scheduling Algorithm	111

5.7.2	Maximum Rate Scheduling Algorithm	113
5.8	The Static and Virtualized Sharing Algorithm	114
5.8.1	Static Sharing Allocation	115
5.8.2	Virtualized Dynamic Sharing Allocation	116
5.9	Simulation results	117
5.10	Conclusion	121
6	Thesis Summary and Future Work	125
6.1	Thesis Summary	125
6.2	Future Work	126
6.2.1	Optimal D2D User Allocation in Virtualized Scheduling Algorithm	127
6.2.2	Energy-Efficient for Green Smart Grid Communication in Virtualized Scheduling Algorithm	127
6.2.3	Green Heterogeneous Networks in Virtualized Scheduling Algorithm	128
	Bibliography	130
	Curriculum Vitae	143

List of Figures

2.1	OFDM with IFFT implementation (Tx).	7
2.2	Illustration of the OFDMA principle.	9
2.3	The evolutionary path of the LTE radio platform technology.	10
2.4	The LTE system architecture.	14
2.5	Frequency and time division duplex.	15
2.6	UL/DL time/frequency structure in case of FDD and TDD.	16
2.7	TDD configuration.	17
2.8	The relationship between a slot, symbols, and RBs.	19
2.9	The relationships between channel bandwidth, and transmission bandwidth configuration.	20
2.10	The transmission bandwidth configuration.	20
2.11	Inputs and outputs for the UL and DL scheduling algorithm.	21
2.12	The information exchange procedure in both UL and DL connection between an eNB, and two UEs.	23
3.1	MNOs sharing radio RBs in a single eNB.	29
3.2	The UEs' data transmission sequence.	30
3.3	EF, AF, and BE considered traffic classes.	32
3.4	Spectral efficiency and transport block size versus SNR.	35
3.5	LTE flowchart for M MNOs, N UEs, and various Traffic Classes considered.	36
3.6	Pseudo-code for the strict priority scheduler.	38
3.7	Pseudo-code for the largest weight delay first scheduler.	40
3.8	The block diagram of the internal scheduler working procedure.	41
3.9	The pseudo-code for the UE's internal scheduler.	42
3.10	MNOs, achieving different schedulers policy, and sharing radio RBs in a single eNB.	44

3.11	Two MNOs with 10 RBs each, and TTI for 3 frames scenario.	44
3.12	UEs per MNOs are distributed as near and far user from the eNB.	47
3.13	The throughput comparison of the S.P. and LWDF schedulers.	48
3.14	The average packet delay for different traffic classes with the S.P. and LWDF schedulers.	49
3.15	The average packet delay per different traffic classes for MNOs -1, and -2 with non-sharing scenario.	49
3.16	Average packet delay with sharing scenario ($w_1 = 0.2$, RB1 = 14, and $w_2 = 0.4$, RB2 = 12).	51
3.17	Average packet delay with sharing scenario ($w_1 = 0.8$, RB1 = 13, and $w_2 = 0.3$, RB2 = 18).	51
3.18	Queue length in the UE-1's buffer before sharing radio RBs.	52
3.19	Queue length in the UE-1's buffer after sharing radio RBs.	52
3.20	Average AF packet delay with respect to variation of weight of sharing.	53
3.21	Average BE packet delay with respect to variation of weight of sharing.	53
3.22	Average packet delay per different traffic classes for MNOs -1, and -2.	55
3.23	Average packet delay with sharing scenario ($w_1 = 0.2$, and $w_2 = 0.4$).	55
3.24	Average packet delay with sharing scenario ($w_1 = 0.8$, and $w_2 = 0.3$).	56
3.25	Two-tier cellular network topology.	58
3.26	Allocation message sequence between the two-tier cellular networks.	59
3.27	The average packets delay (EF and non-EF traffic) for UE_M before, during, and after passing through the micro-cell footprint.	63
4.1	UEs from different SPs sharing eNB in a single cell.	66
4.2	The flowchart of the heuristic allocation algorithm in SS and DS scenarios.	81
4.3	The average BIP and heuristic transmit power in SP1.	85
4.4	The average BIP transmit power versus the average channel gain.	86
4.5	The average BIP transmit power versus the number of active UEs.	87
4.6	The average BIP and heuristic transmit power in SP1 versus the average channel gain.	87
4.7	The average BIP and heuristic transmit power in SP1 versus the number of active UEs.	88

4.8	The average UL transmission rate per TTI in SPs-1, and 2.	89
4.9	The normalized battery life versus the average channel gain.	89
4.10	The normalized running time versus the average channel gain.	90
4.11	The normalized running time versus the number of active UEs in SP1.	91
5.1	Basic network topology of multiple eNBs sharing one MME/S-GW.	93
5.2	UE's path of a mobile going through two handoffs and two changes of direction before cell termination.	97
5.3	The pseudo-code for the rate of HO for different mobility speeds.	97
5.4	Handover algorithm.	99
5.5	LTE handover message sequence.	100
5.6	Macro Diversity Handover.	103
5.7	Fast Base Station Switching.	103
5.8	The range of RSRP reported by UE versus SNR.	107
5.9	Hybrid handover scheme.	111
5.10	The pseudo-code for HY-HO scheduling algorithm.	112
5.11	The rate of handover versus mobility speeds for cell radius of 1 Km.	119
5.12	The average packets delay (EF and non-EF traffic) for mobility speed 150 Km/hr versus distance from eNB.	120
5.13	The average packets delay (EF and non-EF traffic) for mobility speed 350 Km/hr versus distance from eNB.	121
5.14	The average packets delay (EF and non-EF traffic) for mobility speeds 150 and 350 Km/hr versus time.	122
5.15	The average packets delay (high dense EF traffic) for mobility speed 150 Km/hr versus distance.	122
5.16	The average packets delay (high dense EF traffic) for mobility speed 350 Km/hr versus distance.	123
5.17	The average packets delay (high dense EF traffic) for mobility speeds 150 and 350 Km/hr versus time.	123

List of Tables

2.1	Mobile speeds and LTE performance with respect to mobility.	12
2.2	UL/DL Frame Configuration for LTE TDD.	16
3.1	List of MCS which are used in LTE.	34
3.2	Defined necessary parameters.	37
3.3	Simulation default Parameters.	47
3.4	Groups' map.	54
3.5	Simulation Default Parameters and Values.	62
4.1	QoS Attributes	67
4.2	Frequently Used Notations	70
4.3	Simulation Default Parameters and Values.	84
5.1	Frequently Used Notations	105
5.2	Simulation Default Parameters and Values.	118

Acronyms

3GPP	Third Generation Partnership Project
4G	Fourth Generation Wireless Systems
ACK	Acknowledge or Acknowledgment
A/D	Analog-to-Digital
AF	Assured Forwarding
AMC	Adaptive Modulation and Coding
Apps	Application Server
ARQ	Automatic Repeat Request
BE	Best Effort
BER	Bit Error Rate
BIP	Binary Integer Programming
BLER	Block Error Rate
BPSK	Binary Phase Shift Keying
BS	Base Station
BSR	Buffer Status Report
BW	Bandwidth
C-OFDM	Coded Orthogonal Frequency Division Multiplexing
CAPEX	Capital Expenditure
CBR	Constant Bit Rate
CDMA	Code Division Multiple Access
CP	Cyclic Prefix
CQI	Channel Quality Indicator
CRC	Cyclic Redundancy Check
CSI	Channel State Information
D2D	Device-to-Device
DFT	Discrete Fourier Transform
DL	Downlink

DRA	Dynamic Resource Allocation
DRX	Discontinuous Reception
DS	Dynamic Sharing
DSL	digital Subscriber Line
DTX	Discontinuous Transmission
DwPTS	Downlink Pilot Time Slot
E-UTRA	Evolved UMTS Terrestrial Radio Access
E-UTRAN	Evolved UMTS Terrestrial Radio Access Network
EDGE	Enhanced Data Rates for GSM Evolution
EF	Expedite Forwarding
eNB	Evolved Node B
EPC	Evolved Packet Core
FDD	Frequency Division Duplex
FDM	Frequency Division Multiplexing
FDMA	Frequency Division Multiple Access
FFT	Fast Fourier Transform
GBR	Guaranteed Bit Rate
GP	Guard Period
GPRS	General Packet Radio Service
GSM	Global System for Mobile Communication
GW	Gateway
HARQ	Hybrid ARQ
HetNet	Heterogeneous Networks
HHO	Hard Handover
HO	Handover
HSPA	High Speed Packet Access
HSPA+	High Speed Packet Access Evolved

HY-HO	Hybrid Handover
ICI	Inter-Carrier Interference
IEEE	Institute of Electrical and Electronics Engineers
IFFT	Inverse Fast Fourier Transform
IMS	IP Multimedia Subsystem
IP	Internet Protocol
ISI	Inter-Symbol Interference
I.S.	Internal Scheduler
kbps	kilo-bits per second
KHz	Kilo Hertz
LBS	Level of Bearer Satisfaction
LP	Linear Programming
LTE	Long Term Evolution
LWDF	Largest Weight Delay First
MAC	Medium Access Control
MC-OFDMA	Multi-Carrier Orthogonal Frequency Division Multiple Access
MCS	Modulation and Coding Scheme
MIMO	Multiple Input Multiple Output
MME	Mobility Management Entity
MMF	Maximum-Minimum Fairness
MNO	Mobile Network Operator
MR	Maximum Rate
NGBR	Non-Guaranteed Bit Rate
OFDM	Orthogonal Frequency Division Multiplexing
OFDMA	Orthogonal Frequency Division Multiple Access
OPEX	Operating Expenditure
PAPR	Peak-to-Average Power Ratio

PC	Power Control
PDB	Packet Delay Budget
PDCP	Packet Data Convergence Protocol
PDU	Protocol Data Unit
PF	Proportional Fair
PGW	Packet Gateway
PHEVs	Plug-in Hybrid Vehicles
PHY	Physical Layer
PLER	Packet Loss Error Rate
PSK	Phase Shift Key
QAM	Quadrature Amplitude Modulation
QCI	QoS Class Identifiers
QoS	Quality of Service
QPSK	Quadrature Phase Shift Keying
RAN	Radio Access Network
RB	Resource Block
RE	Resource Element
RF	Radio Frequency
RLC	Radio Link Control
RN	Relay Node
RRC	Radio Resource Control
RRM	Radio Resource Management
RSRP	Reference Symbol Received Power
RSRQ	Reference Signal Received Quality
RSSI	Received Signal Strength Indicator
S-GW	Serving Gateway
S1-U	S1 - User Plane

SC	Single Carrier
SC-FDMA	Single Carrier - Frequency Division Multiple Access
SFN	Single Frequency Network
SHO	Soft Handover
SIB	System Information Block
SLA	Service of Level Agreement
SNR	Signal-to-Noise Ratio
SPs	Services providers
SS	Static Sharing
S.P.	Strict Priority
TB	Transport Block
TDD	Time Division Duplex
TTI	Transmission Time Interval
UE	User Equipment
UL	Uplink
UMTS	Universal Mobile Telecommunications System
UPE	User Plane Entity
UpPTS	Uplink Pilot Time Slot
VBR	Variable Bit Rate
VoIP	Voice over Internet Protocol
VRB	Virtual Resource Blocks
WCDMA	Wideband Code Division Multiple Access
Wi-Fi	Wireless Fidelity
WiMAX	Worldwide Interoperability for Microwave Access

Chapter 1

Introduction

Emerging broadband wireless access technologies nowadays face the long-term challenge of properly addressing air-link channel limitations and reconciling these limitations with the growing demand for services with fast mobility and widespread coverage. One of the most demanding and challenging scenarios is the high-mobility scenario [1, 2].

The Third Generation Partnership Program-Long Term Evolution (3GPP-LTE) system adopts the orthogonal frequency division multiplexing (OFDM) and multi-input multi-output (MIMO) techniques [3] in order to satisfy the fast-growing demand of wireless data, wherein services providers (SPs) revenues in LTE systems are not growing at the same rate as the traffic volume. In order to handle the rapid increase in mobile data traffic, more suitable business models with higher capacities should be deployed.

Coded orthogonal frequency division multiplexing (C-OFDM) which is a form of OFDM where error correction coding is incorporated into the signal, has been developed into a popular scheme for wideband digital communication, and is used in applications such as digital television and audio broadcasting, digital subscriber line (DSL) broadband internet access, wireless networks, and Fourth Generation (4G) mobile communications. The primary advantage of OFDM over single-carrier schemes is its ability to cope with severe channel conditions (for example, narrowband interference and frequency-selective fading due to multipath) without complex equalization filters [4].

Channel equalization is simplified because OFDM may be viewed as using many slowly

modulated narrow band signals rather than one rapidly modulated wideband signal [5]. The low symbol rate makes the use of a guard interval between symbols affordable, making it possible to eliminate intersymbol interference (ISI) and utilize echoes and time-spreading to achieve a diversity gain, i.e. an improvement in the signal-to-noise ratio (SNR).

Modern wireless communication systems strive to achieve two very contrasting objectives, namely increasing system performance while well as improving energy efficiency for green communications [6]. In fact, both these goals have been heavily focused on since the adoption of early wireless systems; while the definition of system performance has evolved over time.

1.1 Thesis Contributions

In our way to evolve towards the future, my main objective is to enhance the quality of services' (QoS) parameters in wireless networks that can stand with the nowadays raising mobile data usage [7, 8]. In this thesis, a variety of optimized techniques that aim to provide innovative solutions for this objective are explored.

The first part outlines the benefits of deploying virtualization in terms of resource sharing concept. Wherein, SPs achieving different schedulers' algorithms can share a single evolved network B (eNB). This part shows how the delay parameter can be improved. The second part, proposed the power allocation problem in a virtualized scheme in LTE uplink (UL) systems. That aims to prolong the mobile devices' battery utilization time per charge. While, the third part proposes the hybrid-Handover (HY-HO) technique that can enhance the system performance in terms of latency and HO reliability for high mobility objects (up to 350 km/hr; wherein, HO will occur more frequent) [9].

The main contributions of this thesis are in proposing the optimal binary integer programming (BIP)-based and suboptimal heuristic (with less computational complexity) algorithms subject to exclusive and contiguous allocation, maximum transmission power, and rate constraints. Moreover, designing the HY-HO based on the combination of soft and hard HO was

able to enhance the system performance in term of latency, interruption time and reliability during HO. The results prove that the proposed solutions can effectively contribute in addressing the challenges caused by the demand for high data rates and power transmission in mobile networks and also in improving QoS parameters [10].

1.2 Thesis Organization

The thesis is organized into six chapters where the technical contributions of this thesis are contained in Chapters 3 to 5. Prior to introducing the technical contributions, in Chapter 2, I provide detailed background on the problem domain with an introduction to communication systems for high-mobility objects, introduce the main task for this thesis, and summarize some of the recent state-of-the-art advances in the area concentrated on in this thesis.

The technical contributions of this thesis begin in Chapter 3. I propose a novel design for a virtualized resources' sharing technique with investigation that analyze and test the users performance in terms of delay QoSs parameter, wherein, SPs using different scheduling algorithms are sharing their physical radio resources blocks (RBs) in one eNB in a virtualized scheme as a promising solution for reducing operational and capital expenditures, leading to potential energy savings, and supporting higher peak rates. The proposed method makes use to schedule traffic with various delay and priority requirements.

The contributions of this chapter was partially presented in IEEE international conference on wireless communications and mobile computing [11], that evaluates the average packets jitter and delays for cases of non-sharing and sharing schemes, with the goal to close the growing gap between the capacities of backbone networks, that yields notable improvements in average packet delay.

In Chapter 4, I concentrate on detailing the focuses on the specification and analysis of a proposed technique for modeling an optimized solution for the simulated sharing scheme methodology used in Chapter 3. Wherein, I proposed a design for a dynamic scheduling pol-

icy framework for an arbitrary number of queues and channels for single-carrier frequency division multiple access (SC-FDMA) UL which meets exclusive and contiguous allocation, maximum transmission power, and rate constraints restrictions while minimizing the average applied transmission power for a time-invariant channel to achieve green communication.

Chapter 4 was partially presented in IEEE international conference on wireless and mobile computing, networking and communications [12]. The major contributions are proposing both optimal BIP-based and suboptimal lower complexity heuristic scheduling algorithms to minimize overall average applied power, and compared their performance in terms of average applied power and computational complexity.

In Chapter 5, I analyze the performance of UEs random-way mobility model and HO algorithms for high-mobility users within the sharing virtualized scenario in LTE systems. A HY-HO technique is proposed to address the shortcomings of the existing approaches and the challenges caused by the demand for high data rates. The HY-HO was able to enhance the system performance in term of interruption time, reliability and latency during HO at the cell boundary.

The contributions of this chapter appear in IEEE international Canadian conference on electrical and computer engineering [13], wherein, the HY-HO virtualized scheme is capable of achieving great improvements with respect to delay when compared to the non-sharing application. Overall, the results confirm that the HY-HO framework yields notable improvements in average packet delay, without degrading QoS.

Finally; Chapter 6 summarizes and draws the main conclusions in this thesis and propose some further research directions in this area.

Chapter 2

Background and Literature Review

This chapter provides an introduction to the main technologies that are related to the scope of this thesis. First, multi-carrier systems OFDM and orthogonal frequency division multiple access (OFDMA) are introduced as the basic technique used in the recent radio LTE networks in both UL/downlink (DL) transmissions. Later, LTE is presented, followed by the description of system architecture jointly with main features and characteristic. At the end of the chapter, a summary is approached as an introduction for the coming thesis's contributions.

LTE is the standard cellular technology for wireless communication of high speed data for mobile phones and data terminals that is emerged as one of the most promising access network technologies, launched by the 3GPP to support diversity of traffic at potentially high rates [14, 15] with greater flexibility for heterogeneous networks and flatter networks. In this chapter, an overview on the state-of-the-art research related to this thesis is provided including background on the 3GPP-LTE systems technology.

2.1 Multicarrier Systems

OFDM, the method of encoding data on multi-carrier subcarriers. OFDM has developed widely for wide band digital communications, with many applicable approaches, for example, audio broadcasting, digital television, and DSL Internet access, power-line networks, wireless

networks, and 4G communications networks.

It is a frequency-division multiplexing (FDM) approach that is used as a digital multiple carriers method. Wherein, a large number of close spaced orthogonal sub-carrier signals are carrying data on multiple parallel data channels. Each subcarrier is modulated with a conventional modulation scheme (such as quadrature amplitude modulation (QAM) or phase-shift keying (PSK)) at a low symbol rate, maintaining total data rates similar to conventional single-carrier (SC) modulation schemes in the same bandwidth.

The main advantage of OFDM over SC techniques is the ability to work with severe channel conditions (like, high frequencies' attenuation in a long copper wire, frequency-selective fading due to multi-path, and narrow band interference) with simple equalization filters. Moreover, the channel equalization is simplified since OFDM may be viewed as using multi-slow narrow band modulated signals instead of one rapid wide-band modulated signal. As a result, the low symbol rate takes the advantage of the guard interval between symbols. That makes it possible to cancel any ISI, utilize echoes and time-spreading to achieve higher diversity gain, i.e. a SNR improvement.

This mechanism facilitates the design of single frequency techniques, where several contiguous transmitters send the same signal at the same frequency, where signals from different distant transmitters can be combined constructively, instead of interfering that would typically occur in normal single-carrier system. OFDM and OFDMA are multi-carrier systems, a brief description of both is presented in this section.

2.1.1 OFDM and OFDMA

The main idea of a multi-carrier modulation is to divide the transmitted bit stream into different sub-streams and send these over many different channels. It is based on the principle of transmitting individually many narrow-band orthogonal frequencies, sub-carriers [16]. The number of sub-carriers is noted as N_s . These frequencies are orthogonal to each other, which cancels the interference between channels. If a data symbol is N_s times longer, compared to

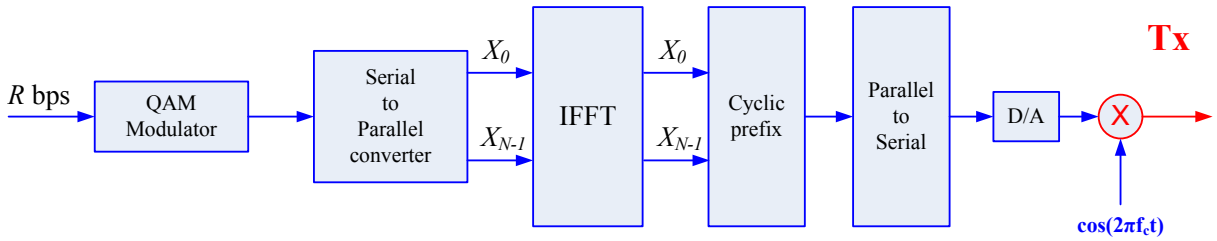


Figure 2.1: OFDM with IFFT implementation (Tx).

SC, it provides to OFDM a much better multi-path resistance, which together with orthogonal carriers allows a high spectral efficiency.

The basic premise of a multi-carrier modulation is to split this wide-band system into N_s linearly-modulated subsystem in parallel, each with Subchannel Bandwidth is:

$$B_N = B/N_s \quad (2.1)$$

where: B is the pass-band bandwidth.

The bandwidth sub-channel is lower than the coherence band (B_C) for N_s sufficiently large and ensures relatively flat fading on each sub-channel. Also, with N_s sufficiently large, the symbol time is much longer than the delay spread, so each sub-channel experiences low ISI degradation.

The input data stream is linearly-modulated, resulting in a complex symbol stream. This symbol stream is divided into N sub-streams via a serial-to-parallel converter, as shown in Figure 2.1.

OFDM theory shows that the inverse Fourier fast transform (IFFT) of magnitude N_s , applied on N_s symbols, realizes one OFDM signal, where each symbol is transmitted on one of the N_s orthogonal frequencies. The IFFT operator realizes the reverse operation of the fast Fourier transform (FFT). The FFT is a matrix computation that allows the discrete Fourier transform (DFT) to be computed. When N_s is power of 2 the complexity of the FFT is reduced.

Since the channel output is a linear convolution instead a circular one (needed for IFFT/FFT),

a special prefix is added to the input called a cyclic prefix (CP), so the linear convolution between the input and impulse response can be turned into a circular convolution.

The CP can also serve to eliminate ISI between the data blocks, since CP samples are also the first samples (as guard interval) of the channel output which are affected by ISI. These samples can be discarded without any loss relative to the original sequence, since there is no new information.

At the receiver section, the ISI associated with the end of a the OFDM symbol is added again to the symbol, which re-creates the effect of a cyclic prefix. The zero cyclic prefix decreases the power transmitted relative to cyclic prefix by $N_s/(N_s + \mu)$, as the prefix does not need any transmit power. However, the received noise is added to the beginning of the symbol, which increases the noise power by $(N_s + \mu)/N_s$.

CP allows the receiver to absorb much more efficiently the delay spread due to the multipath and to maintain frequency orthogonality. This CP is a temporal redundancy that must be taken into account in data rates computations. The ratio μ/N_s is chosen taking some considerations into account. If the multipath effect is important, a high value of this ratio is needed, which increases the redundancy and then decreases the useful data rate. On the other hand if the multipath effect is lighter, a relatively smaller value of this ratio can be used.

OFDM transmission was originally conceived for a single user; therefore, it had to be associated to a multiple user access scheme so that several users could be served. OFDMA is the scheme to be used. OFDMA allows the access of multiple users on the available bandwidth. Each user is assigned a specific time-frequency resource.

OFDMA subcarriers are divided into subsets of subcarriers, each subset representing a sub-channel, as shown in Figure 2.2).

In the DL, a sub-channel may be intended for different receivers or groups of receivers; in the UL a transmitter may be assigned one or more sub-channels. The subcarriers forming one sub-channel may be adjacent or not.

The multiple access has a new dimension with OFDMA. A DL or an UL user will have a

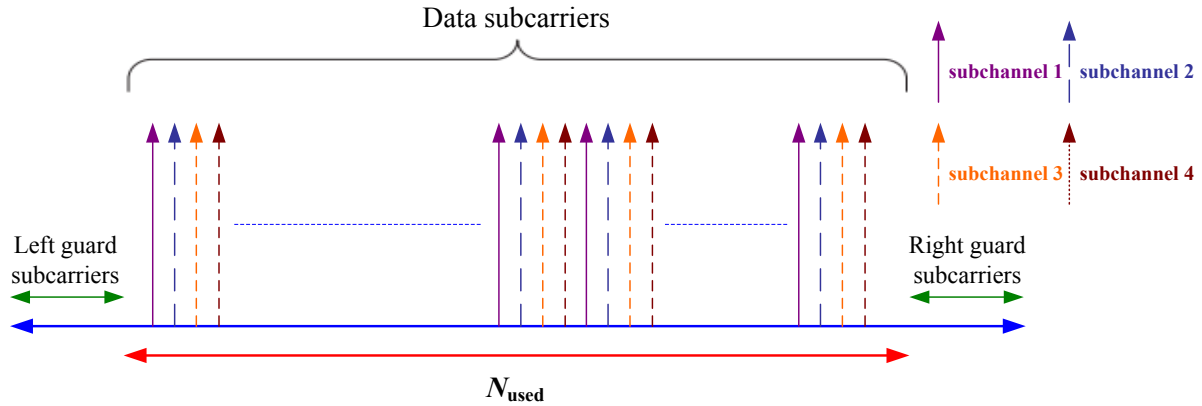


Figure 2.2: Illustration of the OFDMA principle.

time and a sub-channel allocation for each of its communications.

2.1.2 Key Challenges

The peak to average power ratio (PAPR) is a very important feature in any communication system. The low PAPR makes it possible for the transmit power amplifier to operate more efficiently, whereas the high PAPR makes the transmit power amplifier to have a high back-off for ensuring linear amplification for the signal.

The operation in the linear region of this response is totally required to eliminate the distortion of the signal, so this peak value is considered to be in that region. Having these peak and average values close together as possible, is preferable, to have the power amplifier operating with its the maximum efficiency.

For N subcarriers, the maximum PAPR is N . In practice, the full coherent addition of all N symbols is improbable, so the observed PAPR is less than N , usually many dB. Moreover, the PAPR increases linearly with the number of subcarriers. Although it is required to have N as large as it can be to keep the over-head associated with the cyclic prefix down, the large PAPR is the expected penalty that must be paid for a large N .

A high PAPR requires high resolution for the receiver analog/digital (A/D) convertor, since the dynamic range of the signal is much larger for high PAPR signals. High resolution A/D

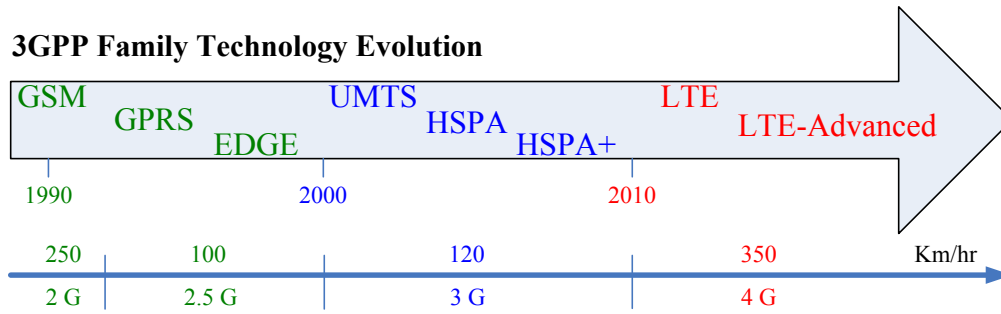


Figure 2.3: The evolutionary path of the LTE radio platform technology.

conversion places a complexity and power burden on the receiver front end.

2.2 Background of LTE Systems

LTE is part of the Global System for Mobile Communications (GSM) evolutionary path for mobile broadband, following General Packet Radio Service (GPRS), Enhanced Data rates for GSM Evolution (EDGE), Universal Mobile Telecommunications System (UMTS), HSPA, and its evolution (HSPA+) [17, 18] as shown in Figure 2.3. Although HSPA and HSPA+ are strongly positioned to be the dominant mobile data technology for the next decade, the 3GPP family of standards must evolve toward the future.

The need for LTE is to provide an extremely highly performance radio access technology that offers full vehicular speed mobility [11, 19], and that can readily coexist with HSPA and earlier networks. And, because of the scalable bandwidth, operators will be able to easily migrate their networks and users from HSPA to LTE over time.

2.2.1 LTE Objectives

The main overall objectives [20] for LTE are:

1. Reduced cost for the operator,
2. Efficient spectrum utilization,

3. Minimizing energy consumed per user,
4. Improved spectral efficiency,
5. Improved system capacity, and coverage,
6. Increased DL and UL peak data rates with reduced latency,
7. Scalable bandwidth with flexible spectrum allocation,
8. All IP network,
9. Support different traffic types,
10. and, satisfying the service of level agreement (SLA) between users per SP, customers, and between SPs sharing the same eNB.

2.2.2 eNBs Main Functions

The following are the functions assigned to eNBs [5, 21] for radio resource management in the E-UTRAN:

1. Radio bearer control,
2. Radio admission control,
3. Connection mobility management,
4. Dynamic resource allocation (scheduling),
5. Inter cell interference coordination,
6. and, load balancing.

2.2.3 LTE Performance of Demands

The LTE performance demands [19] could be simplified as:

1. Data rate: For 20 MHz spectrum, the target for peak data rate is 50 Mbps for UL, and 100 Mbps for DL,
2. Bandwidth: flexible usage of spectrum from 1.4 MHz to 20 MHz,
3. Peak spectral efficiency: for DL is of average 3.2 bps/Hz, and for UL is 1.05 bps/Hz,
4. Spectral efficiency of cell edge: is 0.04-0.06 bps/Hz/user for DL and 0.02-0.03 bps/Hz/user for UL,
5. Average cell spectral efficiency: for DL is 1.6-2.1 bps/Hz/cell and for UL it is 0.66-1.0 bps/Hz/cell,

6. Data type: All packet switched data (voice, video, and data),
7. Packet call throughput: DL avg. 256 Kbps, and for UL is 15 Kbps,
8. Average user throughput: DL is 3.6 Mbps, and for UL is 0.45 Mbps,
9. Latency: is less than 50 ms (for dormant to active). The user-plane latency is less than 5 ms from user equipment (UE) to server,
10. Call setup time: 50 ms,
11. Broadcast data rate: 3.072 Kbps,
12. Modulation types supported: BPSK, QPSK, 16QAM, 64QAM,
13. Access schemes: SC-FDMA has been chosen as the UL access scheme for its low peak-to-average power ratio (PAPR) properties compared to multi-carrier orthogonal frequency division multiple access (MC-OFDM) in DL,
14. Security: is used at good level with the earlier systems starting from GSM.

2.2.4 LTE Performance with Respect to Mobility

Table 2.1 summarizes the LTE performance versus various mobility speeds, and shows that the LTE is able support high mobility up to 350 km/h [9, 22], and is at good level compared to the earlier wireless systems shown in Figure 2.3.

Table 2.1: Mobile speeds and LTE performance with respect to mobility.

Mobile speed		Mobility	LTE performance
Stationary	0 Km/hr	Low mobility	Optimized high performance
Walking	3 : 5 Km/hr	Low mobility	Optimized high performance
Race walkers	14 Km/hr	Low mobility	Optimized high performance
Vehicular	15 : 120 Km/hr	Medium mobility	Marginal degradation
High speed	120 : 350 Km/hr	High mobility	Maintain connection with QoS
Extremely high	up to 900 Km/hr	Extremely high	Not supported

2.2.5 LTE Traffic Quality of Services

The QoSs' requirements and recommendations differ according to the type of traffic [23, 24], such that the QoS for voice traffic include:

1. Loss \leq 1 percent. (packet error loss $\leq 10^{-2}$),
2. One-way latency (mouth-to-ear) should be \leq 100 ms,

3. Packet delay ≤ 20 ms,

and, unlike voice, video uses a variety of packet sizes and packet rates to support a single video stream, and the QoS recommendations for video traffic include:

1. Packet delay ≤ 150 ms,
2. Packet error loss : $\leq 10^{-3}$,
3. The average bit rate varies between of 64 kbps to 1.2 Mbit/s,

while, the QoS recommendations for data traffic include:

1. Packet delay ≤ 300 ms,
2. Packet error loss : $\leq 10^{-3}$.

The LTE system architecture is shown in Figure 2.4, where the evolved-[UMTS] terrestrial radio access network (E-UTRAN) [25], uses a simplified single node architecture consisting of the eNB [26] to communicate with users' equipments (UEs), while the eNB communicates with other eNB using X2-C and X2-U interfaces for control and user plane respectively, for example in mobile end UE HO situations. The eNB communicates with the evolved packet core (EPC) using the S1 interface; specifically with the mobile management entity (MME) and the user plane entity (UPE) identified as serving gateway (S-GW), using S1-C and S1-U interfaces for control plane and user plane respectively, that supports a many-to-many relation between MMEs/UPEs and eNBs, and by its turn is connected by the internet protocol (IP) Multimedia Subsystem (IMS), and the application server (Apps). The MME and the UPE are preferably implemented as separate network nodes so as to facilitate independent scaling of the control and user plane.

2.2.6 LTE Spectrum Flexibility

The most important value in the LTE requirements in terms of spectrum flexibility is the ability to use LTE based radio access in unpaired and paired spectrum [20]. Therefore, LTE

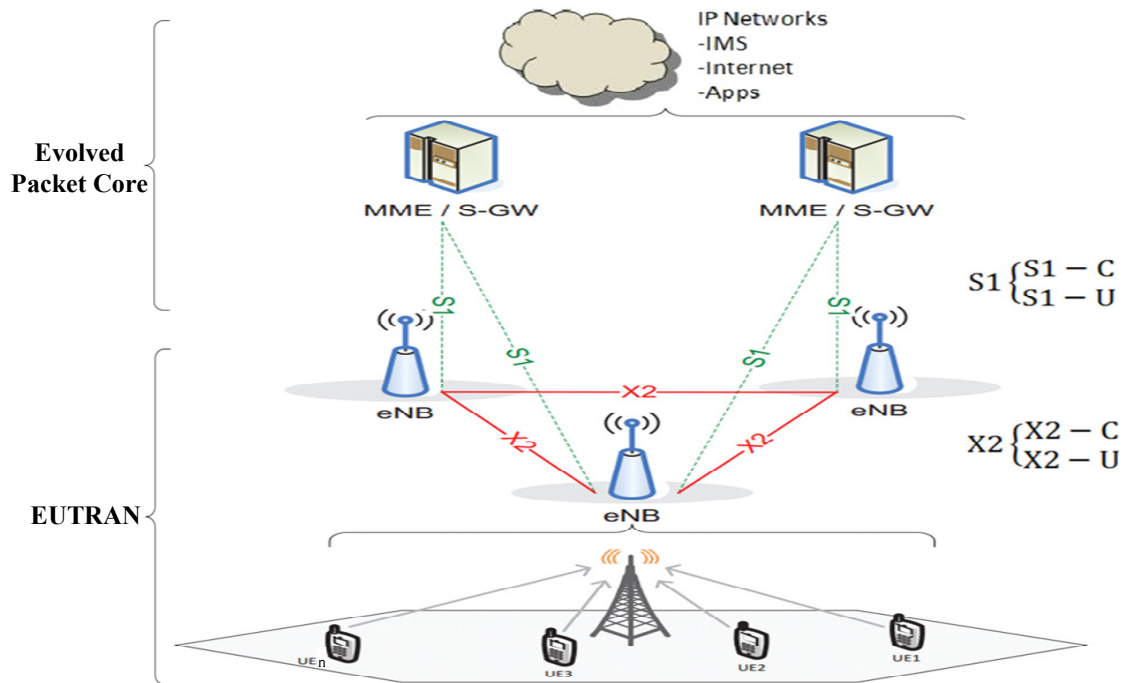


Figure 2.4: The LTE system architecture.

is able to support both frequency- and time-division-based duplex transmissions. Frequency division duplex (FDD) [27] as illustrated to the left in Figure 2.5 implies that DL and UL transmission take place in different, sufficiently separated, frequency bands. Time division duplex (TDD), as illustrated to the right in Figure 2.5, shows that DL and UL transmission can take place in non-overlapping, different time slots. Then, TDD can work in unpaired spectrum, whereas, FDD requires paired spectrum.

LTE also can support half-duplex FDD (illustrated in the middle of Figure 2.5). In half-duplex FDD, the transmission and reception at a certain terminal are separated in both frequency and time. The base station can still uses full duplex as it may schedule different transmissions in UL and DL; that is the same case in the GSM operation.

The main advantage with half-duplex FDD is the reduced complexity as no duplex filter is required in the terminal, which is much beneficial in case of multi-band terminals that otherwise would require many sets of duplex filters.

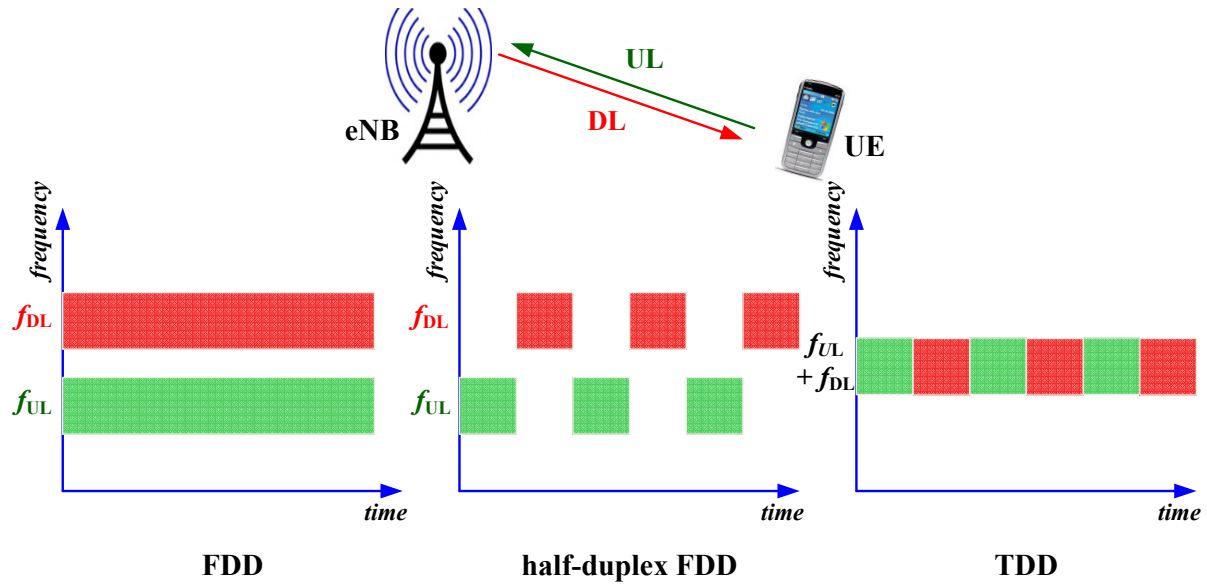


Figure 2.5: Frequency and time division duplex.

2.2.7 LTE Frame Structure

The LTE frame structure is set for two types: type-1 LTE FDD, and type-2 LTE TDD mode systems. Type-1 frame structure that works on both half duplex and full duplex FDD modes [27]. That type of radio frame usually has duration of 10 ms and consists of 20 slots, each slot has the equal duration (0.5 ms). The sub-frame consists of two slots, one radio frame has 10 sub-frames. In the FDD mode, DL and UL transmission is divided in frequency domain, so half of all sub-frames can be used for DL and half for UL, in radio frame interval of 10 ms. Type-2 frame structure consists of two identical half frames of 5 ms duration each. Both half frames have 5 sub-frames with duration of 1 ms.

TDD mode uses frame structure type 2. In this structure, the slots, sub-frames and frames have the same duration, but each subframe can be allocated to either the UL or DL [20, 23, 24], using one of the TDD configurations as shown in Figure 2.6.

One sub-frame consists of two slots and each slot has duration of 0.5 ms. There are some special sub-frames which consist of three fields; guard period (GP), DL pilot time slot (DwPTS) and UL pilot time slot (UpPTS). These three fields are individually configurable, but each sub-frame shall have a total length of 1ms.

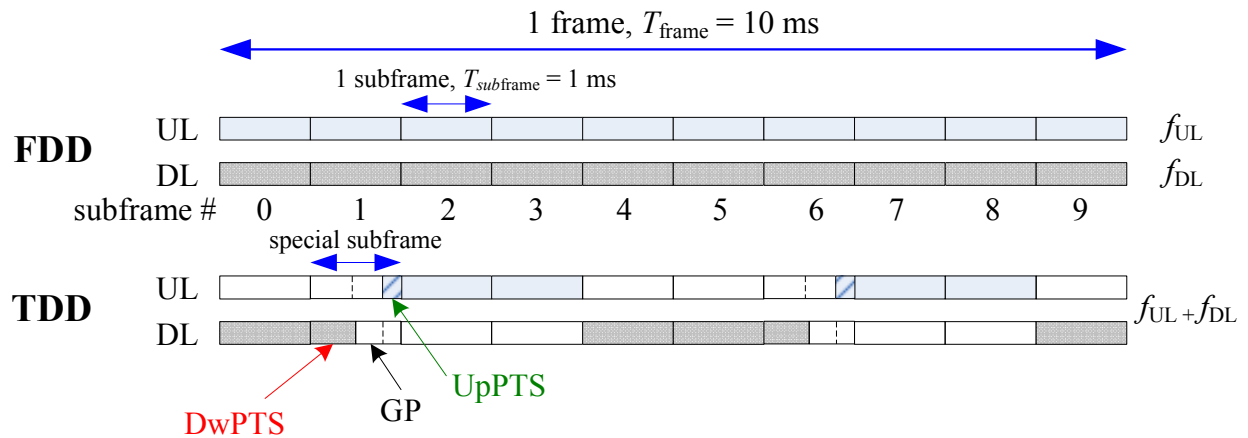


Figure 2.6: UL/DL time/frequency structure in case of FDD and TDD.

There are seven UL/DL configurations used for either 5 ms or 10 ms switch-point periodicities. Note that, a special sub-frame exists in half frames in case of 5 ms switch-point time-period whereas, for 10 ms switch-point time-period the special frame exists only in the first half-frame. Table 2.2 shows the UL/DL frame configuration for LTE TDD, and simplified in Figure 2.7.

Table 2.2: UL/DL Frame Configuration for LTE TDD.

Configuration	DL to UL	SF ₀	SF ₁	SF ₂	SF ₃	SF ₄	SF ₅	SF ₆	SF ₇	SF ₈	SF ₉
0	5 ms	DL	SF	UL	UL	UL	DL	SF	UL	UL	UL
1	5 ms	DL	SF	UL	UL	DL	DL	SF	UL	UL	DL
2	5 ms	DL	SF	UL	DL	DL	DL	SF	UL	DL	DL
3	10 ms	DL	SF	UL	UL	UL	DL	DL	DL	DL	DL
4	10 ms	DL	SF	UL	UL	DL	DL	DL	DL	DL	DL
5	10 ms	DL	SF	UL	DL						
6	5 ms	DL	SF	UL	UL	UL	DL	SF	UL	UL	DL

Where, SF is a subframe and it is used for guard time, DL is a subframe and it is used for DL transmission, and UL is a sub-frame and it is used for UL transmission.

Different cells can have different TDD configurations, which are advertised as part of the cells system information. Configuration 1 might be suitable if the data rates are similar on the UL and DL, for example, while configuration 5 might be used in cells that are dominated by DL transmissions. Nearby cells should generally use the same TDD configuration, to minimize

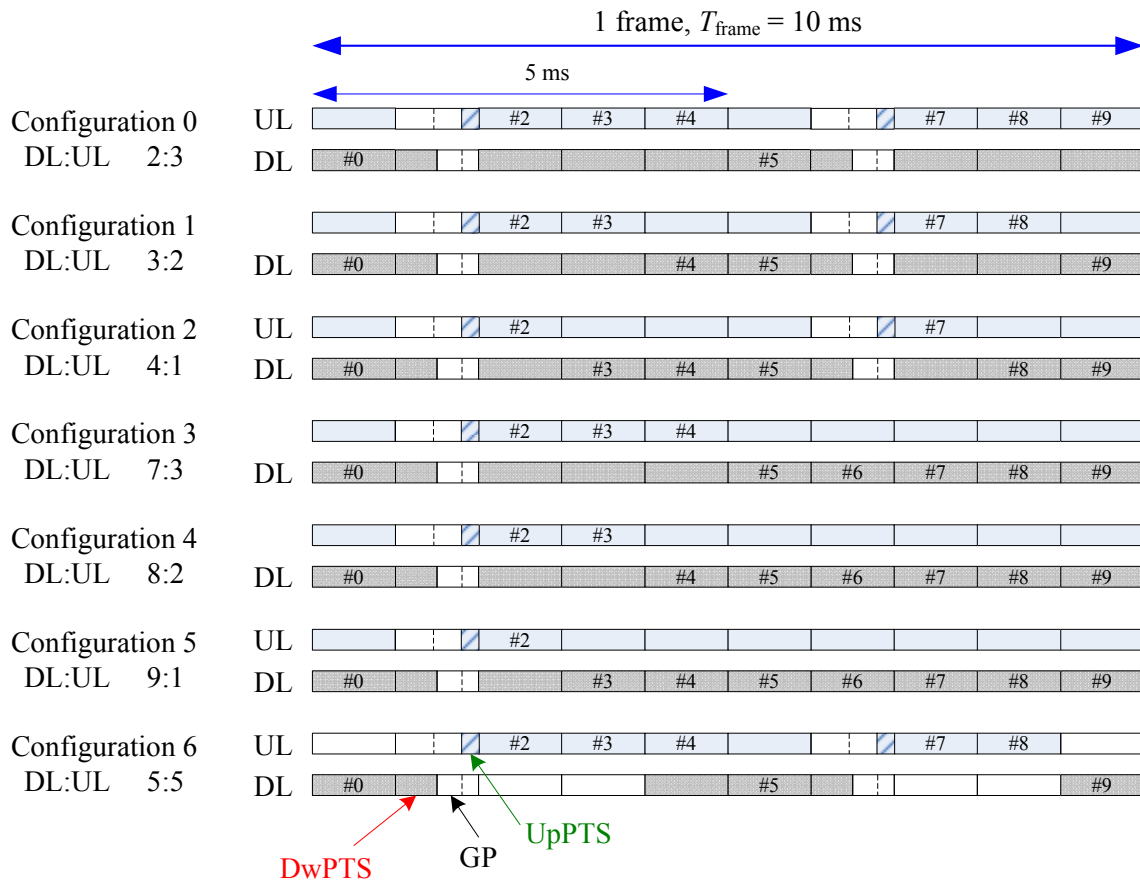


Figure 2.7: TDD configuration.

the interference between the UL and DL.

Special subframes are used at the transitions from DL to UL transmission. They contain three regions. The special DL region takes up most of the subframe and is used in the same way as any other DL region. The special uplink region is shorter, and is only used by the random access channel and the sounding reference signal. The two regions are separated by a guard period that supports the timing advance procedure described below. The cell can adjust the size of each region using a special subframe configuration, which again is advertised in the system information.

Figure 2.8 shows the relationship between a slot, symbols, and physical radio RBs. The sub-carriers are divided into RBs, which is the basic resource allocation unit for scheduling in 3GPP-LTE system. N_{RB} is the symbol used to indicate the maximum number of RBs for a given bandwidth. This allows the system to split the sub-carriers into small parts, without mixing the data across the total number of sub-carriers for a given bandwidth. The basic unit is a resource element (RE), which spans one symbol by one sub-carrier. Each resource element usually carries two, four or six physical channel bits, depending on whether the modulation scheme is QPSK, 16-QAM or 64-QAM. Resource elements are grouped into RBs, each of which spans 0.5ms (one slot), by 180 kHz (12 sub-carriers). The base station uses RBs for frequency-dependent scheduling, by allocating the symbols and sub-carriers within each sub-frame in units of RBs.

The LTE signal can be represented in a two dimensional map. The horizontal axis is time domain and the vertical axis is frequency domain. The minimum unit on vertical axis is a sub-carrier and on horizontal axis is symbol [20].

In the frequency domain structure, any SC-FDMA/OFDMA band is made up of multiple small spaced channels, and each of these small channels is called as "sub-carrier". Space between the channel and the next channel is always same regardless of the system BW of the LTE band. So, if the system BW of the LTE channel changes, number of the channels (sub-carriers) change, but the space between channels does not change. In Figure 2.9, the rela-

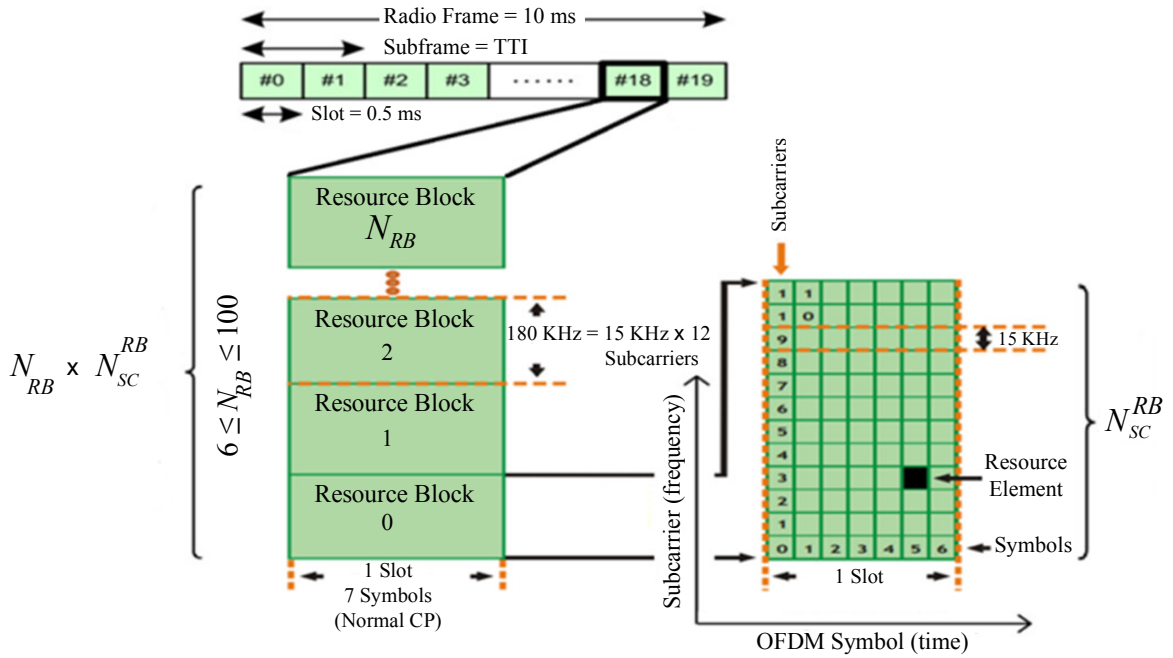


Figure 2.8: The relationship between a slot, symbols, and RBs.

tionships between channel bandwidth, and transmission bandwidth configuration is illustrated. Also, another important part of the LTE benefits is in terms of spectrum flexibility (1.4 MHz to 20 MHz) [28] as shown in Figure 2.10.

2.2.8 UL/DL Information Exchange

In UL transmission of LTE, there are still some additional carrying signals needed such as; reference signal, random access preamble and control signal, etc. These signals are specified as a sequence signalling and have constant amplitude with zero auto-correlation.

These signals are not part of SC-FDMA modulation scheme. On the other hand, the base stations scheduling algorithm has to decide the contents of every DL scheduling command and UL scheduling grant, on the basis of all the information available to it at the time. Each bearer is associated with a buffer occupancy, as well as information about its quality of service such as the priority and prioritized bit rate.

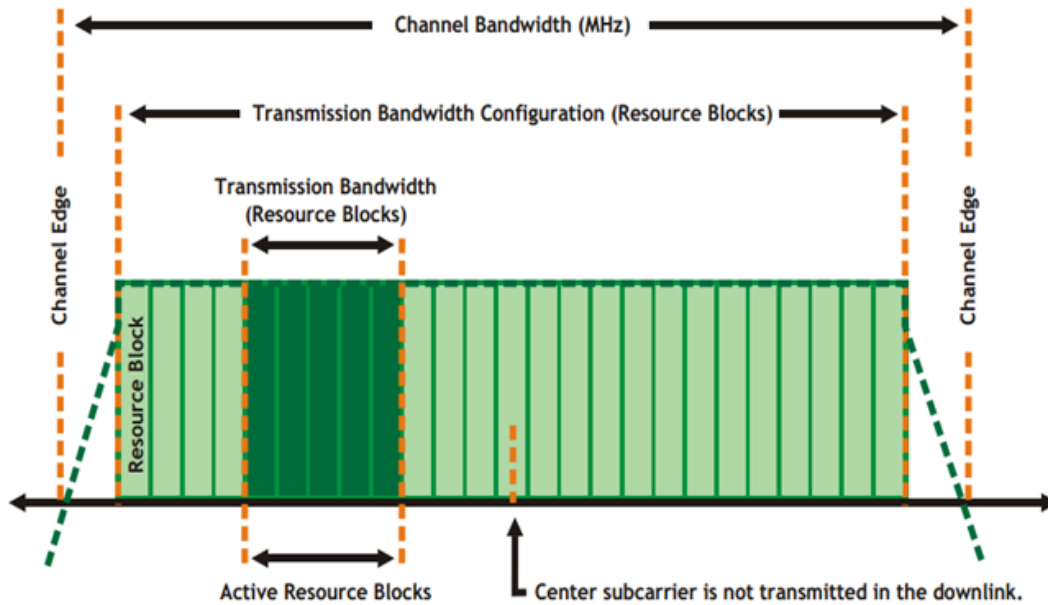


Figure 2.9: The relationships between channel bandwidth, and transmission bandwidth configuration.

Channel Bandwidth (MHz)	Maximum Number of Resource Blocks (Transmission Bandwidth Configuration)	Maximum Occupied Bandwidth (MHz)
1.4	6 × 180 KHz	1.08
3	15	2.7
5	25	4.5
10	50	9.0
15	75	13.5
20	100	18.0

Figure 2.10: The transmission bandwidth configuration.

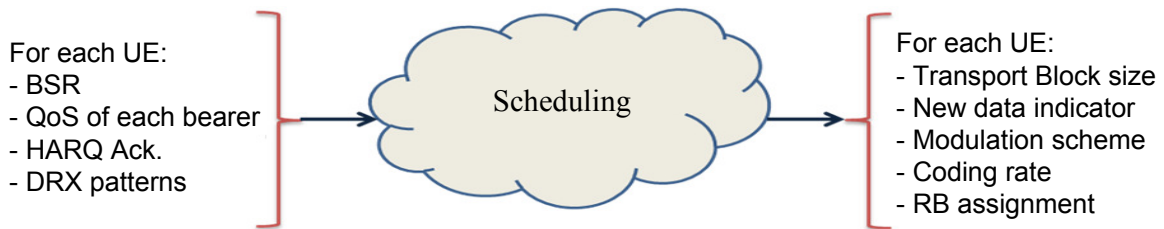


Figure 2.11: Inputs and outputs for the UL and DL scheduling algorithm.

To support the scheduling function, the mobile returns hybrid automatic repeat request (HARQ) acknowledgments (Acks) [29], channel quality indicators and rank indications [30]. The eNB also knows the discontinuous reception (DRX) pattern for every UE in the cell and can receive load information from nearby cells about their own use of the sub-carriers. Figure 2.11 shows the most common of the main inputs and outputs commands and data exchange.

With the use of this information, the scheduler has to determine how much information in bits are required to send to each user, even to send a new transmission or a re-transmission and how to classify new transmissions through the available bearers. It also needs to determine the used modulation schemes and coding rates, spatial multiplexing, and the allocation of RBs to every mobile UE.

The UL scheduler usually follows the same concept, although some of the inputs and outputs are different. For example, the eNB does not have the full knowledge about the UL buffer occupancy and does not tell the UEs which channels they shall use for their transmissions. Moreover, the eNB calculate its channel quality data from the sounding procedure, instead of the UEs' channel quality indicators (CQIs).

The UL scheduler follows the same principles, although some of the inputs and outputs are different. For example, the eNB does not have complete knowledge of the UL buffer occupancy and does not tell the UEs which logical channels they should use for their UL transmissions. In addition, the eNB derives its channel quality information from the sounding procedure, instead of from the UEs channel quality indicators.

The given example in Figure 2.12 introduces one SP, serving two users, the first user (UE-1) is considered to be the near user (1.2 Km far from the eNB), has high SNR (SNR_h), while UE-2 is the far user (1.8 Km far from the eNB), has low SNR (SNR_l). The figure shows an overview of the information exchange procedure in both UL and DL connection between an eNB, and UE-1, and 2, considering an already ongoing transfer data, noting that TDD is considered, using type Frame 2, with Configuration 2, where DL:UL = 3:2, functioning with packet data convergence protocol (PDCP), where the eNB scheduler takes its scheduling mapping decision every half frame, and one frame time period, where The UE transmits buffer status report (BSR) medium access control (MAC) control elements to tell the base station about how much data it has available for transmission.

Where, the UE sends the BSR in three situations:

1. if data is ready for transmission on the channel with high priority than the previously storing buffers were,
2. or if data is ready for transmission when the transmit buffers were empty,
3. or if the timer expires while data is waiting for transmission.

The mobile expects the base station to reply with a scheduling grant. Considering the CQI [30], which is the indicator that carries the information on how good or bad the communication channel quality is, as it is the information that UEs send to the network and practically it implies the following two indications :

1. Current communication channel quality,
2. Data transport block size,

that in turn can be directly translated into throughput, and the buffer status report include the QoS of each Bearer, sounding measurements, modulation schemes, and the transport block (TB) size.

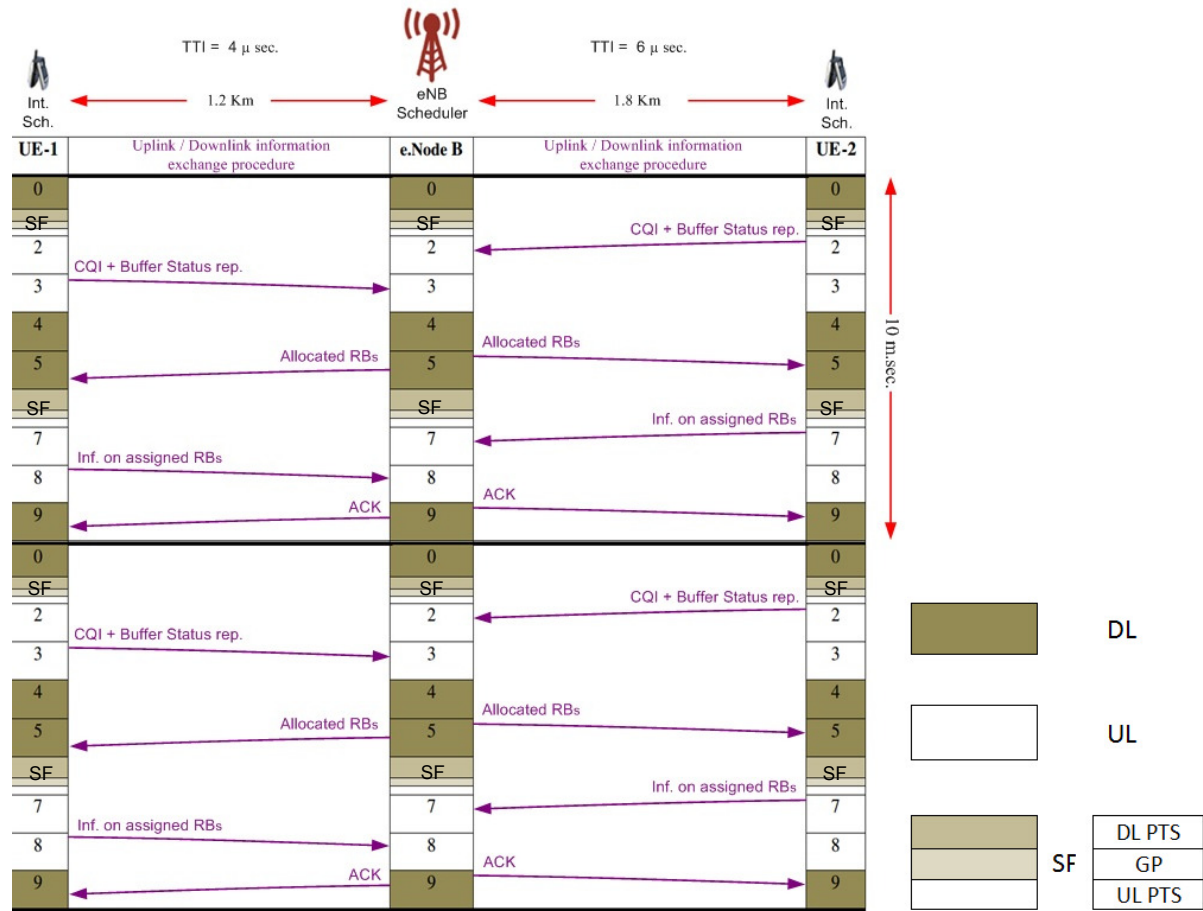


Figure 2.12: The information exchange procedure in both UL and DL connection between an eNB, and two UEs.

2.3 Chapter Summary

In this chapter, an overview on the recent radio platform LTE technology that depends on the OFDM communication method is presented. LTE system use SC-FDMA for UL transmission and OFDMA for DL transmission. This system is capable of reaching a peak data-exchange rate of 50 Mbps for UL transmission and 100 Mbps for DL transmission; the main motivation for our research is to model our research problems in order to make an effective contribution.

Nevertheless, there has been a small amount of pioneering work in this area trying to enhance and contribute the wireless QoSs' parameters. This has been accomplished by making various assumptions or simplifications to the system or simply by focusing on a subset of the overall scheduling problem. In the coming chapters, I propose several different approaches in this research domain.

Chapter 3

Sharing Resources in 3GPP-LTE Systems

Framework

Nowadays, much research and standardization efforts are evolving in order to withstand more capable facilities at high effective points. The purpose of this work is to address some of these issues by demonstrating several novel dynamic allocation sharing algorithms in LTE systems. This algorithm will help in increasing the performance over a broader range of subscriber access scenarios.

Specifically, this Chapter proposes a novel dynamic scheduling sharing algorithm that can support guaranteed QoS for multiple types of applications in the wireless networks. The proposed algorithm reduces the packet delay and jitter for delay-sensitive applications, such as narrow-band voice. This considerably enhance the related delay performance without degrading QoS parameters for all service types.

3.1 Introduction

Recently, network sharing has been proposed as an integral part of the next-generation networking architecture for vehicular communications, and is considered to be a promising solution to provide low-cost framework, and accommodate increased traffic demands [31, 32].

Sharing radio resources management in LTE systems leads to successful virtualization of the wireless access networks that have received much attention by network operators. Virtualizing the wireless resources enables MNOs to create multiple logical networks based on a single physical substrate.

Recently, there has been a dramatic increase in the amount of network data traffic, primarily driven by the rising number of users demanding increased data rates. Moreover, a wide range of increasingly bandwidth-intensive services are continuing to emerge (e.g., storage extension/virtualization, grid computing, packet video teleconferencing, and so on) [11].

A mobile network operator (MNO), commonly known as a service provider, wireless carrier, cellular company, or mobile network carrier [33], is a provider of the wireless services communications that controls all the necessary elements to rent/sell and deliver services to the end UE including the spectrum allocation, network and back haul infrastructure, customer care, provisioning systems, billing, and marketing and repair organizations.

This chapter proposes a novel dynamic scheduling sharing resources algorithm for different types of applications in access networks. The framework scheme shares MNOs' resources while maintaining different scheduling strategies. The proposed algorithm considerably improves related delay performance without degrading QoS. The research below offers detailed simulations to study the performance of the proposed algorithm and validate its effectiveness.

3.2 Related Work

During the latest basic literature, MNOs sharing RBs have gained significant attention. Jing *et al.* in [27] presented the resource sharing on the relay link according to the buffer state at the relay nodes (RNs) for urban scenarios without applying a power control (PC) optimization, and their results including the suburban scenarios are also provided in [34].

In latter approach, Zaki *et al.* in [35], proposed an LTE air interface virtualization scheme wherein a hypervisor is added on top of physical resources, that takes the responsibility of vir-

tualizing the eNB into a number of virtual eNBs that are then used by different MNOs. As an extension to [36], the discussed some practical scenarios in [37]; where MNOs share multiple eNBs. The managed in the sharing process is controlled by the so-called hypervisor. Moreover, two traffic models (best effort model and the guaranteed bit rate model) have been considered for resource sharing.

Kokku *et al.* in [38] proposed and evaluated a flow-level virtualization scheme of wireless resources on base stations in worldwide interoperability for microwave access (WiMAX) cellular systems. The proposed solution enables customized flow scheduling per slice and takes into account the level of isolation and resource utilization trade-off. Each slice can be seen as a virtual MNO and contains a number of flows. The goal of achieving dynamic and efficient resource sharing is moved to the scheduler by Min *et al.* in [39]; which can instantaneously adapt to changes in system conditions, rather than relying on semi-static radio interface sub-frame allocation.

In addition, in [40], O. Bulakci *et al.* presented the relay-enhanced networks, where a combination of resource allocation on the relay link based on the number of attached UEs; and a throughput throttling scheme achieving max-min Fairness (MMF) in the end-to-end two-hop communication have been proposed.

Some advanced resource sharing mechanisms are discussed such as the schemes based on interference graph by Necker *et al.* in [41], or game theory by Menon *et al.* in [42]. Game theory based resource sharing models the resource allocation as the outcome of a game. In [43, 44], Bulakci and Kokku investigated the cooperative methods relying on information exchange between the cells that yield significant performance improvement comparing to non cooperative solutions, but at the cost of high signaling overhead.

Roth *et al.* in [45], investigated the time-division and frequency-division multiplexing of relay and access link transmissions on the DL excluding the resource sharing within the links. Another framework for wireless network virtualization that separates SPs from network operator is reported by Fu *et al.* in [46]. Wherein, the SPs are in charge for QoS management, while

spectrum management is maintained by the network operator.

3.3 System Modeling Framework

In the LTE architecture, the eNB is the node between the UE and the core network. It is responsible for the radio resource management (RRM) functions (transmission power management, mobility management and radio resource scheduling) [47, 48, 49]. As the bandwidth of wireless communication system is scarce and very expensive, the RRM is workable with OFDMA. Then the radio resource scheduling is a significant process in which the available radio resources are assigned to all active UEs efficiently in terms of QoS requirements.

The LTE sharing framework is shown in Figure 3.1. Let k denotes the number of MNOs sharing the eNB. Each MNO has various numbers of UEs, as well as its own associated EPC, RBs and scheduling algorithm. The eNB establishes multiple radio bearers per UE to support multiple traffic types.

In the considered frame work scenario, the eNBs scheduler algorithm explore the contents of every UL scheduling requested grant [50] and, reply to UEs with the decided scheduling mapping commands specifying the assigned RBs, power control entity, modulation and coding scheme (MCS) on the basis of all the information available to it at the time, FDD is considered, functioning with PDCP, where the eNB Scheduler takes its scheduling mapping decision every one sub-frame time period (1 ms), where The UE transmits BSR MAC control elements to inform the base station (eNB) about how much data available for transmission. Considering the CQI, and the BSR include the QoS of each Bearer, sounding measurements, modulation schemes, and the TB size.

3.3.1 Data Transmission Sequence

The sequence of data transmission for M UEs is shown in Figure 3.2. The UEs receive UL traffic from upper layers. Data from multiple logical channels are queued in the radio link



Figure 3.1: MNOs sharing radio RBs in a single eNB.

control (RLC) sub-layer buffers. Information about buffered data sizes is sent to the eNB over the UL control channel known as the BSR. The eNB's scheduler performs allocation decisions according to the SPs' scheduling policy. And based on the mapped decisions, the eNB sends the maps to the UEs over the the DL control channel. The UEs' allocation map consists of the assigned RBs, power control entity and MCSs [30, 51].

The RBs chunk and MCS that is assigned to a user specifies the UL transport block (TB) size. Noting that, how the TB is shared between a user's buffers is left to the UE policy [11]. In the UE's MAC sub-layer, the MAC protocol data unit (PDU) is performed according to the received map. The MAC PDU extrapolates the data from all RLC PDUs and the MAC header. The MAC passes the MAC PDU to the physical layer (PHY), that adds the cyclic redundancy check (CRC) bits to the MAC PDU and transmits the whole packet as a TB over the UL channel to the eNB.

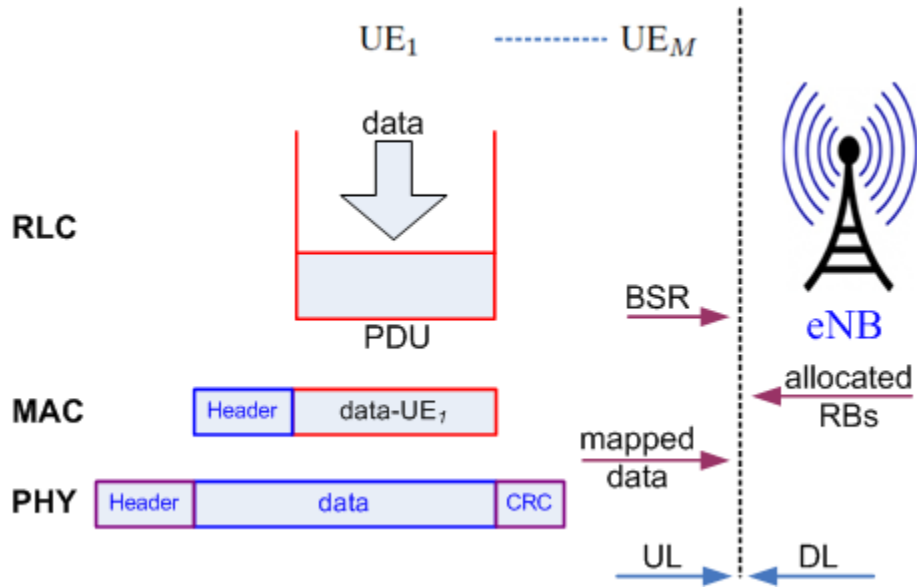


Figure 3.2: The UEs' data transmission sequence.

3.3.2 LTE Traffic Classes

The LTE sharing framework is shown in Figure 3.1. Let k denotes the number of MNOs sharing the eNB. Each MNO has various numbers of UEs, as well as its own associated EPC, RBs and scheduling algorithm. The eNB establishes multiple radio bearers per UE to support multiple traffic types [52].

In order to support different classes of service with different packet jitter and delay requirements, three prioritized service classes are introduced: expedite forwarding (EF) [53] with the highest priority for strictly delay sensitive services typically constant bit rate (CBR) voice transmission, assured forwarding (AF) with medium priority for services of non-delay sensitive variable bit rate (VBR) services such as video stream, and best effort (BE) with the lowest priority for delay tolerable services, which include web browsing and background file transfer [11].

A key motivation was the inherently non-deterministic nature for AF and BE. Packets in dedicated bearers are generated at the application layer by 3 different traffic generators: Voice traffic, trace based, and infinite buffer.

The voice traffic application generates G.729 voice flows. In particular, the voice flow

has been modeled with an ON/OFF Markov chain, where the ON period is exponentially distributed with a mean value of 3 s, and the OFF period has a truncated exponential probability density function with an upper limit of 6.9 s and an average value of 3 s [54, 55]. During the ON period, the source sends 20 bytes-sized packets every 20 ms (*i.e.*, the source data rate is 8 kb/s), while during the OFF period, the rate is zero because the presence of a voice activity detector is assumed. The trace-based application sends packets based on realistic video trace files, available in [56] using H-264 compression format. The BE application generates packets with VBR, assuming Packets arrive according to Poisson distribution, with an exponential inter-arrival mean time and size of 200 ms, and 2400 bits. Figure 3.3 shows a simplified explanation for the considered traffic classes.

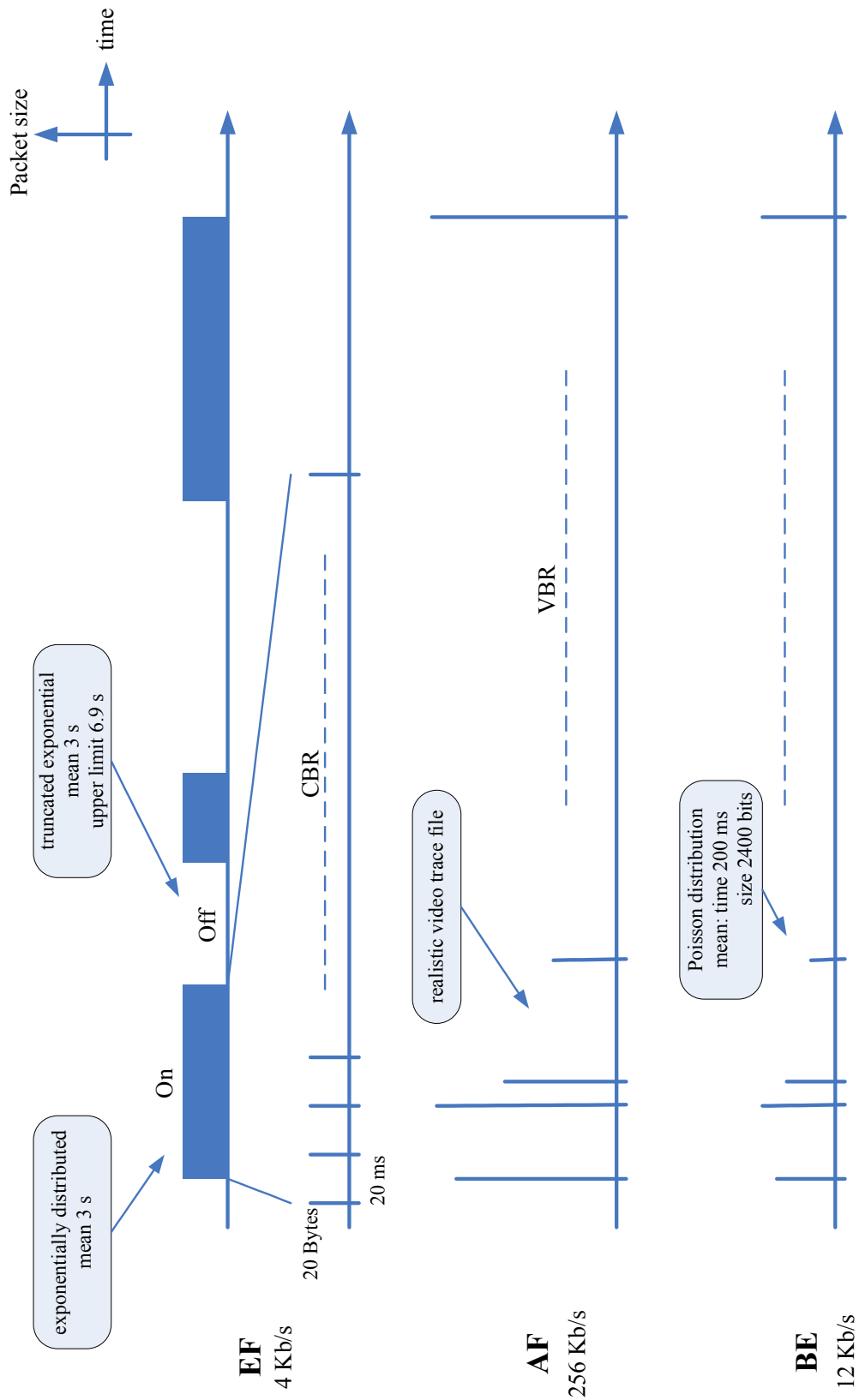


Figure 3.3: EF, AF, and BE considered traffic classes.

3.3.3 Transmission Block Size and MCSs

In LTE, the subframe has a duration of 1 ms. The available spectrum is divided into RBs. The RB is defined in both frequency and time domains. It consists of a contiguous set of 12 subcarriers (180 kHz with subcarrier spacing of 15 KHz) from each OFDM symbol and has a duration of 0.5 ms.

The overall TB size is a function of the spectral efficiency (ζ_s) of the selected MCS s and the number of allocated RBs. The total RB bandwidth is $12 \times BW$, where BW is the subcarrier bandwidth. The total TB size, that can be transmitted per subframe over R RBs for UE $_{m_n}$ is given by:

$$T_{m_n,R,s}(t) = \lfloor 12(N_{sym} - N_{OH}) \times \zeta_c(t) \times \|R\| \rfloor \quad (3.1)$$

where N_{sym} is the number of symbols per subcarrier in a given subframe, while N_{OH} is the number of overhead symbols per subcarrier (usually 3 symbols). The value $N_{OH} \geq 0$ allows any additional overhead per TB. When normal cyclic prefix is used ($N_{sym} = 14$ symbols); each subframe consists of 11 symbols per subcarrier, each with a duration of $T_s = 66.7\mu s$.

The total number of symbols in one RB per subframe is $12 \times 11 = 132$ OFDM symbols. Therefore, the TB size can be calculated as:

$$T_{m_n,R,s}(t) = \lfloor 132 \times \zeta_c(t) \times \|R\| \rfloor, \quad (3.2)$$

where, ζ_c is the spectral efficiency of the MCS c . The received SNR determines the MCS [57, 58, 59] that should be used to deliver TB with a 10% block error rate. The MCS selection scheme is enacted using a lookup table that maps the received SNR to MCS [30, 60]. Table 3.1 shows MCSs that are used in LTE and how they are mapped to the received SNR for BLER 10%. Figure 3.4 shows the spectral efficiency and TB size versus SNR investigated from Table 3.1.

The channel between eNB and UEs is modeled as a block Rayleigh fading, which is constant over each RB bandwidth, but changes independently over RBs and UEs. The channel is

Table 3.1: List of MCS which are used in LTE.

Index	Modulation	Coding rate	ζ_c	SNR (dB)
0	-	-	0 bits	-6.7536
1	QPSK	78/1024	0.15237	-6.7536 : -4.9620
2	QPSK	120/1024	0.2344	-4.9620 : -2.9601
3	QPSK	193/1024	0.3770	-2.9601 : -1.0135
4	QPSK	308/1024	0.6016	-1.0135 : +0.9638
5	QPSK	449/1024	0.8770	+0.9638 : +2.8801
6	QPSK	602/1024	1.1758	+2.8801 : +4.9182
7	16QAM	378/1024	1.4766	+4.9182 : +6.7005
8	16QAM	490/1024	1.9141	+6.7005 : +8.7198
9	16QAM	616/1024	2.4063	+8.7198 : +10.515
10	64QAM	466/1024	2.7305	+10.515 : +12.450
11	64QAM	567/1024	3.3223	+12.450 : +14.348
12	64QAM	666/1024	3.9023	+14.348 : +16.074
13	64QAM	772/1024	4.5234	+16.074 : +17.877
14	64QAM	873/1024	5.1152	+17.877 : +19.968
15	64QAM	948/1024	5.5547	+19.968

assumed to be frequency non-selective, constant over each RB bandwidth, but changes independently over RBs and users.

3.3.4 LTE Frame work Scenario

The flowchart of the LTE frame work is illustrated in Figure 3.5, assuming M MNOs, each with N users, and UE is expected to send various types of traffic classes, the internal scheduler per user sends its BSR (in its long format that stands on more than one bearer, and up to four bearers), and the CQI. The BSR is assumed to include how much data is available for transmission, QoS, sounding references measurements, modulation schemes, etc.

Each MNO work with its associated EPC, and its own radio physical RBs. The eNB establishes multi-radio bearers for each user to support multi-traffic types. Each bearer is only assigned to a UE. The number of the working bearers is controlled by an admission control procedure. Each MNO owns a set of RBs R , and there are no intersection between the MNOs RBs.

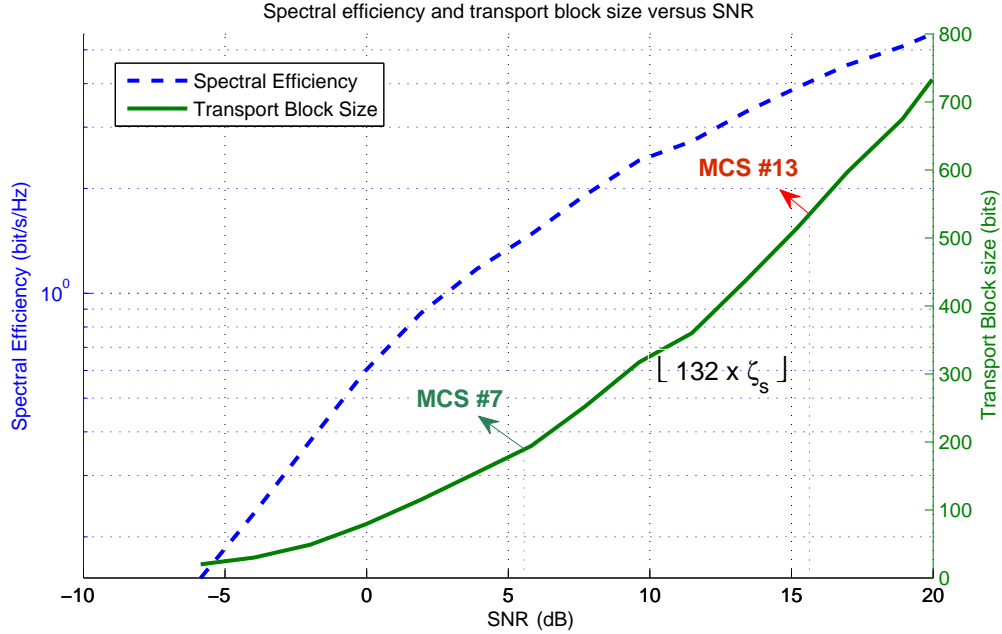


Figure 3.4: Spectral efficiency and transport block size versus SNR.

3.4 The Considered Scheduling Algorithms

Packet scheduling revenues in radio platform technology standard LTE systems are the charge of allocating resources to active flows in both frequency and time domain. Many schedulers have been discussed in [7, 11, 51, 61, 62, 63], comparing their data throughput, delay, fairness, etc; trying to reach the most effective performance among the schedulers resources allocation algorithms, as resource allocation for each UE is usually based on the comparison of per-RB metrics: the k -th RB allocated to the j^{th} user. Its metric $m_{j,k}$ is varified, i.e., if it satisfies the equation:

$$m_{j,k} = \max_i \{m_{i,k}\} \quad (3.3)$$

Herein, the presented framework is for 2 MNOs: MNO-1 cares about fairness between users, but with priority appliance among traffic classes, so; it will apply strict priority (S.P) scheduling; However, MNO-2 cares more about achieving revenues by transmitting the maximum weight of packets delay; largest weight delay first (LWDF) scheduling could be applied,

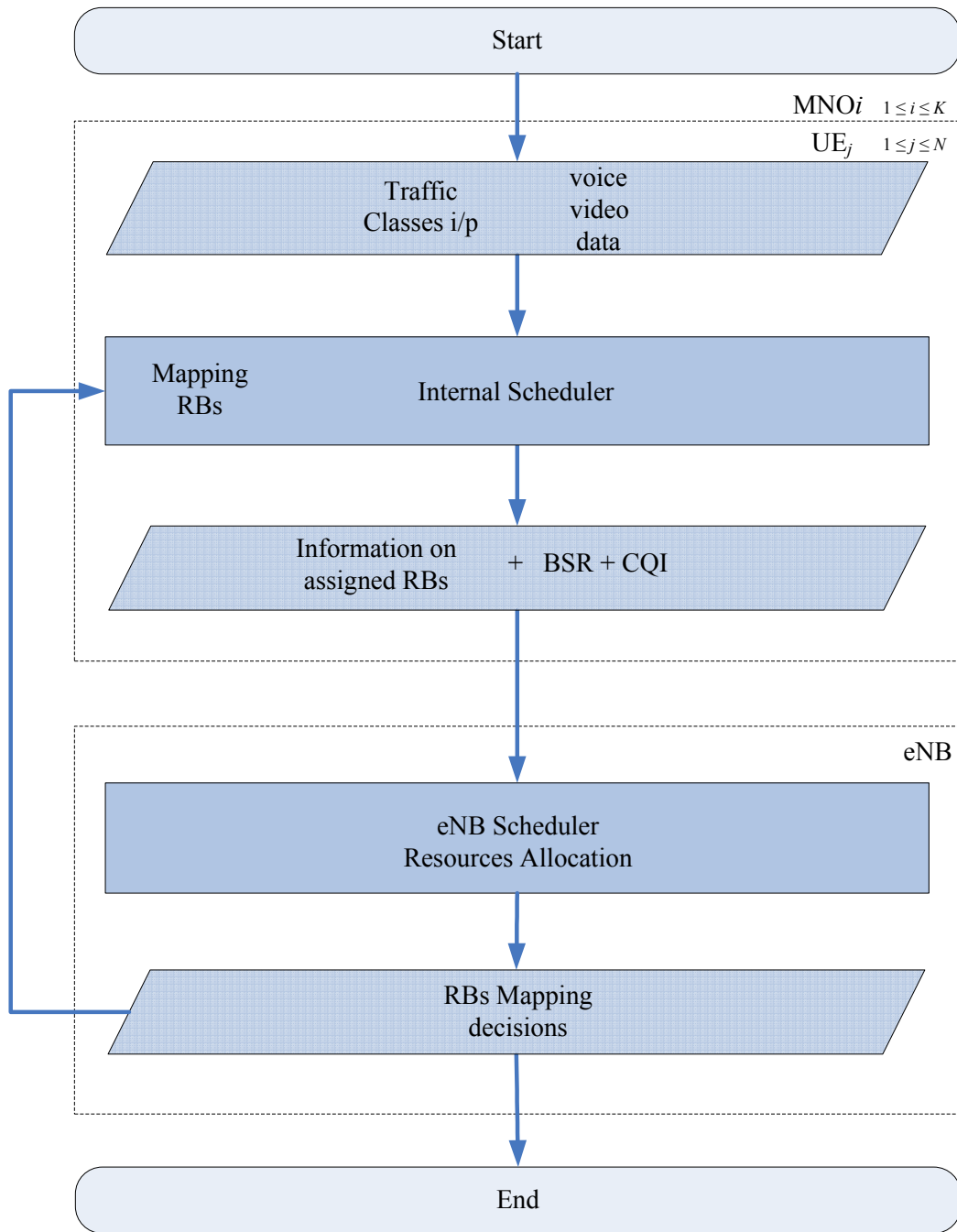


Figure 3.5: LTE flowchart for M MNOs, N UEs, and various Traffic Classes considered.

Table 3.2: Defined necessary parameters.

Parameter	Definition
av_{RBs}	Number of available RBs at definite TTI
$D_{HOL,ij}$	Head of line delay for traffic class i for UE_j
N	Total number of RBs
N_{cl}	Number of Traffic Classes
n_{i_RBj}	Number of RBs allocated to UE_j for Traffic Class i
n_{ij}	Number of needed RBs to satisfy traffic i for UE_j
n_{RBj}	Number of RBs allocated to UE_j
RB_{BW}	Size of available RB that could be allocated to UE_j
RBS_i	RBs BW allocated to UE_j
S_i	Needed BW to satisfy traffic i (in bits) by all UEs
T_i	Delay threshold for traffic class i
TTI	Transmission Time Interval
U	Total number of UEs
V_{ij}	BSR size of queue i for UE_j , where $i = 1$ for EF $i = 2$ for AF $i = 3$ for BE
W_{ij}	Weight factor of delay for traffic class i for UE_j
δ_i	Acceptable packet loss rate for traffic class i
$[.]*$	The new value of $[.]$

followed by internal scheduler (I.S.) per UE, that distribute RBs among the traffic classes' queues. In order to formularize the considered schedulers policies, it is helpful to consider some necessary parameter definitions as shown in Table 3.2.

3.4.1 The Strict Priority Scheduling Algorithm

The S.P. scheduling algorithm allocate RBs according to the priority of the considered traffic class, while maintaining fairness between UEs. The pseudo-code for the S.P. scheduler is shown in Figure 3.6.

3.4.2 The LWDF Scheduling Algorithm

The guaranteed delay services, in particular, need that all packets have to be received within a specific deadline to avoid packet drops. This aim can be ensured by considering into the metric data about the exact packet timing, that is both the time when the packet was sent

```

1 : For each simulated TTI do
2 :    $av_{RB_s} = N_{RB}$  // Total available RBs
   // phase i: RBs Allocation for traffic Class i (Priority-i)
3 :   For  $i = 1$  to  $N_{cl}$  do
4 :     If  $av_{RB_s} > 0$  Then
5 :       For  $j = 1$  to  $N_{UE_s}$  do
   // Requested RBs to satisfy traffic i for UEj
6 :          $n_{ij} = \text{Ceil} \left\{ \frac{v_{ij}}{RB_{BW}} \right\}$ 
7 :       End For
8 :        $S = \sum_{j=1}^{N_{UE_s}} n_{ij}$  // total requested RBs by traffic i for UEj
9 :       For  $j = 1$  to  $N_{UE_s}$  do
   // Allocated RBs for Traffic Class i for UEj
10:         $n_{i\_RBj} = \min \left( n_{ij}, \text{floor} \left\{ \frac{n_j \times av_{RB_s}}{S} \right\} \right)$ 
11:      End For
12:    End If
13:     $av_{RB_s} = N_{RB} - \sum_{j=1}^{N_{UE_s}} n_{i\_RBj}$  // Available RBs
14:    Repeat
15:      For  $j = 1$  to  $N_{UE_s}$  do
16:        Sort  $UE_s$  by  $\left[ \frac{n_{ij}}{n_{i\_RBj}} > 1 \right]$  Descending
17:        If  $av_{RB_s} > 0$  Then
18:           $n_{i\_RBj}^* = n_{i\_RBj} + 1$ 
19:           $av_{RB_s}^* = av_{RB_s} - 1$ 
20:        End If
21:      End For
   // Satisfy either allocation request or vanished available RBs
22:      Until  $\left[ \frac{n_{ij}}{n_{i\_RBj}} \leq 1 \text{ or } av_{RB_s} = 0 \right]$ 
   // Total available RBs after allocation to traffic i for UEj
23:       $av_{RB_s} = N_{RB} - \sum_{i=1}^{N_{cl}} \sum_{j=1}^{N_{UE_s}} n_{i\_RBj}$ 
24:    End For
25:     $n_{RBj} = \sum_{i=1}^{N_{cl}} n_{i\_RBj}$  // Number of RBs allocated to UEj
26:  End For // End of Simulation

```

Figure 3.6: Pseudo-code for the strict priority scheduler.

and its deadline. LWDF policy is defined mostly for real-time operating system and wired networks [64], that aim at avoiding deadline expiration. Intuitively, the more the head of line delay approaches the expiration time, the more the user metric increases. LWDF metric is based on the system parameter δ_i , representing the acceptable probability for the j^{th} user that a packet is dropped due to deadline expiration, that could be expressed by:

$$W_{ij} = \alpha_{ij} \times D_{HOL,ij} \quad (3.4)$$

$$\alpha_i = -\log(\delta_i)/T_i \quad (3.5)$$

where: $W_{i,j}$ is the weight factor of delay for traffic class i for UE_j ,

T_i is the Delay threshold for traffic class i ,

δ_i is the acceptable packet loss rate for traffic class i ,

$D_{HOL,ij}$ is the head of line delay for traffic class i for UE_j .

In fact, α_i weights the metric so that the user with strongest requirements in terms of acceptable loss rate and deadline expiration will be preferred for allocation. The pseudo-code for the LWDF scheduler is shown in Figure 3.7. noting that:

$$N_{RB} \geq \sum_{j=1}^{N_{UES}} n_{RB_j} \quad (RBs) \quad (3.6)$$

$$S_i = \sum_{j=1}^{N_{UES}} V_{ij} \quad (bits) \quad (3.7)$$

$$RBS_j = \sum_{j=1}^{N_{UES}} n_{RB_j} \times RB_{BW} \quad (bits) \quad (3.8)$$

To reduce control signalling overhead, the LTE standard recommends that, for each sub-frame, only one MCS should be used for all allocated users RBs [11, 12, 30]. The RBs chunk and MCS that is assigned to a user determine the UL TB size. However, how the TB is shared between users buffers is left to the user; As distributing the TB into a different users bearers is

```

1 : For each simulated TTI do
2 :    $av_{RB_s} = N_{RB}$  // Total available RBs
3 :   For  $i = 1$  to  $N_{cl}$  do
4 :     For  $j = 1$  to  $N_{UE_s}$  do
5 :       // Requested RBs to satisfy traffic  $i$  for  $UE_j$ 
6 :        $n_{ij} = \text{Ceil} \left\{ \frac{v_{ij}}{RB_{BW}} \right\}$ 
7 :     End For
8 :   End For
9 :   For  $i = 1$  to  $N_{cl}$  do
10 :    For  $j = 1$  to  $N_{UE_s}$  do
11 :      Calculate  $W_{ij}$  for traffic class  $i$  for  $UE_j$ 
12 :    End For
13 :    Sort  $UE_s$  by [Largest Weight Delay ( $W_{ij}$ )] descending
14 :    // RBs Allocation for traffic Class  $i$  for  $UE_j$ 
15 :    For  $i = 1$  to  $N_{cl}$  do // Priority per traffic classes
16 :      For  $j = 1$  to  $N_{UE_s}$  do
17 :        If  $av_{RB_s} > 0$  Then
18 :          // Allocated RBs for traffic class  $i$  for  $UE_j$ 
19 :           $n_{i\_RB_j} = \min(n_{ij}, av_{RB_s})$ 
20 :          // Available RBs
21 :           $av_{RB_s} = N_{RB} - \sum_{i=1}^{N_{cl}} \sum_{j=1}^{N_{UE_s}} n_{i\_RB_j}$ 
22 :        End If
23 :      End For
24 :    End For
25 :  End For // End of Simulation

```

Figure 3.7: Pseudo-code for the largest weight delay first scheduler.

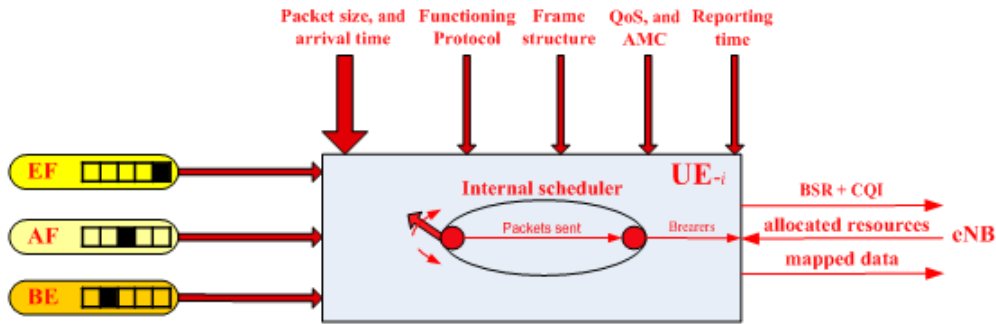


Figure 3.8: The block diagram of the internal scheduler working procedure.

assumed to be handled by UE as guaranteed bit rate (GBR) bearers should be satisfied before non-GBR (NGBR) bearers, and within the same radio bearer category, the allocated resources are distributed proportionally according to the UE's I.S. policy.

3.4.3 The UE's Internal Scheduler

The UE's I.S. targeting to perform scheduling between its traffic classes, where the scheduler distributes the received grant among the different active RBs according to the priority of their highest flow based on latest buffer status information (which may have changed since the buffer status was reported) taking into account the cell load, priority of other UEs data, etc. The block diagram of the I.S. working procedure is shown in Figure 3.8. The pseudo-code for the UE's I.S. is shown in Figure 3.9.

3.5 Sharing Radio Resources Strategy

Nowadays, the networks' resources sharing has been considered to be as an important part of the next-generation networking architectural. The total RBs R set is assumed to be fully pooled and accessible to the MNOs [11, 32]. RBs are assigned in accordance to the following agreement:

1. Each bearer per MNO should receive at least the level of bearer satisfaction (LBS). In

```

1 : For    each simulated TTI    do
2 :     For    j = 1 to NUEs do
           // Available BW allocated for UEj
3 :         avRBSj = nRBj x RBBW
4 :         If    avRBSj > 0 Then
           // phase i: mapping RBs for traffic i (Priority-i)
5 :             For    i = 1 to Ncl do
6 :                 If    avRBSj > 0 Then
7 :                     If    Vij ≤ avRBSj Then
           // Mapped traffic i BW (in bits) for UEj
8 :                         Uij = Vij
9 :                         Vij = 0
10:                    Else
11:                        Uij = avRBSj
           // Buffer size at definite TTI
12:                        Vij* = Vij - avRBSj
13:                        avRBSj* = avRBSj - Uij
14:                    End If
15:                End If
16:            End For
17:        End If
18:    End For
19: End For // End of Simulation

```

Figure 3.9: The pseudo-code for the UE's internal scheduler.

this case, the LBS is typically defined in terms of throughput, jitter, minimum delay, or a combination of two or more of them. This condition ensures isolation among users, and between MNOs on the bearer-level. And Also, it protects their LBS from other MNOs traffic fluctuations.

2. MNOs should be able to perform their own preferred scheduling algorithms to achieve their SLA. MNOs have various QoS requirements to satisfy their own billing and charging models. To meet each MNO's SLA while maximizing their revenues, MNOs can apply various scheduling algorithms.

Now, let's considered the system modeling using the two MNOs, and with resources sharing. The MNOs share R radio RBs in a single eNB as seen in Figure 3.10. The shared radio access network connects MNOs, and manages the radio resources allocation between them according to the MNOs sharing agreement conditions.

And as mentioned before that; each MNO owns a set of RBs $\{R_i\}$ such that

$$R_i \cap R_j = \emptyset, \text{ and } R = R_i \cup R_j. \quad (3.9)$$

Here, another parameter which is the blocking rate (B_r) should be defined, that is the ratio between the number of blocked requests and the total number of requests in long interval simulation time TTI. For example, consider two MNOs with 10 RBs each, and TTI for 3 frames with RBs allocation per frame (10 ms), as in Figure 3.11.

From Figure 3.11, and considering non sharing resources scenario, B_r can be calculated as $3/57 \approx 5\%$, but in case of resources sharing, B_r is calculated to be $1/57 \approx 1.7\%$ since there is only 1 blocked request in the third frame (considering 100 weight of sharing between MNOs), also the gain which is how much free RBs used to cover MNOs request in the TTI per frame, is calculated to be $(2/57)/3 \approx 1.2\%$ per frame. Later on, the weight of sharing between MNOs will be illustrated.

And in addition for the previous considerations, it is assumed that each bearer per MNO

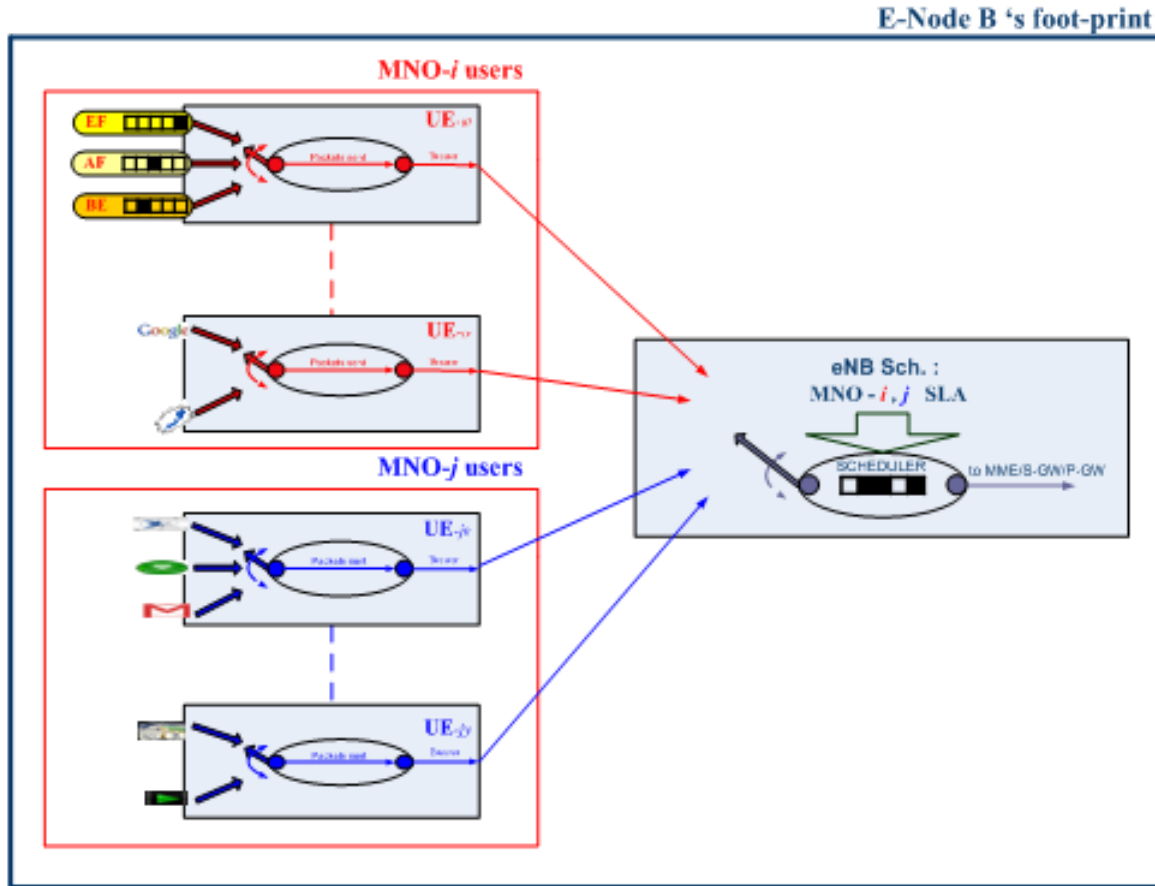


Figure 3.10: MNOs, achieving different schedulers policy, and sharing radio RBs in a single eNB.

MNO	Frame #1	Frame #2	Frame #3
MNO-1	request 8 RBs (2 RBs free)	request 11 RBs (1 RBs blocked)	request 9 RBs (1 RBs free)
MNO-2	request 9 RBs (1 RBs free)	request 8 RBs (2 RBs free)	request 12 RBs (2 RBs blocked)



Figure 3.11: Two MNOs with 10 RBs each, and TTI for 3 frames scenario.

should receive at least the LBS, which it would otherwise receive in the case of a non-RB sharing scenario. For example, when one of the MNO has a high traffic load, the other MNO bearers still receive LBS that is the same as in the case of a non-RB sharing scenario.

MNOs can share an eNB, allowing MNOs to customize their scheduling, taking into consideration the importance of satisfying the user SLA per MNO, minimizing energy consumed per user, and applying scheduling policy per users and traffic classes. This resources sharing can help deliver various benefits as:

1. Sharing the high-cost mobile network hardware deployment among multiple MNOs reduces the operating expenditure (OPEX) and capital expenditure (CAPEX), as sharing can save as much as 60 billion over a period of 5 years worldwide [11, 32, 59].
2. Networks sharing of one common infrastructure between multiple MNOs would reduce the network physical components (for example antenna masts) which minimizes their environmental impact leading to potential energy savings.
3. Facilitating a new business models in the wireless market (For example, operators without LTE licenses, spectrum, or network resources would be able to provide LTE services by renting parts of the LTE radio resources from the MNOs).
4. Efficient utilization of the existing radio resources.
5. Introducing the multi-MNOs multiplexing gain that would support higher peak rates owing to radio resource aggregation.
6. Facilitates a new business models, and contributes to better resource utilization.

The scheduling algorithm that aims to maximize the total aggregate utility. The scheduler objective is to optimally allocate RBs to each bearer such that the total bearer utilities are maximized. It is considered that, each bearer is associated with a utility function. Also, I assume all utility functions are linear. Let the utility function of bearer m be U_m . If bearer m is assigned the RB r , the bearer utility is U_m . At every TTI, the optimization problem can be expressed as:

$$\max \sum_{r=1}^R \left(\sum_{m=1}^M U_m(r) \beta_{m,r} \right) \quad (3.10)$$

subject to:

$$\sum_{m=1}^M \beta_{m,r} \leq 1, \quad \forall r \in R \quad (3.11)$$

where, $\beta(m, r)$ is a binary number indicator that is equal to 1 if the RB r is assigned to bearer m , and 0 otherwise.

A framework of sharing resources of network consolidation in the context is proposed, where MNOs have different spectrum band licenses. MNOs combine their spectrum bands on a single physical eNB. The optimization problem in Equation (3.10) can be modified to be:

$$\max \sum_{r=1}^R \left(\sum_{m=1}^M U'_m(r) \beta_{m,r} \right) \quad (3.12)$$

subject to:

$$\sum_{m=1}^M \beta_{m,r} \leq 1, \forall r \in R \quad (3.13)$$

where, $U'_m = w \times U_m$ if $m \in M_1$ and $U'_m = U_m$ if $m \in M_2$, w is defined to be the weight of sharing in resources such that $0 \leq w \leq 1$, for example, if $w = 0$, this implies that there is no sharing in resources between MNO-1, and -2, while if $w = 1$, this makes 100 % sharing in MNOs resources.

$$s(r, m) = \arg \max_{i \in M} U_i^i, \quad (3.14)$$

where, $s(r, m)$ represents RB r to be assigned to bearer m , that is much higher than non-sharing by factor w .

3.6 Simulation Results

Detailed simulation studies are conducted in order to test the performance of the proposed protocol. The scheme is tested using a discrete event simulator developed in MATLAB [65], and the key simulation parameters are summarized in Table I. To emulate the self-similar characteristics of AF and BE traffic, self-similar traffic models for all UEs are generated.

Furthermore, in order to overcome the extreme uncertainty of self-similar traces and simulate conclusive results, the outputs of multiple iterative simulation runs are averaged for each result. Thus, all results are averaged over 10^4 Monte-carlotrails of fading channels. Noting

Table 3.3: Simulation default Parameters.

Parameter	Value	Parameter	Value
UEs/MNO-1 (M_1)	2 (UE-1, 2)	UEs/MNO-2 (M_2)	2 (UE-3, 4)
RBs/MNO-1	10	RBs/MNO-2	10
MNO-1 scheduler	S.P.	MNO-2 scheduler	LWDF
Fading	Rayleigh	Simulation time	80 s
$SNR_f(UE - 1, 3)$	10 dB	$SNR_h(UE - 2, 4)$	15 dB
δ	0.1	P	27 dBm
Channel Estimation	Perfect dB	σ^2	1 dB

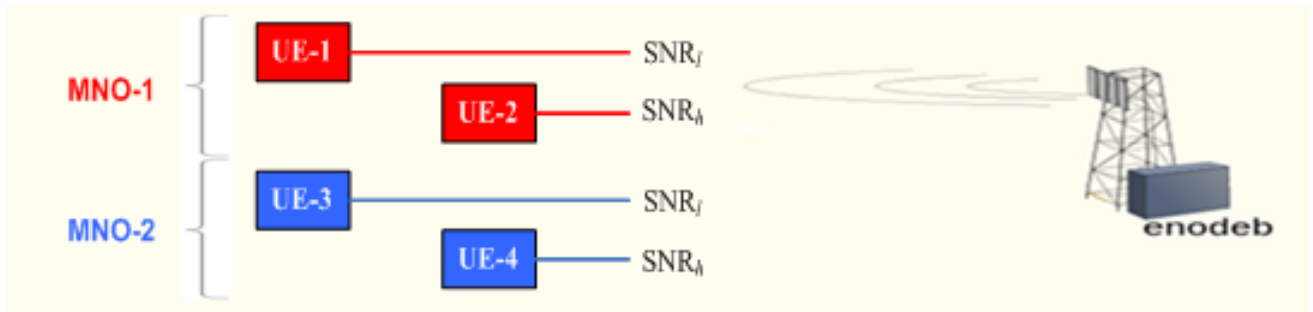


Figure 3.12: UEs per MNOs are distributed as near and far user from the eNB.

that, these classes are extended from the Application class that provides methods and parameters common to all of them, such as starting/stopping time instants. The simulation default parameters are shown in Table 3.3.

It is considered two users for each MNO, one UE is close to eNB and has average SNR of SNR_h dB, while the other UE is far from the eNB and has average SNR of SNR_f as shown in Figure 3.12. Also, it is considered that each user has only one bearer.

To simplify the simulations, it is also assumed that the total network load is evenly distributed amongst all UEs (the UEs are equally weighted). Figure 3.13 compares the throughput between the S.P. and LWDF schedulers, that shows throughput improvement in LWDF over S.P. scheduler; while Figure 3.14 shows the average packet delay for different traffic classes among the 2 MNOs. The delay of the AF class is noticed to be higher than BE within the first active 15 UEs, that is because of the higher arrival rate, but over 15 UEs, it starts to proceed as the AF has an over priority on the BE traffic class. Moreover, EF traffic in MNO-2 cannot

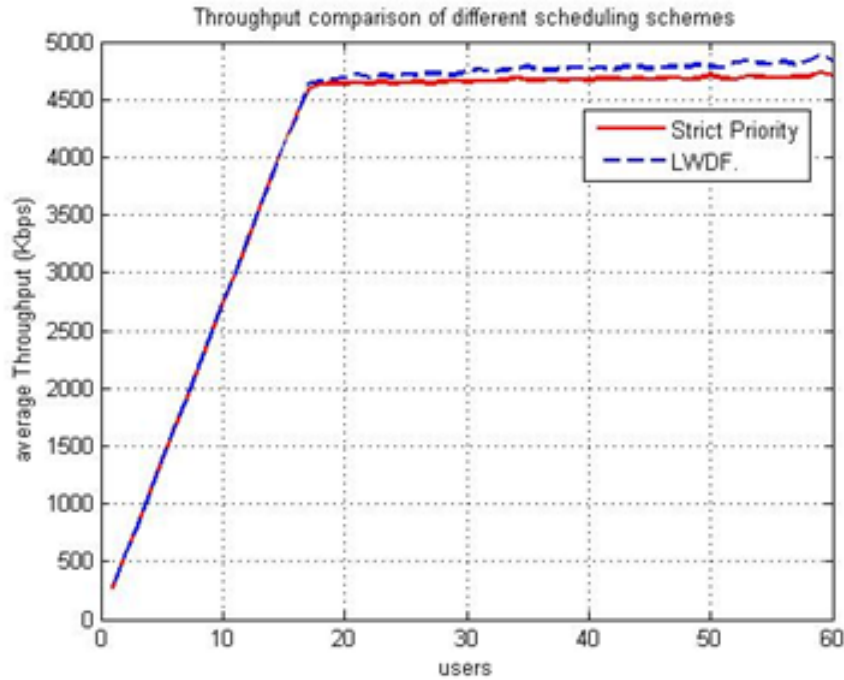


Figure 3.13: The throughput comparison of the S.P. and LWDF schedulers.

support over 18 UEs as it will not satisfy its QoS, which could be handled by MNO-1 that can go over 60 UEs as it has strict priority to EF traffic class.

However, users with the same channel quality are treated differently. This is because the MNOs apply different scheduling policies. As a result, the proposed scheme allows MNOs to run a custom bearer scheduler on the same eNB. To reiterate, user-1 and user-3 have the same low channel quality (SNR_l), and user-2 and user-4 have the same high channel quality (SNR_h). In Figure 3.15, the average packet delay per different traffic classes for MNOs -1, and -2 in the case of a non-sharing scheme.

3.6.1 Case Study and Results Analysis

It is considered that according to the SLA there is only a fair weight of sharing between the MNOs. For example, if $w=0.7$, this means that each MNO is sharing 70% of its resources with the other MNO. Then, in the considered example, each MNO is allowing 7 from its 10 RBs,

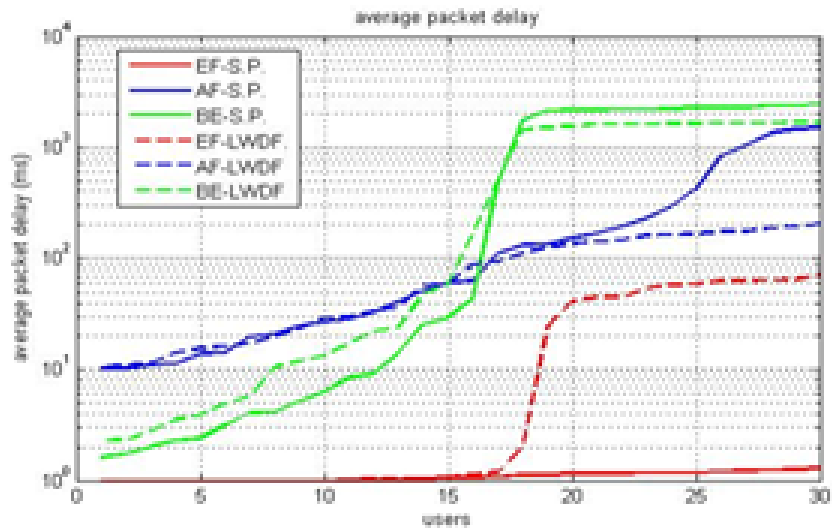


Figure 3.14: The average packet delay for different traffic classes with the S.P. and LWDF schedulers.

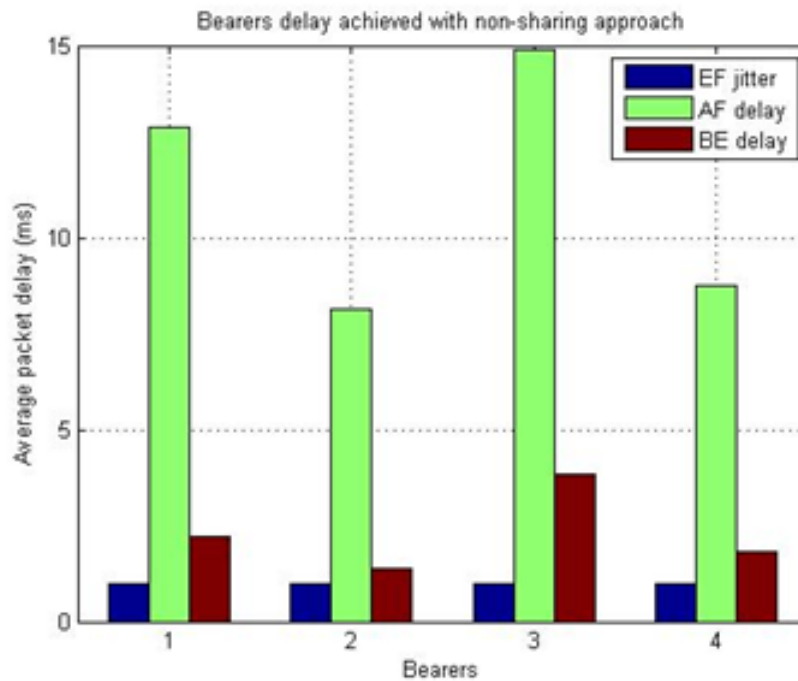


Figure 3.15: The average packet delay per different traffic classes for MNOs -1, and -2 with non-sharing scenario.

and then each MNO can use 17 RBs among its two users (depending on how much RBs are free in the MNO).

Figure 3.16 shows another assumption, considering the SLA between two MNOs is with different weight of sharing resources per each. That might happen among MNO with varied budgets sharing the same eNB. The considered model assumes that the weight of sharing resources for MNO-1 $w_1 = 0.2$, that means that 2/10 from the RB1 (10 RBs) are allowed to be shared for MNO-2; similarly, the weight of sharing resources for MNO-2 $w_2 = 0.4$, that means that 4/10 from the RB2 (10 RBs) are allowed to be shared for MNO-1; hereby, MNO-1 can use 14 RBs, and MNO-2 can use 12 RBs among there users.

Figure 3.17 shows another example for the previous concept; where the weight of sharing resources for MNO-1 $w_1 = 0.8$, indicate that 8/10 from RB1 (10 RBs) are allowed to be shared for MNO-2; similarly, the weight of sharing resources for MNO-2 $w_2 = 0.3$, indicate that 3/10 from RB2 (10 RBs) are allowed to be shared for MNO-1; hereby, MNO-1 can use 13 RBs, and MNO-2 can use 18 RBs among there users. Both Figures show how the delay has been improved with the sharing scheme, noting that mostly EF class has 1ms delay which is the minimum delay could be satisfied.

Figures 3.18, and 3.19 show the queue length in the buffer before and after sharing the radio RBs, and how the delay has been improved with the sharing scheme. Hereby; I simulate the results showing how the parameter w affects the sharing between the MNOs. As w increases, the scheduler allocates more resource in favour of MNO-1's users which results in the averaged data rate. The considered model is as described before in Table 3.4, and 3.5; But here the sharing is varied by 10 each time of simulation, starting from 0 sharing till it reach 100.

Figures 3.20, and 3.21 present the average AF, and BE packets' delay variation with respect to different weight definitions, that clarify the effect of the weight of sharing on transmission time enhancement. The comparison can be seen between SPs (as they are performing with different schedulers' algorithm) or between UEs (within the same SP).

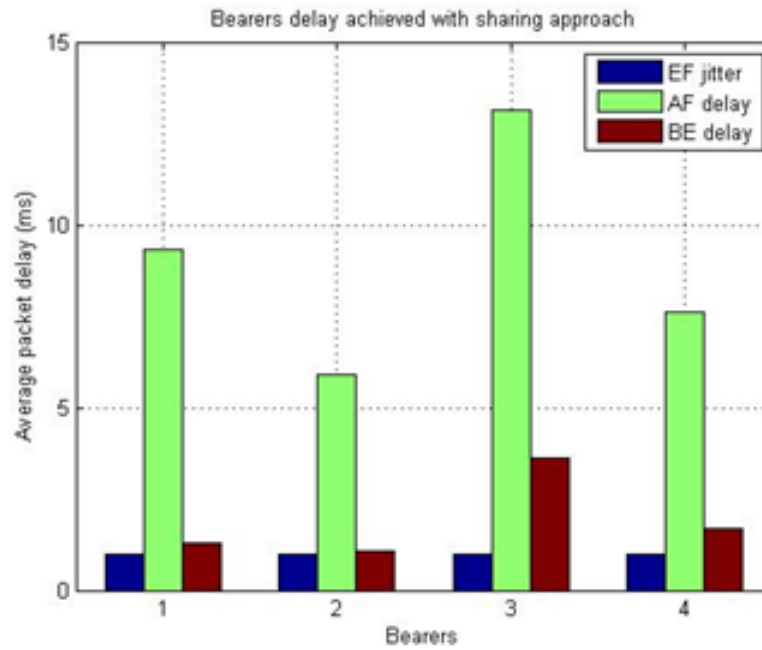


Figure 3.16: Average packet delay with sharing scenario ($w_1 = 0.2$, RB1 = 14, and $w_2 = 0.4$, RB2 = 12).

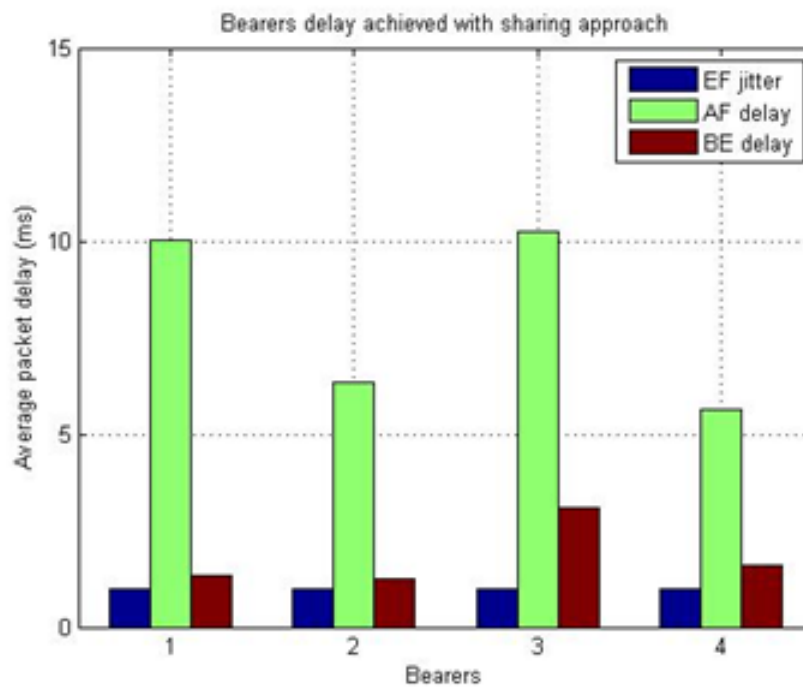


Figure 3.17: Average packet delay with sharing scenario ($w_1 = 0.8$, RB1 = 13, and $w_2 = 0.3$, RB2 = 18).

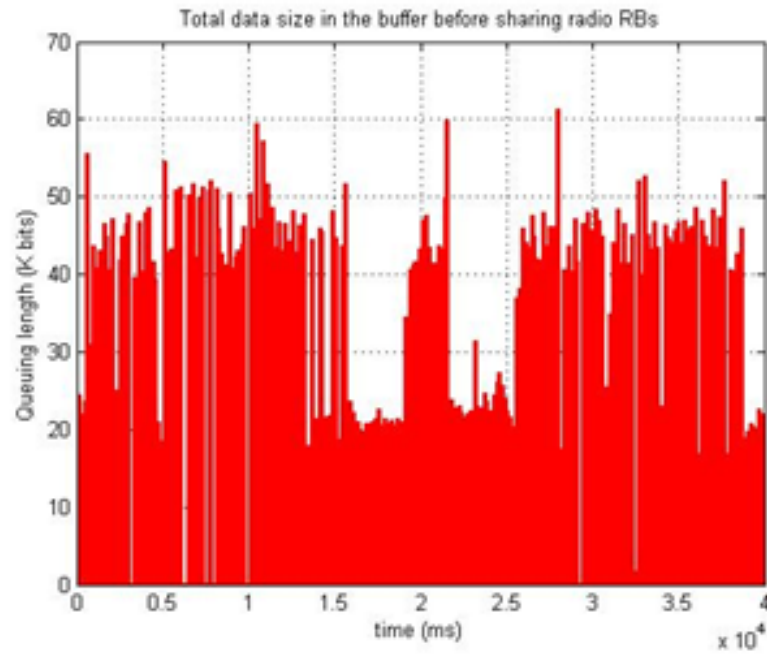


Figure 3.18: Queue length in the UE-1's buffer before sharing radio RBs.

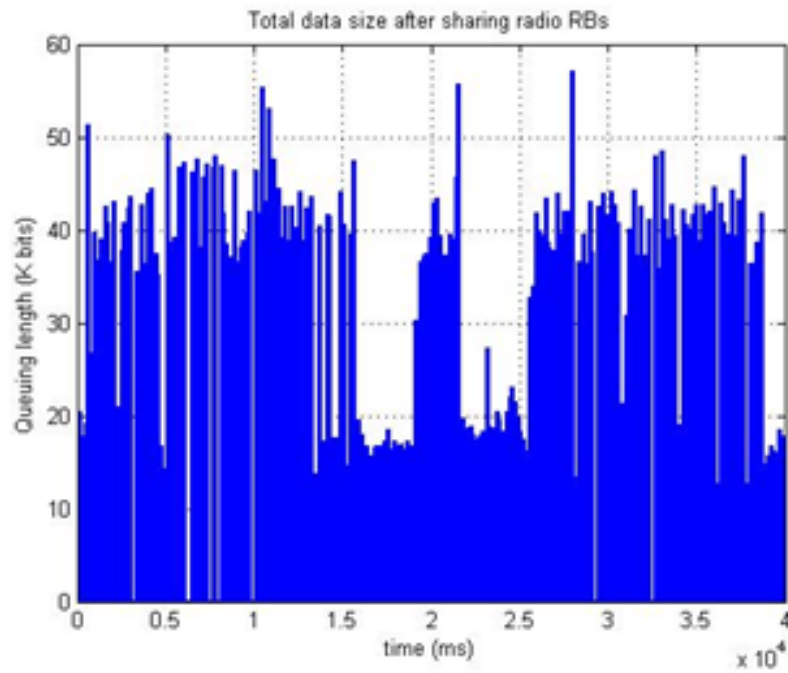


Figure 3.19: Queue length in the UE-1's buffer after sharing radio RBs.

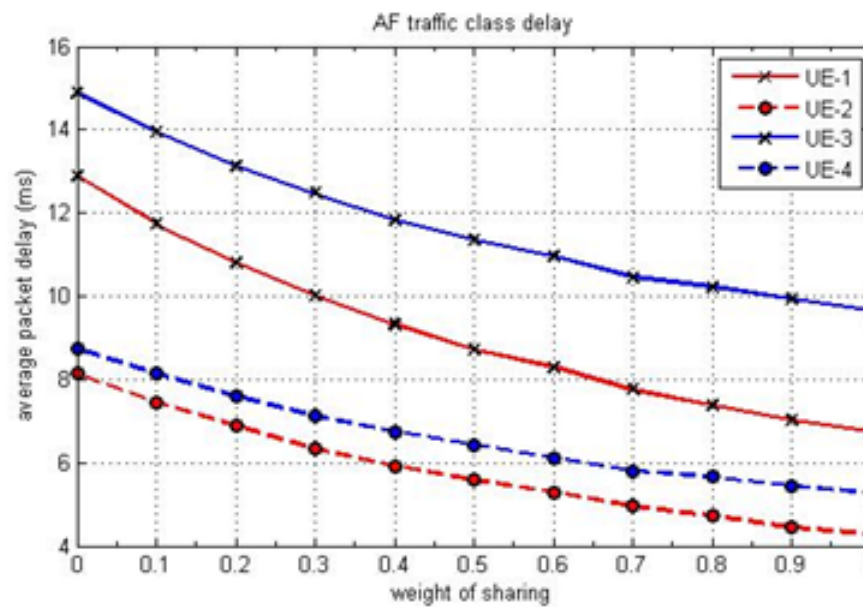


Figure 3.20: Average AF packet delay with respect to variation of weight of sharing.

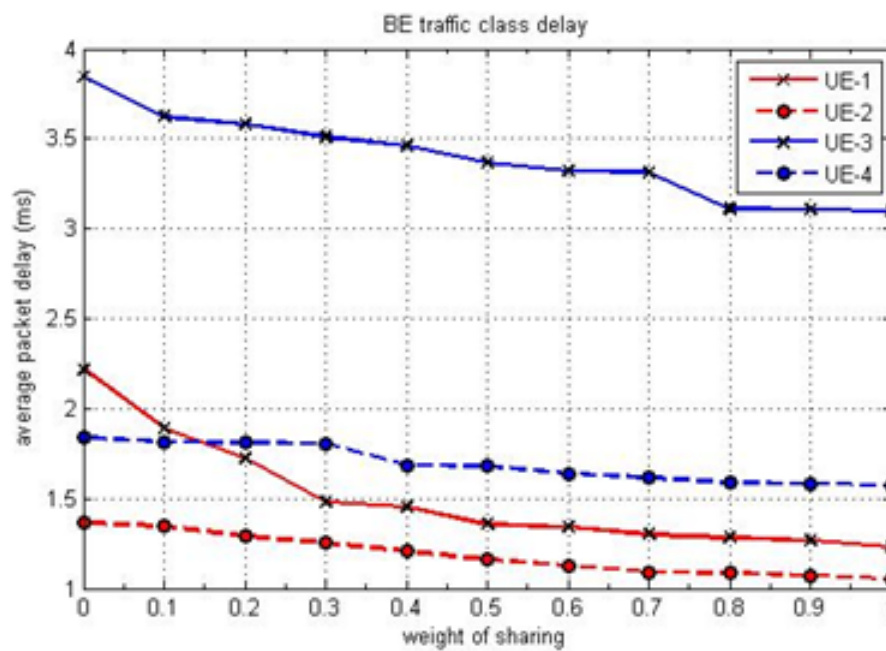


Figure 3.21: Average BE packet delay with respect to variation of weight of sharing.

Table 3.4: Groups' map.

Group	# Users	MNO	Average SNR
Group-1	10	MNO-1	SNR_l
Group-2	10	MNO-1	SNR_h
Group-3	10	MNO-2	SNR_l
Group-4	10	MNO-2	SNR_h

3.6.2 Larger Scale Scenario

As an extension for the previous results, the sharing approach performance for a larger scale scenario is presented here, where each MNO has 20 users grouped into four groups as seen in Table 3.4. The same simulation parameters are chosen as in the previous section.

The result for the large scale scenario is similar to that for the small scale scenario. Different groups with equal average SNR are treated differently as a result of different customized schedulers for different MNOs. Interestingly, the MNOs have the same number of users, number of RBs, average channel SNRs. Figure 3.22 shows the average packet delay per different traffic classes for MNOs -1, and -2 in case of non-sharing scenario, while Figures 3.23 and 3.24 show the average packet delay per different traffic classes for the sharing scenario with various weights.

3.7 Virtualization and Resources Sharing in Two-Tier Cellular Networks

Enhancement of QoSs parameters is a challenging requirement in the Fifth Generation (5G) networks. Delay sensitive applications such as voice traffic, online gaming, and live video are easily affected especially in high data traffic with limited available resources. In this Section, I aim to enhance the delay performance of such applications by utilizing the extra resources available in two-tier cellular network architecture with macro- and micro-cells. Virtualization

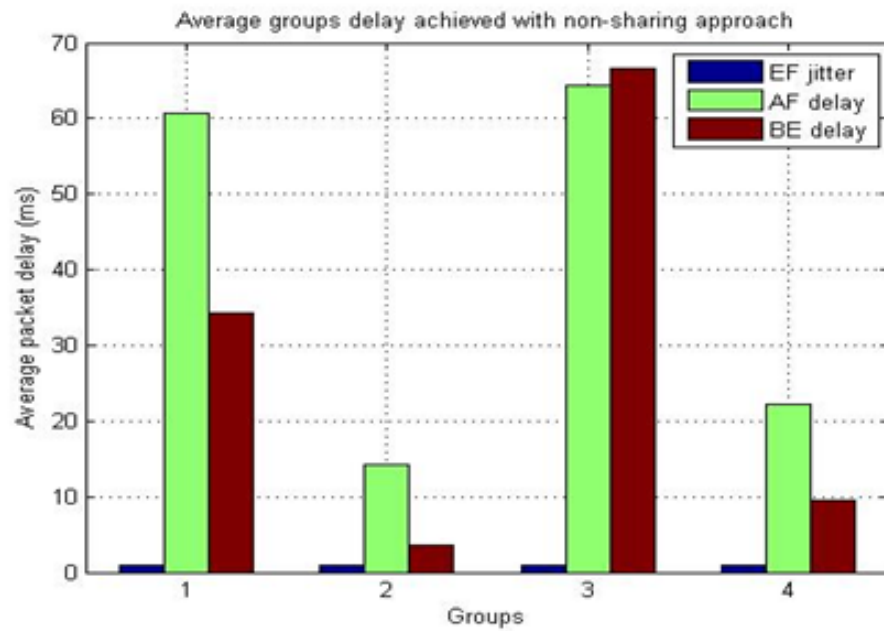


Figure 3.22: Average packet delay per different traffic classes for MNOs -1, and -2.

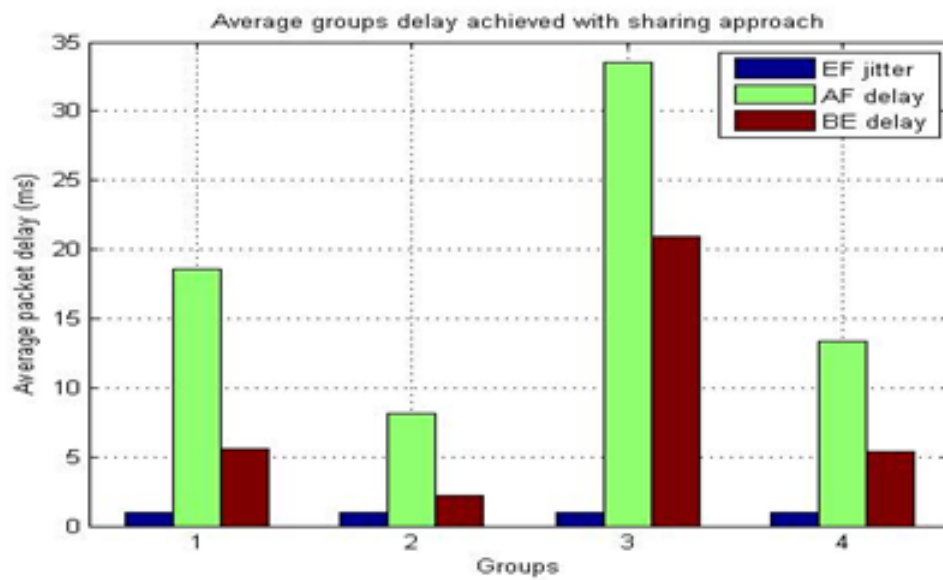


Figure 3.23: Average packet delay with sharing scenario ($w_1 = 0.2$, and $w_2 = 0.4$).

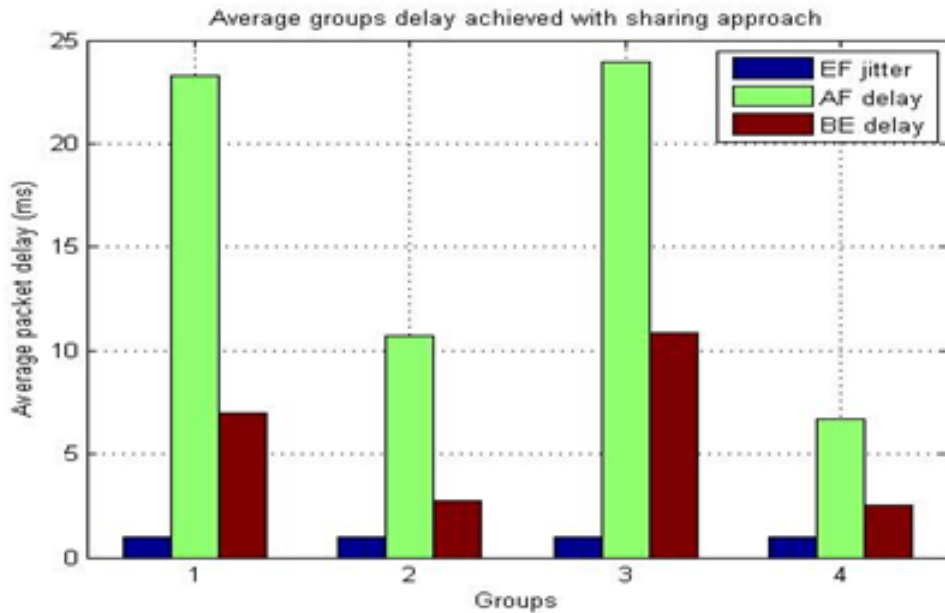


Figure 3.24: Average packet delay with sharing scenario ($w_1 = 0.8$, and $w_2 = 0.3$).

is considered by allowing users belonging to the macro-cell to be allocated resources of the micro-cell when located in the micro-cell range. The average delays for various traffic types are evaluated to verify the framework's performance effectiveness before and after resources sharing scenario. Simulation results show that the proposed framework considerably reduces UE's average delay when compared with the non-sharing scheme.

3.7.1 Recent Relevant Research Work

A solution to meet the increase mobile data demand is the deployment of two-tier networks. Such networks comprise of a regular cellular network overlaid with shorter range hotspots such as micro-cells and offer an economically efficient solution to increase cellular system capacity [66].

Moreover, two-tier networks can also increase spectrum efficiency due to the ability to reuse frequency spectrum assigned to macro-cells using a universal frequency reuse fashion [67]. However, cross-tier interference needs to be maintained below a specific threshold to ensure QoS parameters are satisfied in both tiers. This can be overcome by employing different

frequency spectrum in the tiers and using 2 radio frequency (RF) antennas in UEs.

Several works in recent literature tackled the issue of resource allocation in two-tier networks [66, 67, 68, 69, 70, 71]. Chandrasekhar *et al.* presented an optimal decentralized spectrum allocation policy for two-tier networks that employ OFDMA subject to a sensible QoS requirement in [66]. Also in [68], Li *et al.* proposed an efficient resource allocation scheme that includes the macro eNBs adopting soft frequency reuse strategy to mitigate cross-tier interference while guaranteeing a minimum data rate for UEs of both networks.

On the other hand, Abdelnasser *et al.* suggest a hierarchical interference management scheme based on joint clustering and resource allocation for femtocells in [67]. They formulate the problem as a mixed integer non-linear problem (MINLP) that is solved by dividing it into two sub-problems. Furthermore, Chen *et al.* study the resource allocation problem in two-tier networks in the DL scenario [71]. The problem is formulated as an MINLP that aims to maximize the capacity of the clustered femtocell network subject to delay constraints of flows with different priorities. The problem is solved by applying stochastic network calculus to transform the delay constraints into alternative minimum capacity requirements [71].

A game-based approach for cell selection and resource allocation in two-tier networks is presented by Gao *et al.* in [69] in which an inter-cell game is performed to optimally choose the cell which an intra-cell game is performed to allocate resources. Marshoud *et al.* propose a genetic algorithm to perform joint power and resource allocation in [70]. The proposed algorithm maximizes the overall system throughput and determines the appropriate serving base station as well as the power and bandwidth allocated to each user.

3.7.2 System Model

Consider a DL scenario, wherein, a two-tier cellular network is deployed as shown in Figure 3.25. Denote the macro-cell SP by SP_M and the micro-cell SP by SP_m . Each SP is assumed to serve active UEs, where UE_M refers to UEs in SP_M , and UE_m refers to UEs in SP_m . Both SPs' eNBs employ different scheduling policies.

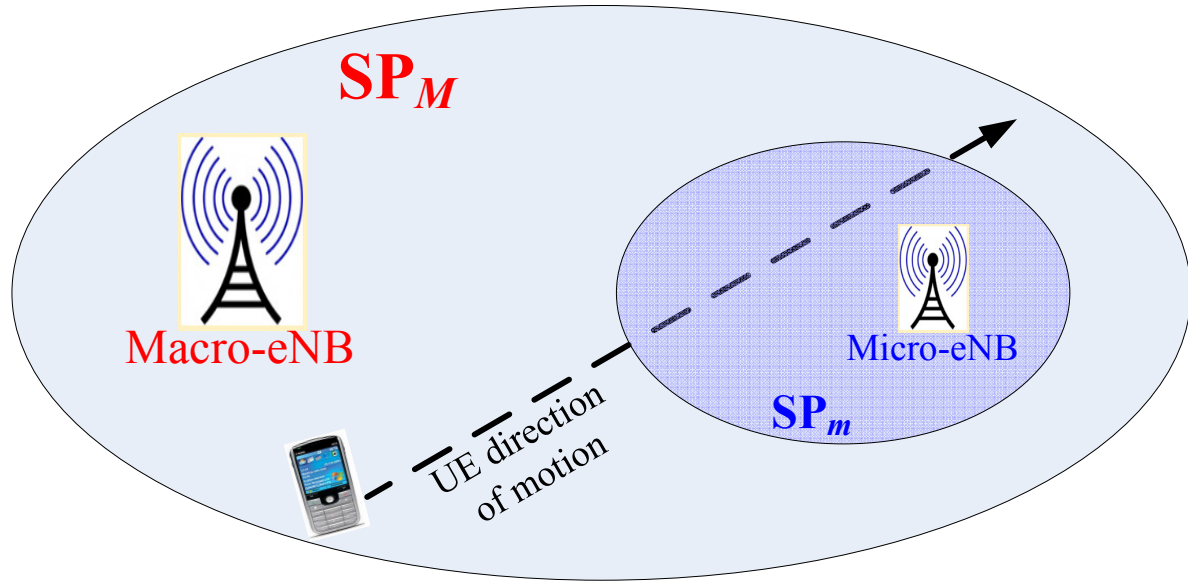


Figure 3.25: Two-tier cellular network topology.

Each SP has access to a number of channels (available RBs). Denote K_M to be the total number of available RBs in SP_M , and K_m to be the total number of available RBs in SP_m . Communications and data exchange between SP_M and SP_m eNBs is assumed using X2 interface, and that the MME and S-GW are unchanged.

Semi-Soft Allocation Technique

The message sequence for RBs allocation for UE_M before, during and after cutting SP_m area of coverage is shown in Figure 3.26 The radio resources control (RRC) is considered between UE_M and SP_M . The UL/DL between the UE, SP_M 's eNB, and the core network, specifically with the S-GW, is also assumed.

The core network (specifically MME) detects the UE location. During the passage of UE_M in the micro-eNB's footprint, UE_M performs RRC configuration and synchronization with the micro-eNB, while the UL/DL is performed through both macro- and micro-eNBs using different RF transceiver modules due to LTE being an OFDM-based system. When UE_M reaches SP_m 's end, the core network (MME) detects the left of UE_M and RRC connection is re-established between UE_M and SP_M .

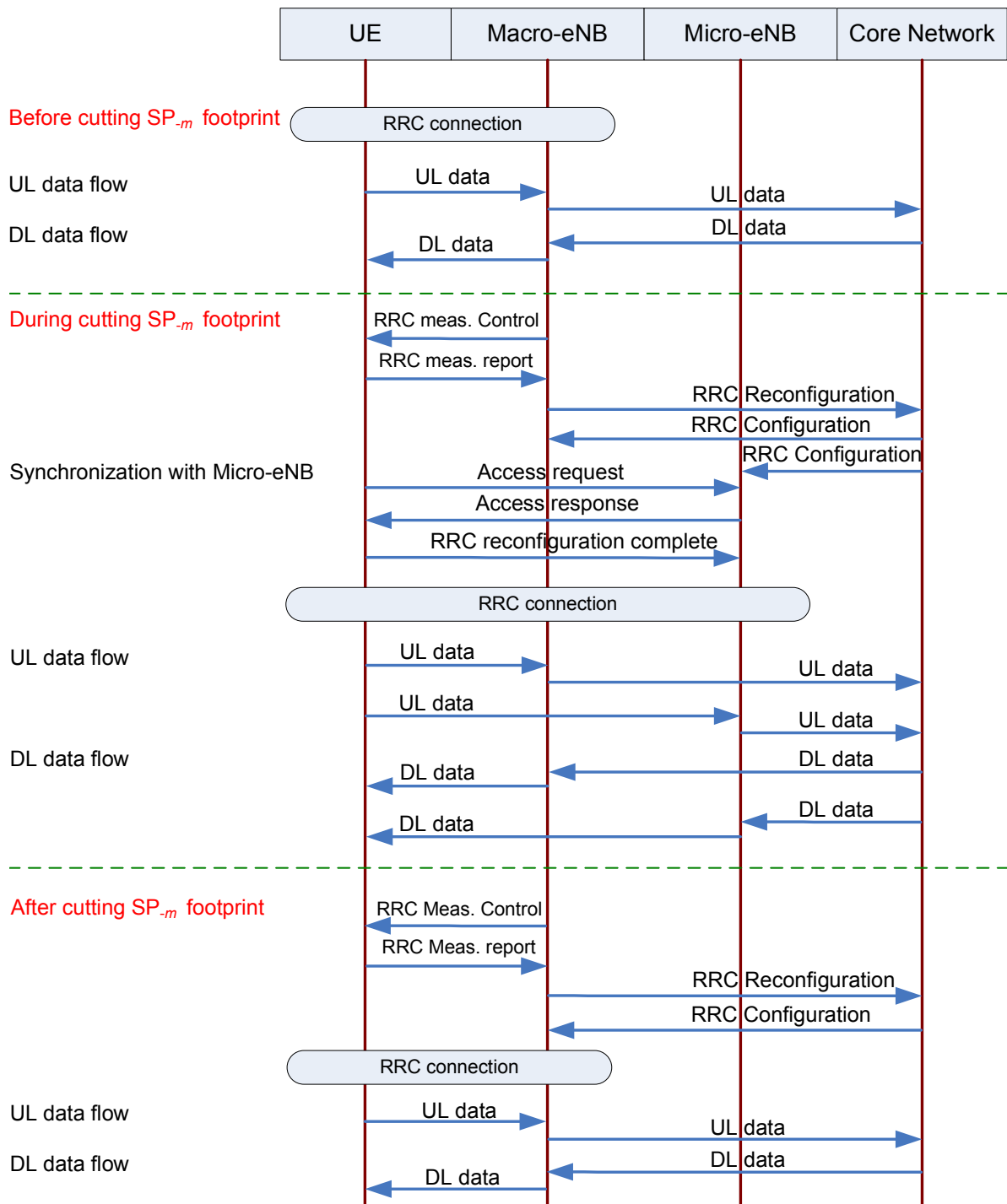


Figure 3.26: Allocation message sequence between the two-tier cellular networks.

To foster customizable schedulers in the evolution, SPs with different utility functions (Ut) are considered. In what follows, the presented framework is for 2 SPs: SP_M is applying S.P. scheduling. On the other hand, SP_m is applying LWDF scheduling, while distributing the allocated RBs among traffic classes' queues is performed by the UE's I.S. according to the priority of their highest flow [11].

The total set of RBs is assumed to be fully pooled. Each SP owns a set of RBs $\{K\}$ with no intersection between the different SPs' RBs, such that:

$$K_M \cap K_m = \phi \quad (3.15)$$

In this work, two scenarios are considered: non-sharing and virtualized sharing radio resources schemes. In non-sharing scheme, SPs allocate their available RBs to their active UEs performing their own scheduling policies, while in the virtualized sharing scheme, SP_m can allocate its available un-allocated RBs (K_m) to UE_M located in its area of coverage and still connected to SP_M due to their speed recognition.

Non-sharing Allocation Scenario

In this algorithm, each SP performs its scheduling individually. The resource allocation problem can be expressed as:

$$\max_t \sum_{i=1,2} \sum_{j=1}^{UE_i} \sum_{r \in k} Ut_{j,r}(t) \psi_{j,r}(t) \quad (3.16a)$$

subject to

$$\sum_{i=1,2} \sum_{j=1}^{UE_i} \sum_{r \in k} \psi_{j,r}(t) = 1, \forall t, k \in K_i \quad (3.16b)$$

$$\psi_{j,r}(t) \in \{0, 1\}, \forall j, r, t \quad (3.16c)$$

Equation (3.16a) represents the objective function that aims to maximize the overall Ut function for all UEs, where Ut and ψ are the decision variables. $Ut_{j,r}$ is the utility function of UE_j assigned by the set of RBs k , and $\psi_{j,k}$ is a binary indicator used to denote whether the UE_j

is assigned by the set of RBs k or not. i refers to the SP, where $i = 1$ denotes SP_M , while $i = 2$ denotes SP_m . Equation (3.16b) represents the exclusive allocation constraint [12], that ensures that at a definite time t , only this set of RBs k is assigned to UE j . Equation (3.16c) shows the bounded values for the binary indicator $\psi_{j,r}$ that is equal 1 if RB r is assigned to UE j and equal 0 otherwise.

Virtualized Sharing Allocation

A virtualized sharing scheme is considered and could be achieved by UE_M ; wherein, the total RBs K_{tot} (K_M + un-allocated RBs in K_m) set is assumed to be accessible to the SP_M . The resource allocation problem can be expressed as:

$$\max \sum_{t=1}^{UE_M} \sum_{j=1}^{UE_M} \sum_{r \in k} U t_{j,r}(t) \psi_{j,r}(t) \quad (3.17a)$$

subject to

$$\sum_{j=1}^{UE_M} \sum_{r \in k} \psi_{j,r}(t) = 1, \forall t, k \in K_{tot} \quad (3.17b)$$

$$\psi_{j,r}(t) \in \{0, 1\}, \forall j, r, t \quad (3.17c)$$

Similarly, Equation (3.17a) represents the objective function. $\psi_{j,r}$ is a binary indicator used to denote whether the UE_j is assigned the set of RBs k or not. Equation (3.17b) represent the exclusive allocation constraint. While, Equation (3.17c) shows the bounded values for the binary indicator $\psi_{j,r}$.

3.7.3 Simulation Results

The scheme is tested using a discrete event simulator developed in MATLAB. The outcomes of multi-repeated simulation runs are averaged for each result. Table 3.5 summarizes the list of simulation parameters and their default values.

All UEs are processing EF traffic with rate 4 Kbit/s, and non-EF (AF, and BE) traffic with

Table 3.5: Simulation Default Parameters and Values.

Parameter	Value
Spectrum allocation (UL, DL)	20 MHz
Number of subcarriers per RB	12 subcarriers
Neighboring subcarrier spacing	15 KHz
RB bandwidth	180 KHz
Macrocell radius	5 Km
Microcell radius	1 Km
UEs/RBs in SP_M (macrocell)	1 UE/1 RB
UEs/RBs in SP_m (microcell)	2 UEs/3 RBs
SP_M scheduler	S.P. scheduling algorithm
SP_m scheduler	LWDF scheduling algorithm
Channel fading	Rayleigh
Iteration #	1e4
SP_M eNB Tx power	46 dBm
SP_m eNB Tx power	13 dBm
Fading	Rayleigh
Coherence time	1 ms
Simulation time	80 s
Cells interference	Avoidance

rate 268 Kbit/s. UE_M is assumed to be moving with a constant speed of 60 Km/hr, and is cutting a distance of 400 m chord in SP_m 's footprint. In this scenario, I consider UE_M can be allocated with RBs (R_m) if SP_m has free RBs to assign and UE_M is in SP_m 's range of coverage.

Figure 3.27 shows the average packet delay (EF and non-EF traffic) for mobile UE_M versus time. The UE's speed is assumed to be constant over the simulation. The Vir. DS scenario ensures less average delays for EF and non-EF traffic than SS. This is due to UEs having access to a larger number of RBs, and thus they can be allocated better channels.

Noting that, mostly the EF class has 1 ms delay, which is the minimum delay that could be satisfied (mapping time period). As in the sharing resources scheme, the scheduler allocates more resources for the immigrant UE_M . Because of the higher arrival rate, the delay of the non-EF classes is noticed to be higher than EF within the entire network. The simulation results show that the sharing virtualized scheme is capable of achieving some improvements with respect to delay when compared to the non-sharing application.

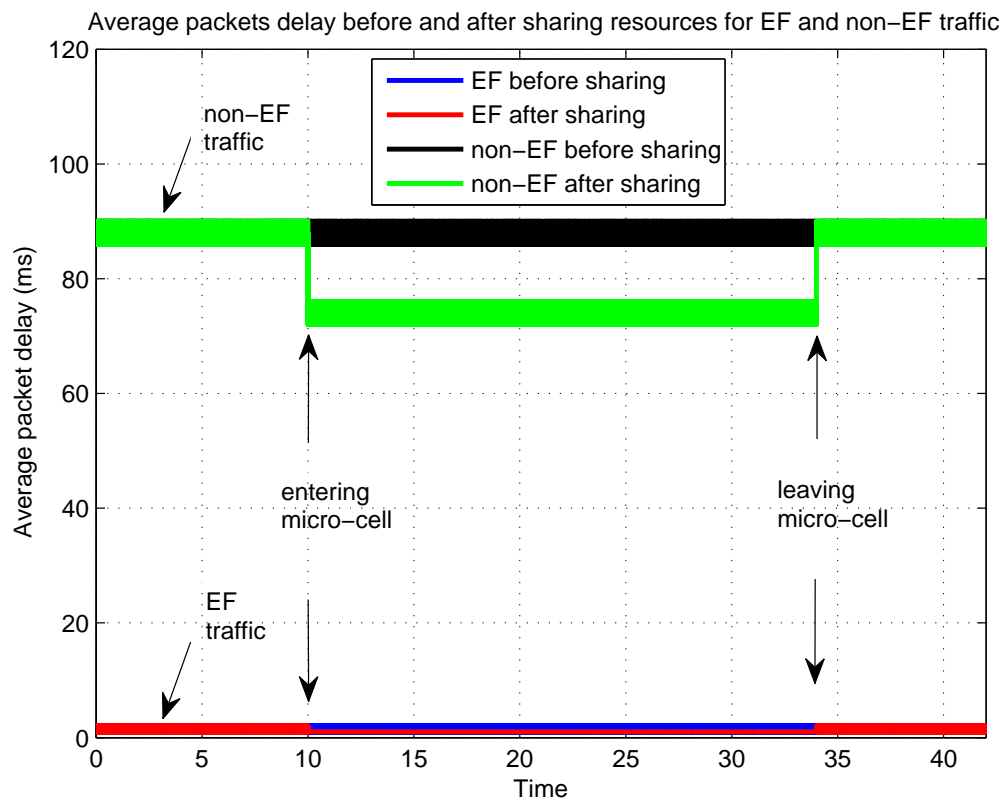


Figure 3.27: The average packets delay (EF and non-EF traffic) for UE_M before, during, and after passing through the micro-cell footprint.

3.8 Chapter Summary

In this Chapter, the framework model is for sharing resources scenario in LTE systems. An overview for the LTE resources allocation, and a comparison between strict priority and LWDF scheduler algorithms strategies in terms of delay and throughput are discussed. I evaluate the average packets jitter and delays for cases of non-sharing and sharing schemes, aiming to enclose the growing gap between the capacities of backbone networks.

From simulation results, it is clear that RBs sharing scheme is capable to achieve much delay improvement as compared to the non-sharing one, allowing MNOs to customize their efforts, schedulers, and control the sharing of multi-MNO resources between them. Overall, the results confirm that sharing framework yields to notable improvements in average packet delay, without degrading QoS support for EF, AF, and BE services. Nonetheless, the performances of AF and BE services are yet to be further improved and QoS to be better delivered.

In the coming chapters, the problem of optimized UL power allocation with different dynamic traffic models, and full resources sharing is consider. Later on, the HO strategy is investigated for various traffic models in a virtualized scheme of sharing SPs' radio resources.

Chapter 4

Efficient Power Allocation in Virtualized 3GPP-LTE Systems

In order to accommodate mobile users' consumed power with the rapid increase of multimedia-rich mobile data, additional network capacities with optimized power allocation scheduling algorithms should be deployed [12, 72]. Motivated by the fundamental requirement of extending the mobile devices' battery utilization time per charge, this work formulates the optimized power allocation problem in a virtualized scheme considered in the 3GPP-LTE UL systems. The proposed framework efficiently shares the eNB's dedicated physical radio RBs of SPs having different requirements under dynamic channel conditions. The target is to reduce the total transmission power for all UEs subject to exclusive and contiguous allocation, maximum transmission power, and rate constraints.

Two algorithms are developed. A BIP-based algorithm is used to solve a simplified version of the problem. A heuristic algorithm is also presented that approaches the BIP-based algorithm's performance. Simulation results show that the proposed framework offers a noticeable transmission power reduction in the virtualized scenario as compared to the non-sharing one.

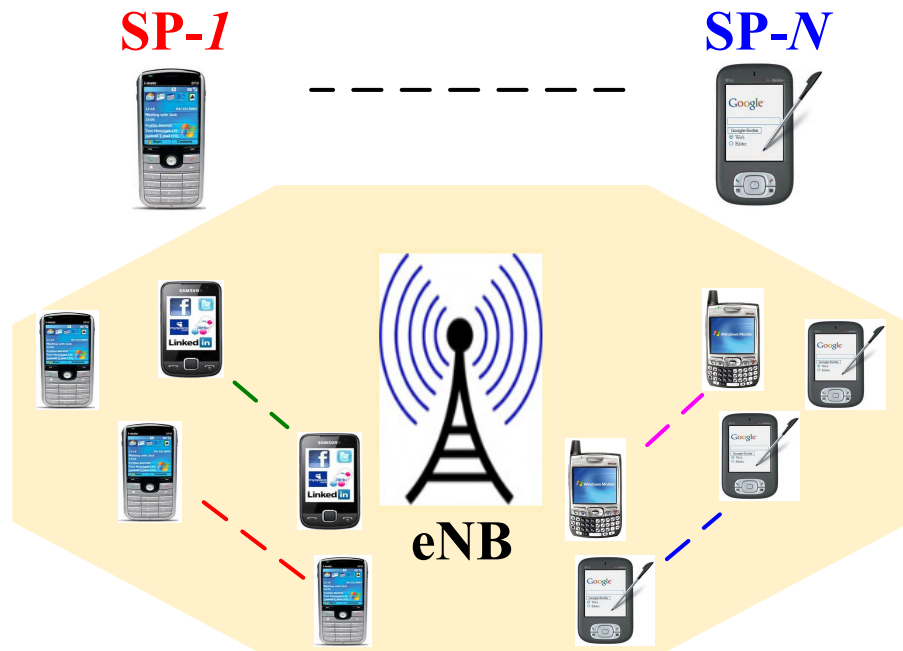


Figure 4.1: UEs from different SPs sharing eNB in a single cell.

4.1 Introduction

Over the years, the growth in data usage per UE has driven an unprecedented increase in UE's power consumption [73]. Moreover, with more demanding user-driven applications, the LTE is expected to reach high data rates, low latency, and packet optimized radio access technology [74, 75, 76]. All of these features directly affect the UE's battery and its lifespan per charge [30].

Most of the previous work [11, 32, 37, 59, 77, 78, 79] focuses on developing scheduling algorithms for the LTE DL transmission. This aims to maximize the total utility of the system in terms of data rate and delay without considering the UE's UL consumed power. In this work, the focus is on finding an optimal solution [80, 81, 82] for resource allocation among users who subscribe to different SPs but are located at the same site (eNB) in UL as shown in Figure 4.1.

The power control entity specifies the UL transmission power for each UE. In order to provide an end-to-end QoS support [83, 84], LTE provides QoS based on each flow's requirements. These flows are organized into logical traffic pipes named bearer services. A set of QoS

Table 4.1: QoS Attributes

QCI	Bearer Type	PDB	PLER	Application
1	GBR	100 ms	10^{-2}	VoIP
2	GBR	150 ms	10^{-3}	Video call
3	GBR	50 ms	10^{-3}	Real time gaming
4	GBR	300 ms	10^{-6}	Buffered streaming
5	non-GBR	100 ms	10^{-6}	IMS signaling
6	non-GBR	300 ms	10^{-6}	Video (buffered streaming)
7	non-GBR	100 ms	10^{-3}	Voice, Video (live streaming)
8	non-GBR	300 ms	10^{-6}	Voice, Video (buffered streaming)

attributes are associated with each bearer (depending on the type of traffic), as shown in Table 4.1.

LTE classifies flows into the QoS class identifier (QCI) [85] which is a scalar number that defines the management of bearer packet transmission, GBR flows for real-time applications and non-GBR flows that are established for non-real-time applications (e.g., buffered video streaming) [25, 86], packet delay budget (PDB) which is the maximum allowable packet delay, and packet loss error rate (PLER) which is the maximum tolerable number of corrupted or lost packets.

The modulation method and multiple access scheme that LTE currently specifies have some disadvantages with regards to power efficiency.

The modulation schemes used in LTE are QPSK, 16QAM and 64QAM [11, 30, 59, 86]. The phase discontinuity in these methods gives rise to out-of-band radiation, which leads to poor power efficiency and higher bandwidth requirement.

LTE has adopted the OFDM based radio interface due to its higher spectral efficiency and resilience against multi-path delay spread (frequency selectivity). In UL transmission, SC-FDMA has been adopted as a transmission technology by the 3GPP community (which enables frequency selective scheduling gains and has the benefit of reduced PAPR) rather than the OFDMA technology used for DL transmission [51].

SC-FDMA's low PAPR allows the power amplifier at the transmitter to operate close to the

saturation point which improves its efficiency. The physical properties of SC-FDMA require that the physical RBs allocated to a single user to be contiguous in frequency.

Power control is a crucial radio network function in cellular systems [30, 77]. It refers to setting output power levels of transmitters, base stations in DL and mobile stations in UL, with an objective to improve system capacity, coverage and user quality, and to reduce power consumption.

In UL, power consumption often acts as a limiting factor to the functionality offered by the mobile devices' batteries. However, batteries' technology is not progressing at the same rate as mobile demand growth and devices' miniaturization. Therefore, there is a primary need to minimize power consumption at UEs as poor power efficiency that leads to shorter battery life.

Also, UL power control has to adapt the radio channel conditions, including path loss, shadowing and fast fading changes. Furthermore, power control has to limit the interference effects from other users within the cell and from neighboring cells.

The orthogonal LTE UL allows multiplexing of terminals with different received UL power within the same cell. However, the high speed data links offered by LTE systems increase the power consumption of the UEs. Thus, it is imperative to develop energy-efficient scheduling algorithms that prolong the UE's battery life per charge.

4.2 Recent Relevant Research Work

In order to assess the current state of the art, the recent approaches to the above energy-optimal problem are reviewed. In general, there are few works found in the literature that attempt to address the above problem directly.

There are however a number of works that focus on addressing subsets of the entire problem. I review these and relevant research here.

Most of the work on power and channel allocation for multi-user multi-channel systems typically focused on OFDMA [77, 87]. In these works, a user can be assigned multiple channels

from any of the available channels by using water filling-based power allocation algorithms. Goodman in [88, 89], proposed the greedy algorithms for the proportional fair scheduling of SC-FDMA systems using utility functions, which is a similar approach to the one proposed in [87] by Song *et al.* for OFDMA proportional fair scheduling. Unfortunately, the proposed algorithms can not guarantee optimality, and does not consider the channel contiguity restriction.

Wong *et al.* in [90] investigated the maximization of the total user-weighted system capacity that depends on maximum allowable transmission and peak power constraint. They used BIP to solve the scheduling problem, disregarding the QoS requirements and the dynamic traffic behavior of UEs.

Dechene and Shami considered power-efficient resource allocation subject to rate and synchronous hybrid automatic repeat request (HARQ) constraints in [91, 92]. The objective was to minimize the weighted sum of the transmission power. Also, the authors assumed fixed data rate to be scheduled every transmission time interval (TTI) without considering maximum power limit constraint. However, practical LTE UL systems limit the maximum transmission power to 23 dBm by Toufik in [21].

In general, MCSs are less power-efficient at higher transmission rates [12]. Thus, transmitting at lower rates with less power can reduce the energy required to transmit the data. However, lower data rates compromise the QoS requirements [93, 94] because that would require to split the data and transmit at lower rates over more subframes to reduce the total transmission power.

The main contribution in this chapter is a novel dynamic scheduling resource sharing algorithm that aims to save power for users in the access network. The objective is to allocate the pooled radio resources to UEs based on the SPs' requirements in high time-frequency resolution that minimizes the total power consumption of the UEs. The framework scheme shares SPs' resources while maintaining different service requirements. The research below offers detailed simulations to study the performance of the considered framework and validate its effectiveness. A BIP-based solution is compared with a heuristic algorithm in terms of transmis-

Table 4.2: Frequently Used Notations

Notation	Definition
C_m	All possible RBs allocation for UE m
$c_{l_{m_n}}$	Column c_l with set of RBs allocated for UE $_{m_n}$
F_t	Finite time length of TTIs
k	RB
K_n	Total number of RBs in SP n
K_{tot}	Total number of RBs in all SPs
m	UE
m_n	UE m in SP n
M_n	Total number of UEs in SP n
M_{tot}	Total number of UEs in all SPs
n	SP
N	Total number of SPs
s	MCS
s_{m_n}	MCS selected for UE $_{m_n}$
S	Total number of MCSs
t	Definite TTI
T_{GBR_n}	GBR specified for any UE in SP n
T_{m_n}	TB of UE m in SP n

sion power and complexity. Simulation results show that the BIP-based algorithm considerably reduces the UE's average transmission power without degrading QoS performance and that the heuristic one achieves comparable performance.

4.3 System Model

Consider a single cell employing SC-FDMA for a multiuser wireless communications, wherein, N SPs share an eNB. The set of SPs is denoted as $\mathcal{N} = \{1, 2, \dots, N\}$. Each SP n is assumed to serve M_n active UEs, where $n \in \mathcal{N}$ and the set $\mathcal{M}_n = \{1, 2, \dots, M_n\}$. Denote UE $_{m_n}$ to be the UE m belonging to SP n . Each SP has access to a number of channels (available RBs), adjacent and located at different frequencies. Denote K_n to be the total number of available RBs in SP n . It is helpful to define some frequently used notations as shown in Table 4.2.

4.3.1 Exclusive and Contiguous Allocation

The main idea of the exclusive and contiguous constraints can be described in the following example. Assume SP n with $K_n = 4$ RBs and $M_n = 2$ UEs. For a particular UE, there are a number of feasible channel allocations available. Here; I denote to a channel allocated to a UE by 1, and 0 otherwise, and form the channel allocation pattern matrix C_{m_n} for UE m_n . The rows of this matrix represent the channel index (RB), and the columns reflect the feasible channel allocation set as follows:

$$C_{m_n} = \begin{bmatrix} 1 & 0 & 0 & 0 & 1 & 0 & 0 & 1 & 0 & 1 \\ 0 & 1 & 0 & 0 & 1 & 1 & 0 & 1 & 1 & 1 \\ 0 & 0 & 1 & 0 & 0 & 1 & 1 & 1 & 1 & 1 \\ 0 & 0 & 0 & 1 & 0 & 0 & 1 & 0 & 1 & 1 \end{bmatrix}, \forall m_n$$

When multiple RBs are assigned to a user (columns 5 to 10), these RBs should be adjacent to each other. Therefore the column $[1 \ 0 \ 1 \ 0]^T$ and its similar non-contiguous allocations are not considered.

To better understand the exclusivity constraint, assume that UE $_{1_n}$ is assigned the best feasible set of RBs found in column 6 (RBs #2 and #3). Then UE $_{2_n}$ in turn has only 2 RBs (RB #1 or #4) to be allocated as follows:

$$C_{2_n} = \begin{bmatrix} 1 & 0 \\ 0 & 0 \\ 0 & 0 \\ 0 & 1 \end{bmatrix}.$$

Thus, the allocation matrix can be represented as $C_{m_n} = [c_1 \ c_2 \ \dots \ c_{L_n}]$ where the total number of columns in C_{m_n} is

$$L_n = \frac{K_n}{2}(K_n + 1) \quad (4.1)$$

Define c_l to be the column containing the selected set of RBs allocated to UE $_{m_n}$, while $\|c_l\|$ is the hamming weight that represents the number of RBs in c_l .

4.3.2 Transmission Block Size

The overall TB size that can be transmitted per subframe over $\|c_l\|$ RBs for UE $_{m_n}$ is given by:

$$T_{m_n, c_l, s}(t) = \lfloor 132 \times \zeta_s(t) \times \|c_l\| \rfloor, \quad (4.2)$$

and thus, the number of RBs can be represented as:

$$\|c_l\| = \frac{T_{m_n, c_l, s} + \epsilon}{132 \zeta_s(t)}, \quad (4.3)$$

where $0 \leq \epsilon < 1$. The received SNR determines the MCS that should be used to deliver TB with a 10% Block Error Rate. The MCS selection scheme is enacted using a lookup table that maps the received SNR to the MCSs [11, 51, 59, 86].

From Figure 3.3, it is clear that transmitting TB over multiple lower level MCSs can be equivalent to transmitting at one higher MCS. Then, I can conclude that the UL transmission power for any UE can be reduced by:

1. increasing the effective SNR by assigning RBs that have less fading [95] (that can not be guaranteed for all TTIs)
2. and/or transmitting TB over longer period of TTIs (more subframes) (but that might affect the GBR traffic and QoS).

4.3.3 Transmission Power Calculation

In SC-FDMA, for adapted continuous-rate with low bit error rate during the t^{th} subframe, an approximation of the instantaneous received effective SNR for an allocated set of RBs c_l for UE m_n over MCS s in TTI t is given by:

$$\gamma_{m_n, c_l, s}(t) = \frac{1}{\|c_l\|} \sum_{j \in c_l} \frac{\sigma_{sig}^2 |h_{m_n, j}(t)|^2 \xi_{m_n}(t) P_{m_n, j, s}(t)}{\sigma_n^2} \quad (4.4)$$

where, $|h_{m_n,j}(t)|$ is the channel frequency response of RB j at TTI t seen by UE $_{m_n}$. The shadowing (long term fading) parameter $\xi_{m_n}(t) = D/d_{m_n}^\alpha(t)$ [96], where D is a normalization constant which accounts for system losses, $d_{m_n}(t)$ is the distance between UE $_{m_n}$ and the eNB at TTI t , and α is the path loss exponent (usually between 2 for open space and 5 for highly built up areas). σ_{sig}^2 and σ_n^2 are the signal and noise variance respectively. Consider $\Omega_{m_n,j}(t)$ to denote $\frac{|h_{m_n,j}(t)|^2 \xi_{m_n}(t)}{\sigma_n^2}$, and $\sigma_{sig}^2 = 1$, then I have

$$\gamma_{m_n,c_l,s}(t) = \frac{1}{\|c_l\|} \sum_{j \in c_l} \Omega_{m_n,j}(t) P_{m_n,j,s}(t) \quad (4.5)$$

To reduce signal overhead, LTE specifies that one power level should be transmitted over the assigned RBs for the same UE [97]. Then it can assumed that $P_{m_n,1} = P_{m_n,2} = \dots = P_{m_n,x} = \dots = P_{m_n,\|c_{l_{m_n}}\|}$. Thus, the total transmission power for the UE $_{m_n,c_l}$ is given by:

$$\sum_{j \in c_l} P_{m_n,j}(t) = \|c_l\| \times P_{m_n,x}(t), \quad \forall x \in c_l \quad (4.6)$$

By substituting in equations (4.4) and (4.5), the UE transmission power can be represented as:

$$\begin{aligned} \sum_{j \in c_l} P_{m_n,j,s}(t) &= \left(\frac{T_{m_n,c_l,s}(t) + \epsilon}{132 \zeta_s(t)} \right)^2 \\ &\cdot \gamma_{m_n,c_l,s}(t) \left(\sum_{j \in c_l} \Omega_{m_n,j}(t) \right)^{-1} \end{aligned} \quad (4.7)$$

4.4 Problem Formulation

The resource allocation in LTE UL requires the following constraints to maintain the physical layer restrictions and the QoS requirements:

1. Power constraint: the LTE standard specifies P_{max} (23 dBm) [30] to be the maximum threshold transmission power that a UE can not exceed.
2. Exclusive allocation constraint: a single RB can only be allocated to one UE at most

within the same TTI to avoid overlapping allocation of available RBs.

3. Contiguous allocation constraint: RBs should be strictly contiguous when multiple RBs are assigned to a single UE.
4. Rate constraint: a minimum GBR must be maintained for all UEs according to each SP's service requirements.

In this work, two scenarios are considered: static sharing (SS) and dynamic sharing (DS) within the efficient power allocation scheduling. In SS, SPs are sharing only the common physical infra-structure eNB without sharing the channels among them; while in DS, the sharing agreement includes the SPs' spectrum. Thus, SPs share their physical RBs (noting that, I consider SPs of adjacent BW spectrum).

4.4.1 Static Sharing Allocation Problem

The radio access network connects multiple SPs and manages the resources allocation between them according to their SLA. Each SP owns a set of RBs K_n with no intersection between the different SPs' RBs, such that:

$$K_n \cap K_v = \phi, \quad \forall n, v \in \mathcal{N} \quad (4.8)$$

The SC-FDMA resource allocation problem involves determining the RB and power allocation that maximizes the total system-utility and minimize the UEs' transmission power, subject to each user's total power constraint.

Assuming an admission control scheme is applied, the resource allocation problem considering SS scenario between SPs can be expressed as:

$$\min \sum_{t=1}^{F_t} \sum_{n=1}^N \sum_{m_n=1}^{M_n} \sum_{j \in c_l} \sum_{s=1}^S P_{m_n, j, s}(t) \psi_{m_n, j, s}(t) \quad (4.9a)$$

subject to

$$\sum_{j \in c_l} P_{m_n, j, s}(t) \leq 23 \text{ dBm}, \forall m_n, s, t \quad (4.9b)$$

$$\frac{1}{F_t} \sum_{t=1}^{F_t} T_{m_n, c_l, s}(t) \geq T_{GBR_n}, \forall m_n \quad (4.9c)$$

$$\sum_{n=1}^N \sum_{m_n=1}^{M_n} \sum_{j \in c_l} \sum_{s=1}^S \psi_{m_n, j, s}(t) = 1, \forall t \quad (4.9d)$$

$$\bigcap_{n=1}^N \bigcap_{m_n=1}^{M_n} c_l \psi_{m_n, j, s}(t) = \phi, \forall j, s, t \quad (4.9e)$$

$$\psi_{m_n, j, s}(t) \in \{0, 1\}, \forall m_n, j, s, t \quad (4.9f)$$

Equation (4.9a) represents the objective function that aims to minimize the overall transmission power for all UEs, where P and ψ are the decision variables. $P_{m_n, c_l, s}$ is the UL transmission power of UE $_{m_n}$ assigned by the set of RBs c_l over MCS s , and $\psi_{m_n, c_l, s}$ is a binary indicator used to denote whether the UE $_{m_n}$ is assigned by the set of RBs $c_{l_{m_n}}$ over MCS s or not.

Equation (4.9b) represents the power constraint as each UE's power can not exceed (P_{max}). $T_{m_n, c_l, s}$ in equation (4.9c) is the TB of UE $_{m_n}$ that assures the rate constraint is satisfied over the finite length F_t of 10 TTIs (10 ms frame). Note that UE $_{m_n}$ has to transmit T_{m_n} bits (target GBR to satisfy the rate constraint). Equation (4.9d) ensures that a UE is allocated only one RB allocation map and uses one MCS.

Equation (4.9e) represents the exclusivity and contiguous allocation constraints. The exclusivity constraint ensures that at most one UE can occupy a given RB during any subframe [77, 97], while the contiguity constraint ensures that RBs for a single transmission are allocated contiguously in frequency for each UE.

4.4.2 Dynamic Sharing Allocation Problem

Assuming an admission control scheme is applied beforehand, the resource allocation problem considering DS scenario between SPs can be expressed as:

$$\min \sum_{t=1}^{F_t} \sum_{m=1}^{M_{tot}} \sum_{j \in c_l} \sum_{s=1}^S P_{m,j,s}(t) \psi_{m,j,s}(t) \quad (4.10a)$$

subject to

$$\sum_{j \in c_l} P_{m,j,s}(t) \leq 23 \text{ dBm}, \forall m, s, t \quad (4.10b)$$

$$\frac{1}{F_t} \sum_{t=1}^{F_t} T_{m,c_l,s}(t) \geq T_{GBR_n}, \forall m \quad (4.10c)$$

$$\sum_{m=1}^{M_{tot}} \sum_{j \in c_l} \sum_{s=1}^S \psi_{m,j,s}(t) = 1, \forall t \quad (4.10d)$$

$$\bigcap_{m=1}^{M_{tot}} c_l \psi_{m,j,s}(t) = \phi, \forall j, s, t \quad (4.10e)$$

$$\psi_{m,j,s}(t) \in \{0, 1\}, \forall m, j, s, t \quad (4.10f)$$

Similar to equation (4.9a), equation (4.10a) represents the objective function that aims to minimize the overall transmission power for all UEs, where P and ψ are the decision variables. $P_{m,c_l,s}$ is the UL transmission power of UE $_{m_n}$ assigned the set of RBs c_l using MCS s , and $\psi_{m,c_l,s}$ is a binary indicator used to denote whether the UE $_{m_n}$ is assigned the set of RBs $c_{l_{m_n}}$ using MCS s or not.

Equation (4.10b) restricts the transmission power of each UE to a maximum of 23 dBm. Similarly, $T_{m,c_l,s}$ in equation (4.11c) is the TB of UE $_m$ that guarantees that the rate constraint is satisfied over the finite length of TTIs time. Note that UE $_m$ has to transmit T_m bits (target GBR to satisfy the rate constraint).

As discussed previously in equations (4.9d) and (4.9e), equation (4.10d) ensures that a UE is allocated only one RB allocation map and uses one MCS while equation (4.10e) represents

the exclusivity and contiguous allocation constraints.

Both problems presented above can not be solved to optimality because they are both dependent on future values that are not available to the eNB. Therefore, the problems need to be simplified in order to solve them.

4.5 Scheduling Framework

Although, it is much desirable to work with the optimal solution for its higher performance, but the computational complexity price in solving encourage us to look for much less complexity algorithms.

To simplify the problems presented in the previous section, a single time slot is considered. Thus, the time index is dropped in both scenarios. In our work, two schemes are considered to solve the problems, a linear BIP based algorithm and a heuristic scheduling algorithm.

4.5.1 The BIP-based Resource Allocation Algorithm

Note that equation (4.9a) forms a combinatorial optimization problem. In order to show how the search space is huge, I first assume that l users are to share the K sub-channels. Due to the sub-channel contiguity constraint, it requires the K sub-channels to be partitioned into exactly l sets, wherein each set has k_l adjacent sub-channels, such that $K = k_1 + \dots + k_l$. To express how complex this is, I assume that the considered case of $K = 24$ subchannels and $M = 10$ users, this would require searching through 5.26×10^{12} possible sub-channel allocations.

This approach indicates reformulating the problem as a pure BIP called the set partitioning problem. A built-in MATLAB function named *bintprog* that performs branch-and-bound search procedure with a linear programming (LP) relaxation per iteration. This problem has the following general form:

$$\min_x c^T x \quad (4.11)$$

subject to

$$A x \leq b, \quad A_{eq} x = b_{eq} \quad (4.12)$$

where c represent the cost $P_{m_n,j,s}$, and x is the binary decision variable that minimize the objective function in equation (4.10a) (represented by $\psi_{m_n,j,s}$). Constraints in equation (4.12) are maintained by linear equality and inequality constrains. Wherein, A and A_{eq} are matrices containing the coefficients of the inequality and equality constraints, while b and b_{eq} are vectors that fulfill these constrains.

The matrices A and A_{eq} are defined as follows. Define the matrix A_{m_n} to be the matrix containing all possible contiguous allocations for all the S different MCSs. Thus, it can be expressed as:

$$A_{m_n} = \underbrace{[C_{m_n}, C_{m_n}, \dots, C_{m_n}]_S} \quad (4.13)$$

To ensure that the GBR constraint and the maximum power constraint are respected, $A_{m_n}^{th}$ is defined to be the matrix that has all the columns in A_{m_n} that achieve a transmission power less than P_{max} and a TB size greater than T_{GBR_n} . Therefore matrix A is defined as:

$$A = [A_{1_n}^{th}, A_{2_n}^{th}, \dots, A_{M_n}^{th}] \quad (4.14)$$

The vector $b = 1_{K_n}$ (vector of all ones) is the upper bound of the inequality constraint. The equality matrix A_{eq} is defined to be:

$$A_{eq} = \begin{bmatrix} \mathbf{1}_{|A_{1_n}^{th}|}^T & \cdots & \mathbf{0}_{|A_{M_n}^{th}|}^T \\ \vdots & \ddots & \vdots \\ \mathbf{0}_{|A_{1_n}^{th}|}^T & \cdots & \mathbf{1}_{|A_{M_n}^{th}|}^T \end{bmatrix} \quad (4.15)$$

where $|A_{m_n}^{th}|$ is the number of columns in $A_{m_n}^{th}$ (number of potential allocation choices for UE $_{m_n}$). $\mathbf{1}_x^T$ is a row vector of length x of ones while $\mathbf{0}_x^T$ is a row vector of length x of zeros. The vector $b_{eq} = \mathbf{1}_{M_n}$ guarantees that only one of the possible allocations is assigned for UE $_{m_n}$.

BIP Complexity

Exploring the wide array of available BIP-based algorithms and evaluating their applicability to our problem instance is beyond the scope of this paper. However it is an interesting area for future research [90]. For the BIP-based algorithm, the worst case scenario is when all the columns of C_{m_n} achieve a power less than P_{max} .

This results in a search space of $\frac{S}{2} K(K + 1)$ for each user. Therefore for M UEs, the maximum search space can be $\frac{S}{2} K(K + 1)^M$. For example, assume a system of one SP that has the following parameters: $K = 10$ RBs, $S = 15$ MCSs, and $M = 5$ UEs. The worst case search space size is 382.18×10^{12} . Such a problem is not practical and clearly hard to solve within fast scheduling period. Thus, it is important to develop a low-complexity heuristic algorithm that can solve the problem faster.

4.5.2 The Heuristic Allocation Algorithm

Although, it is much desirable to work with the optimal solution for its higher performance (as shown in Chapter 3), but the computational complexity price in solving encourage us to look for much less complexity algorithms. In this section, suboptimal iterative heuristic algorithm is proposed to solve the BIP with lower computational time and less complexity. Its objective is to minimize the total users summation costs by assigning RBs to the UEs iteratively. The algorithm needs a maximum of KM iterations to assign all the RBs to all UEs. For each iteration, the algorithm finds the best RB for each UE.

The suitable RB for UE $_{m_n}$ is defined as the RB which has the highest instantaneous $\Omega_{m_n,k}$ and satisfies the contiguous constraint of UE $_{m_n}$. Then, the change in the user's cost value after assigning the best RB is calculated for each user. That leads to decreasing the power by increasing the UE's BW of transmission that efficiently satisfies its constraints.

The heuristic algorithm proposed belongs to the greedy allocation algorithm family, based on a "steepest ascent" in the objective function. It can be explained simply as follows: first, the algorithm is initialized by defining the number of SPs, their corresponding UEs (with their

queue's size indicated in the UEs' BSR at a definite TTI), and their RBs. Each SP performs its target scheduling algorithm. It is assumed that the bits are stored one by one in the queue and that the queue is infinitely long.

Two scenarios are considered (static/dynamic sharing). Figure 4.2 illustrates the flowchart for the heuristic algorithm in SS and DS scenarios.

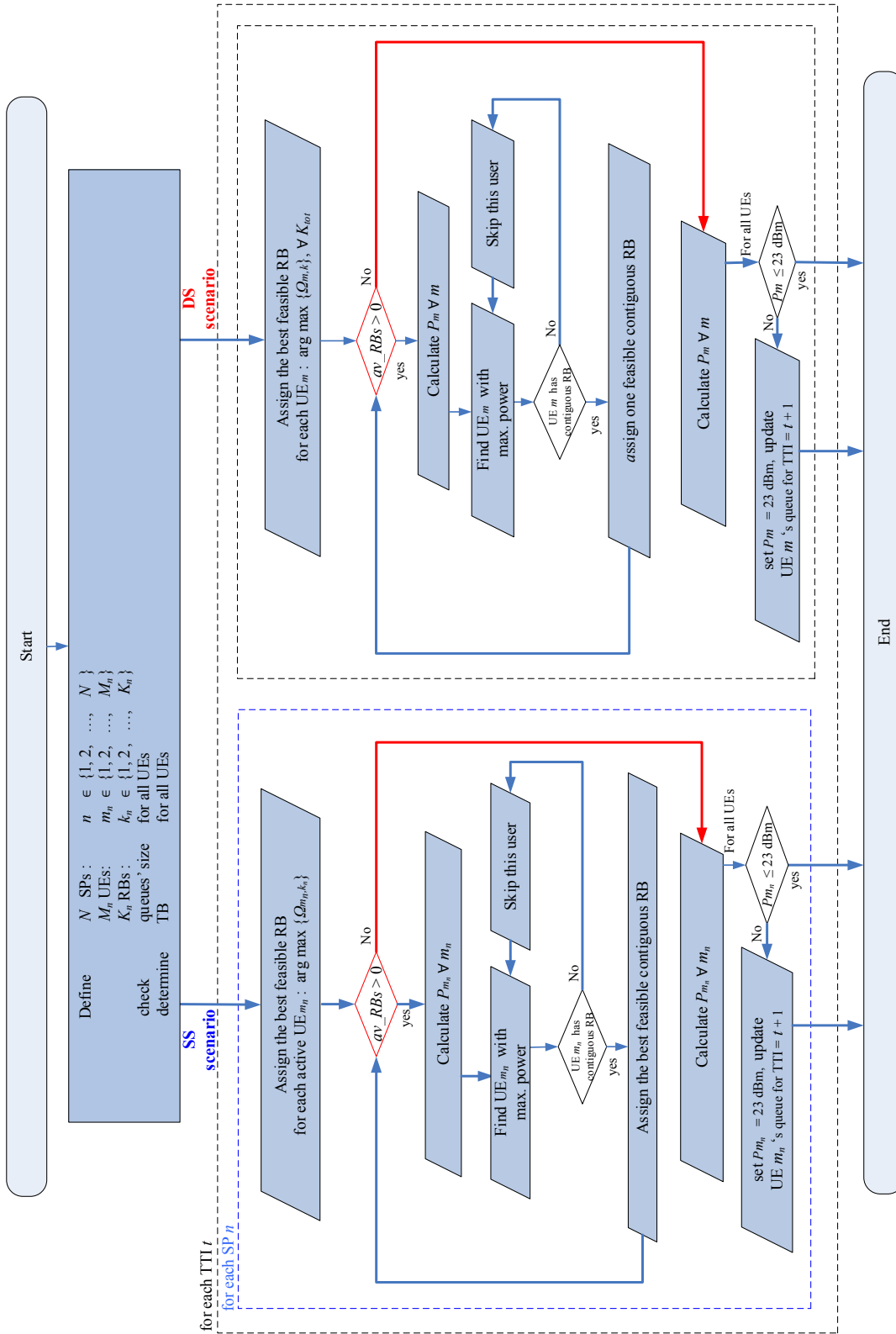


Figure 4.2: The flowchart of the heuristic allocation algorithm in SS and DS scenarios.

Static Sharing Scenario

In this algorithm, each SP performs its scheduling individually with its own available RBs (*av_RB*s). The algorithm first initiates and defines all the needed sets, checks the content of all UEs' queues, and determines the TB size for all UEs. Then it moves to the RB allocation part as follows: the best feasible RB for each UE_{*m_n*} is assigned, and the free *av_RB*s are calculated. Then the transmission power for all UEs is calculated, and the UE with maximum power is assigned with the best feasible contiguous RB. This is repeated until all the RBs are assigned. After assigning all RBs (*av_RB*s = 0), all UEs' transmission power are calculated, and are limited to P_{max} (power constraint).

In case of $P_{m_n} > 23$ dBm, P_{m_n} is set to P_{max} and the UE's queue is updated for the next TTI ($t + 1$). The update will affect the TB that should be satisfied in the next TTI (e.g. if the TB for the considered UE is 400 bits/TTI, it will be recalculated to be 400 + the amount of unsend bits from previous interval bits/TTI).

Dynamic Sharing Scenario

The same steps used in the SS scenario are used in the DS scenario. The only difference is that each SP assigns the best feasible RB to its UEs from the set K_{tot} that contains all RBs from all the different SPs.

In the special case where SPs have different number of users, fairness between UEs (in terms of number of allocated RBs) can only be considered if SLA (between SPs) indicates specific weights of sharing among them [11, 12]. In this case, SPs with fewer UEs can only share a limited number of adjacent RBs (if available) with other SPs.

Heuristic Complexity

When considering the heuristic scheduling algorithm, the order of complexity is $O(KM)$. This is because the algorithm needs K iterations to assign all the RBs. In each iteration, at most 2 operations are needed for each user due to the contiguity constraint. Substituting with

the previous example parameters, the worst case complexity is in the order of 200 operations, which is significantly less than the BIP-based algorithm complexity.

4.6 Simulation results

The scheme is tested using a discrete event simulator developed in MATLAB [65]. Furthermore, in order to combat the extreme uncertainty of self-similar traces and deliver conclusive results, the outcomes of multiple repeated simulation runs are averaged for each result. The solvers and the MATLAB simulator run on i7 core 3400 MHz with 12 GB of memory. Table 4.3 summarizes the list of simulation parameters and their default values.

In this work, 2 SPs performing DS are considered, leading it to allocate more RBs than the SS scenario. It is assumed that the total network load is evenly distributed amongst all UEs, i.e., that the UEs are equally weighted. Each mobile or UE is equipped with a single transmit antenna with 0 dB gain. UEs are assumed to be uniformly distributed over the entire network and are all moving at a pedestrian speed of 3 km/hr.

SP-1's scheduler is considered to assure $\text{GBR} = 400 \text{ kb/s}$ (implying that UEs/SP-1 are able to transmit TB size ≥ 400 bits per TTI), while SP-2's scheduler assures $\text{GBR} = 200 \text{ kb/s}$ (TB size ≥ 200 bits per TTI). An urban environment is assumed with path-loss exponent of 4.5. All existing UEs are assumed to be active.

The average BIP and heuristic transmit power in SP1 is depicted in Figure 4.3. The results show that the DS scenario ensures less UL power consumption than the SS. This is because users have access to a larger number of channels, and thus they can be allocated better channels.

In Figure 4.4, the average BIP transmit power versus the average channel gain is plotted. Three main points are observed. The first is that the DS scenario ensures less UL transmission power than SS. This is due to UEs having access to a larger number of RBs, and thus they can be allocated better channels. The second is that the average transmission power decreases as

Table 4.3: Simulation Default Parameters and Values.

Parameter	Value
Spectrum allocation (UL, DL)	20 MHz
Carrier frequency	2 GHz
Number of subcarriers per RB	12 subcarriers
Neighboring subcarrier spacing	15 KHz
RB bandwidth	180 KHz
Slot duration	0.5 ms
Cell radius	1 Km
MCS	QPSK, 16QAM, 64QAM
UEs in SP1	5 UEs
UEs in SP2	5 UEs
RBs available in SP1	10 RBs
RBs available in SP2	10 RBs
GBR should be satisfied by SP1	400 bits/TTI
GBR should be satisfied by SP2	200 bits/TTI
Channel fading	Rayleigh
Iteration #	1e4
P_{max}	23 dBm
Channel Estimation	Perfect
σ_{sig}^2	1
σ_n^2	1
ϵ	0
Coherence time	1 ms
Cells interference	Avoidance
path-loss exponent	4.5

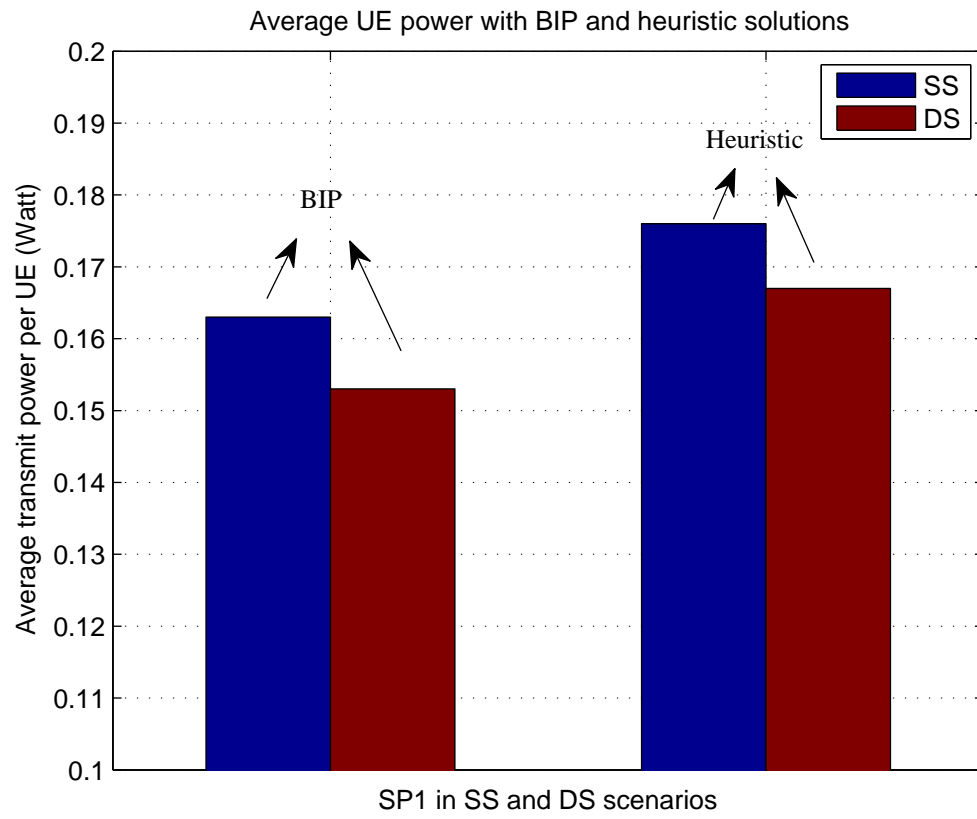


Figure 4.3: The average BIP and heuristic transmit power in SP1.

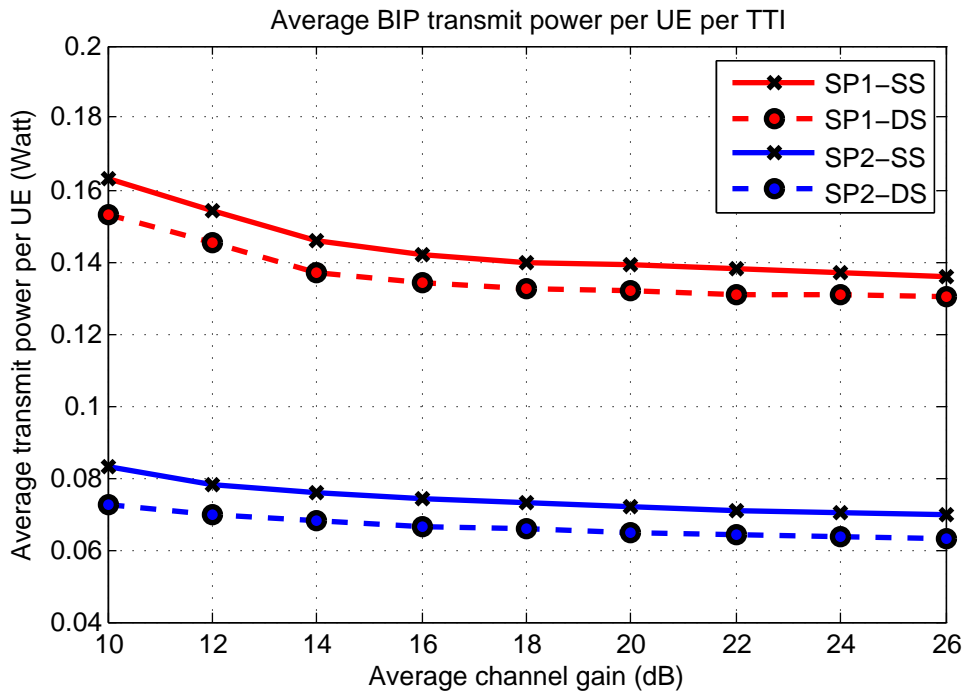


Figure 4.4: The average BIP transmit power versus the average channel gain.

the average channel gain increases. This is expected since the channel improves as the average gain increases, allowing the users to be allocated better channels. The third observation is that the lower the GBR requirement, the lower the average transmitted power. This is due to the fact that a smaller TB size needs fewer number of RBs to be satisfied and thus lower transmission power can be used.

Figure 4.5 shows the average BIP transmit power versus the number of active UEs. Due to the higher competition for RBs, which results in less number of RBs being allocated to each user, it is observed that the average transmission power increases as the number of users increases.

Figures 4.6 and 4.7 present the average BIP and heuristic transmit power in SP1 versus the average channel gain and the number of active UEs. The same observations as in Figures 4.5 and 4.6 are evident here. Furthermore, these figures show that the heuristic achieves comparable performance to the BIP-based scheme.

Figure 4.8 shows the average UL transmission rate per TTI in SPs-1, and 2, and it ensures

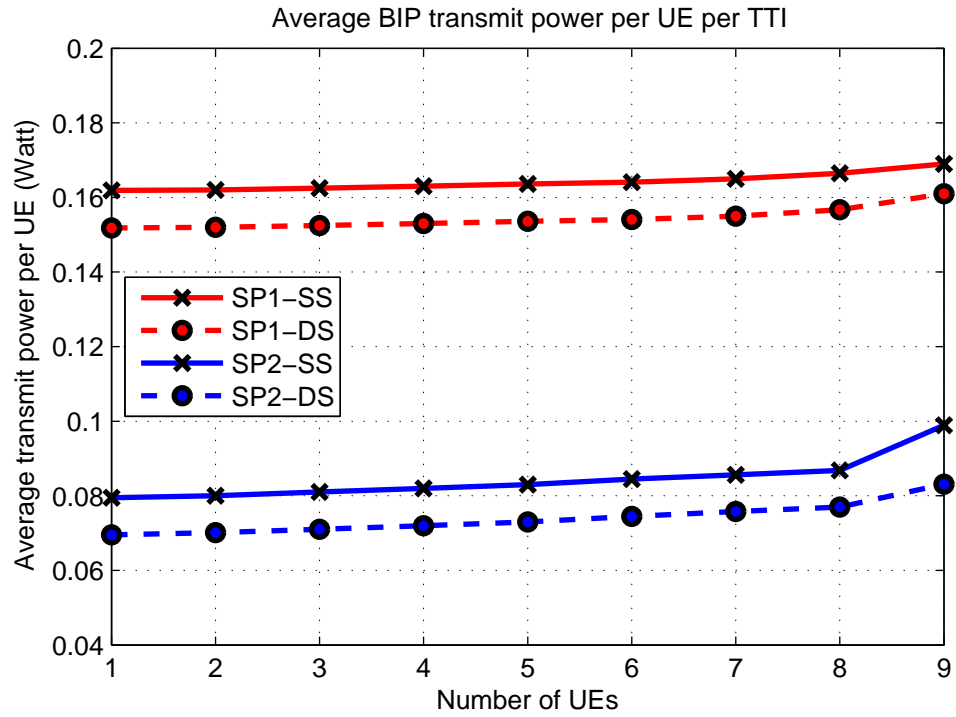


Figure 4.5: The average BIP transmit power versus the number of active UEs.

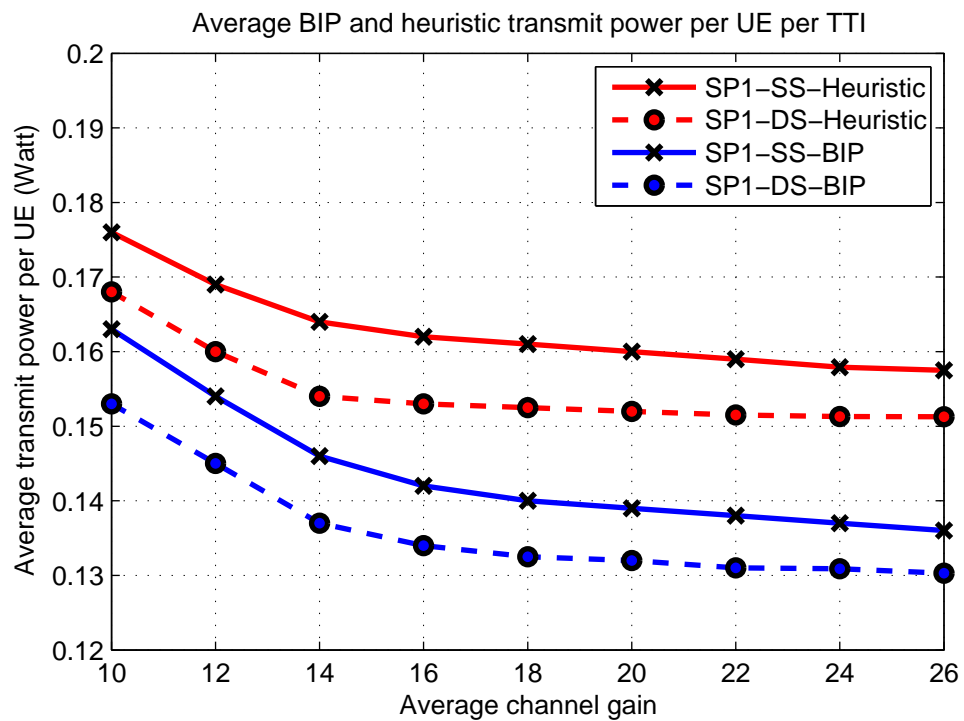


Figure 4.6: The average BIP and heuristic transmit power in SP1 versus the average channel gain.

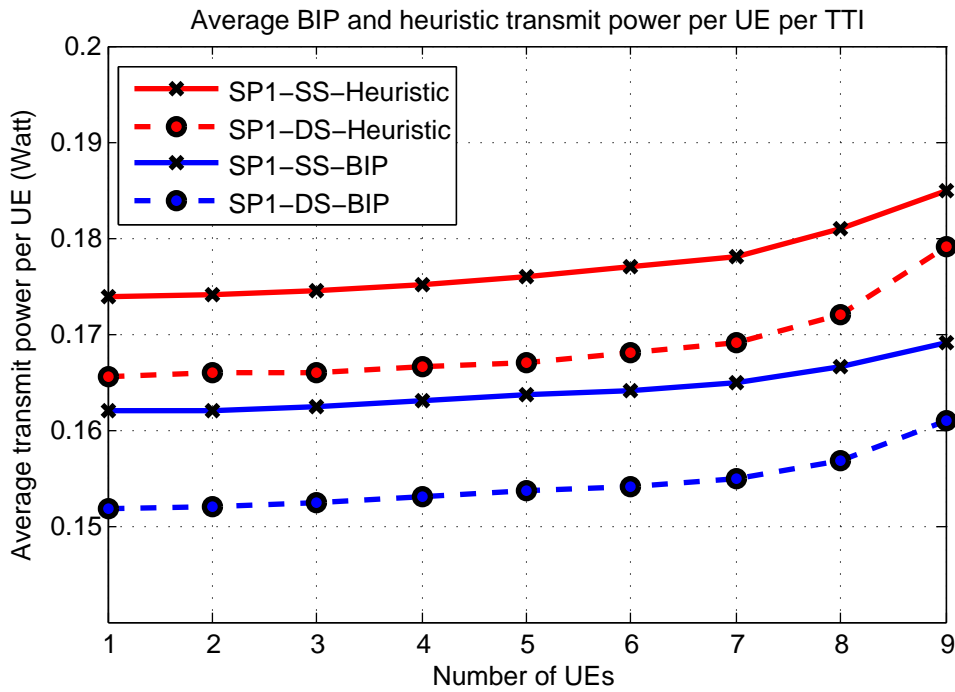


Figure 4.7: The average BIP and heuristic transmit power in SP1 versus the number of active UEs.

that, the GBR is equal to 200 Kbit/s in SP2 and 400 Kbit/s in SP1. The figure shows the efficiency of both the BIP-based solution as well as the heuristic, as both were able to satisfy the rate requirement of both SPs.

To better visualize the efficiency of this framework, it is assumed that UEs transmit data until the total energy consumption reaches 80 Watt (that is equivalent to transmitting at maximum power threshold (200 mW) for 400 TTIs) [30]. The normalized battery life comparison between the considered SS and DS scenarios in SP1 is illustrated in Figure 4.9. It is clear that the proposed schemes prolong the battery life by around 20 % to 53 % for the BIP-based scheme and 14 % to 30 % for the heuristic one.

Figures 4.10 and 4.11 plot the normalized running time (computed using the MATLAB functions *tic* and *toc*) versus the average channel gain and the number of active UEs respectively. As discussed before, the complexity of both schemes is dependent on the number of RBs and the number of users. Moreover, the heuristic has a smaller computational complexity

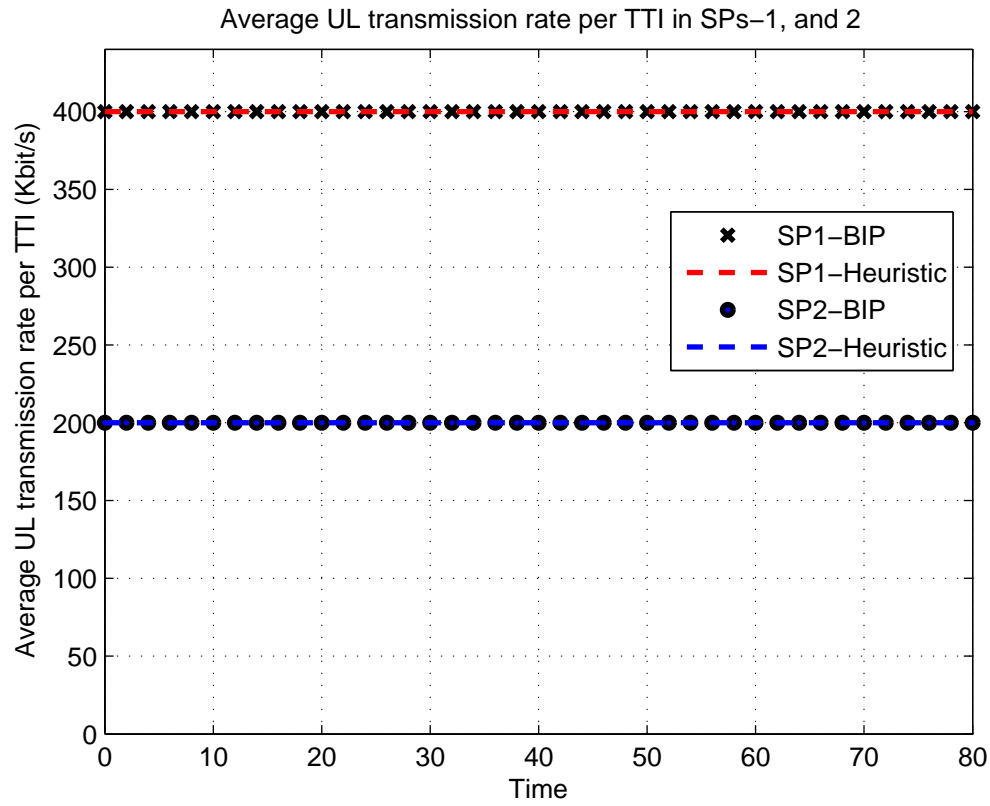


Figure 4.8: The average UL transmission rate per TTI in SPs-1, and 2.

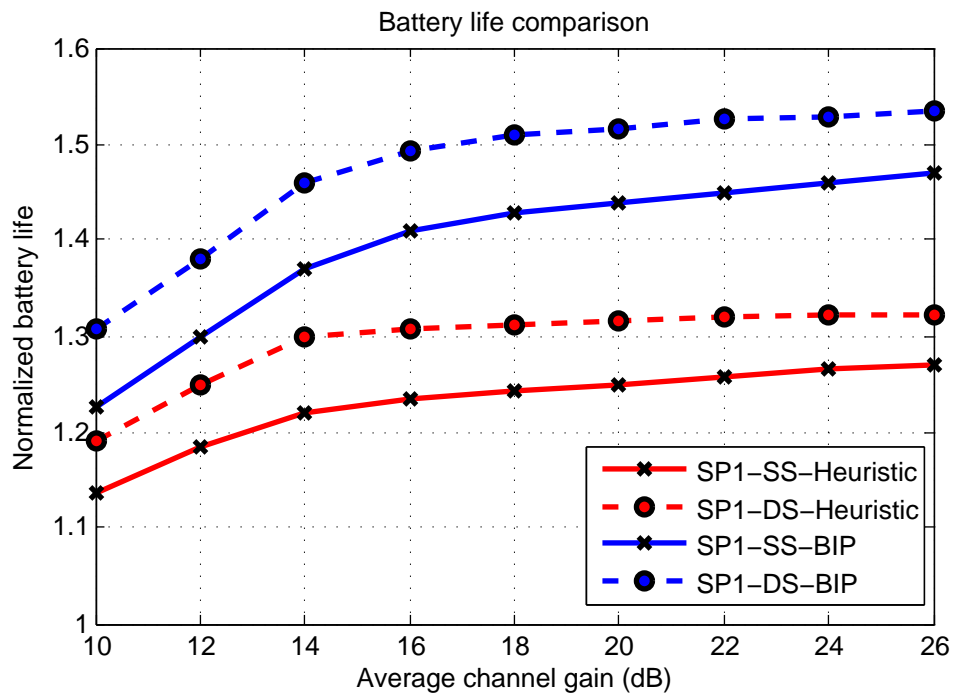


Figure 4.9: The normalized battery life versus the average channel gain.

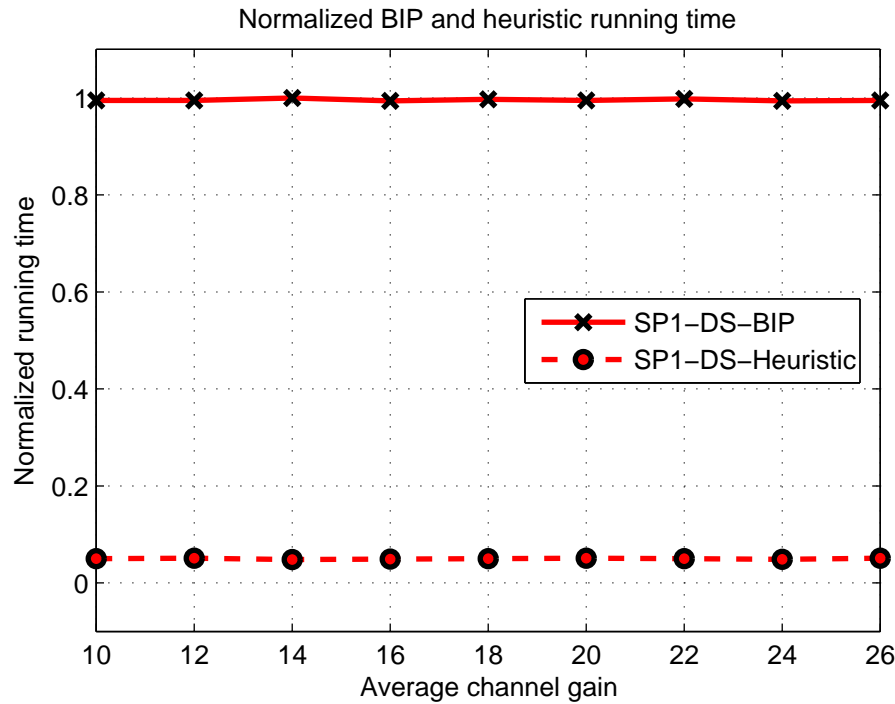


Figure 4.10: The normalized running time versus the average channel gain.

compared to the BIP-based scheme.

4.7 Chapter Summary and Conclusion

The represented work pertains to power-efficient scheduling in a virtualized UL LTE systems to achieve green communication. Both the QoS requirements and the channel fading parameters were considered. The average SPs' transmission power for all UEs in both SS and DS scenarios was evaluated. This improvement allowed SPs to customize their efforts, schedulers, and control the sharing of their resources among them.

A BIP-based scheduling algorithm with high computational complexity was developed. A lower complexity heuristic algorithm was also presented. Although, both algorithms are implementable, however, the heuristic is more reasonable for its less complexity and less computational time with affordable and guaranteed QoSs. Simulation results confirmed that sharing a framework yields notable improvements in terms of power saving without degrading QoS

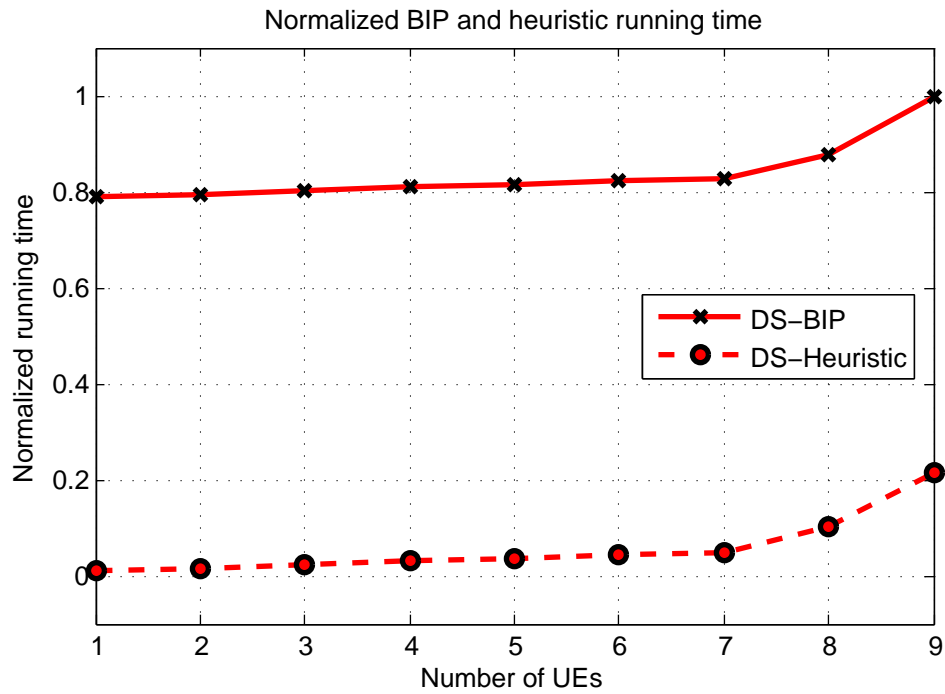


Figure 4.11: The normalized running time versus the number of active UEs in SP1.

performance under different practical realistic scenarios.

Furthermore, it was shown that the DS scenario outperforms the SS scenario due to the larger pool of RBs available for users. Moreover, it was observed that the heuristic algorithm achieved comparable performance with the BIP-based algorithm while having a lower complexity.

Chapter 5

Intra-MME/S-GW Handover in Virtualized 3GPP-LTE Systems

As it is expected that mobility speeds to support can reach up to 350 km/h, the HO will occur more frequent. As a result, the system performance in terms of delay shall be degraded. So, more efficient radio resource management with enhanced HO techniques, and load balancing is required to support fast and seamless HO.

Many applications are appearing every day, specially with the expected evolution in mobility and wireless communications. The most popular high mobility applications are the high-speed rail that are significantly higher in speed than regular rail traffic. Thus, UEs operating their smart applications need to be satisfied with their provided QoSs assigned.

The presented framework to follow pertains to the SPs' resources dynamic sharing scenario, wherein SPs achieving a different schedulers' policy are sharing eNB. This allows SPs to customize their efforts and provide service requirements.

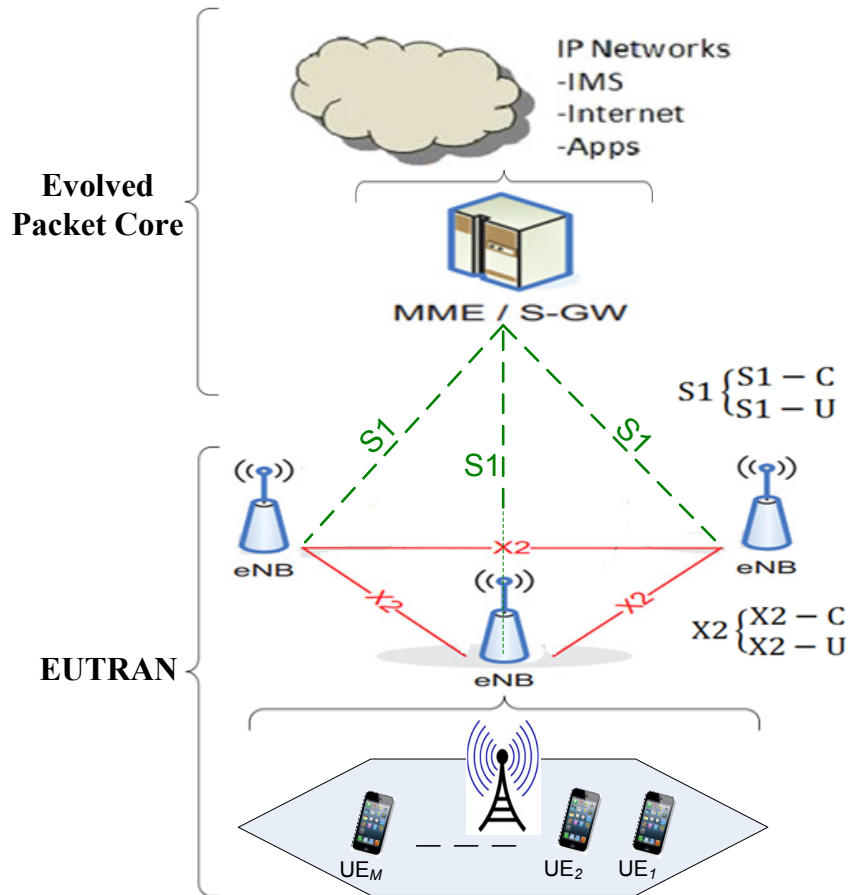


Figure 5.1: Basic network topology of multiple eNBs sharing one MME/S-GW.

5.1 Introduction

One of the important aims of LTE, and any wireless technology, is to provide fast and seamless HO from one cell to another.

Accessing services with high mobility speed will degrade the efficiency and reliability of the wireless system especially during frequent HO.

Figure 5.1 shows the LTE system topology architecture. The E-UTRAN uses a simplified node architecture consisting of the eNB to communicate with UEs, while the eNB communicates with other eNB using X2-C and X2-U interfaces for control and user plane respectively.

The eNB communicates with the EPC using the S1 interface; specifically with the MME and the UPE identified as S-GW, using S1-C and S1-U interfaces for control plane and user

plane respectively, that supports a many-to-many relation between MMEs/UPEs and eNBs, and by its turn is connected by the IMS, and Apps.

The MME and UPE are preferably implemented as separate network nodes so as to facilitate independent scaling of the control and user plane. Intra E-UTRAN HO is used to hand over a UE from a source eNB to a target eNB using X2 interface when MME is unchanged. I assume that S-GW is also unchanged.

5.2 Recent Relevant Research Work

Until now, the existing HO techniques have some flaws such as inter-cell interference coordination, interference mitigation technologies, latency, unreliability and some data loss. Therefore, a new HO technique is essentially required to improve the HO performance.

In [98], the design and evaluation of an LTE test suite encompassing various mobility scenarios was reported. In [9, 99, 100], a fractional soft handover scheme based on the carrier aggregation is applied with single frequency reuse, without discussing the issues of the ignorance of LTE for soft HO (SHO) technique.

Kim *et al.* in [2], considered the state-of-the-art HO schemes with various deployment scenarios in WiMAX networks and 3GPP LTE-advanced candidate systems. They focused on IEEE 802.16m based.

Chen *et al.* in [101], proposed a framework of HO decision in LTE networks under high-speed mobility scenario. Tom *et al.* in [102] analyzed a fixed-point and classical A3 event HO algorithms in the LTE high-speed rail network without discussing the existing challenges in LTE HO operation. Han *et al.* in [103], HO delay and interruption time performance of LTE networks are measured without considering solutions to decrease that delay.

The main contribution in this chapter is proposing a HY-HO technique as feature work based on the combination of hard [HO] (HHO) and SHO techniques. The combination is expected to enhance the system performance in term of latency. Also, reducing the transmission

overhead on the serving cell results in a balanced network traffic.

To the best of my knowledge, there are no previous works that investigate and analyze the HO techniques in DS-virtualized (Vir.) scheme for LTE systems. This chapter considers DS resources Vir. scheduling algorithm for different types of traffic applications in access networks. The framework scheme shares SPs RBs while maintaining different scheduling strategies.

The research below offers detailed simulations to study the performance of the considered work and validate its effectiveness during and after the HO operation.

5.3 Users Mobility

Mobility models usually represent the motion of mobile UEs, and clarify how their position, speed and acceleration change with time [64, 104]. These models are frequently used for simulation purposes when investigating new communications techniques. Mobility management schemes for mobile communication systems use these mobility models in order to predict future user positions [49, 105].

The trade-off of improving the QoSs parameters, in turn improved error performance and would inherently require increased cost expenditures. In mobility modeling, it is important to simulate the system and evaluate its performance. The simulation has several key parameters, including the mobility model used and the pattern of communications traffic. Mobility models characterize user movement patterns, i.e. the different behaviours of subscribers. Traffic models describe the condition of mobile services.

The action of a UE's motion can be described using both analytical and simulation models. The input for analytical mobility models makes simplifying assumptions regarding users movement behaviour. Such models can easily provide the performance parameters for simple cases using mathematical calculations.

Random way-point model is considered. In random-based mobility simulation models, the mobile UEs move randomly without restrictions. The destination, speed and direction are

chosen independently of other nodes. This kind of model has been used in many simulation studies. Two variants, the random walk model and the random direction model are variants of the random way-point model.

When the random direction model is used, the UE randomly chooses the speed direction, that remains constant during the time, and moves toward the simulation boundary area. Once the simulation boundary area is reached, the UE chooses a new speed direction.

When the random walk is used, the UE randomly chooses the speed direction and moves for a given distance which depends on the user velocity. The UE changes its speed direction after covering this distance.

In the mobility model class, the speed and direction variables are used to define the speed and the travel direction of the UE, respectively.

A mobile starts its motion through the system at call initiation with the above initial conditions. If the total call duration is long enough, the mobile will go through its first change of direction, and a new time until its next change of direction will be drawn at that point. The process is repeated until call termination, with the mobile possibly going through several handoffs in the mean time. An example is provided in Figure 5.2 where a mobile goes through two handoffs and two changes of direction before call termination.

Each call contributes a certain number of channel occupancy time samples, according to the number of handoffs it went through. In the example illustrated in Figure 5.2 three samples have been generated; one between call initiation and handoff 1, the second between handoff 1 and handoff 2, and the third one between handoff 2 and call termination. Once a sufficient number of samples have been generated, statistics for the channel occupancy time distribution can be obtained.

Let the position of a UE at time t be denoted by $X_i(x_i, y_i) \in \mathbb{R}^2$, where $\mathbb{R}^2 = \{(x, y) : x, y \in \mathbb{R}\}$. Assuming that, the UE changes its position according to:

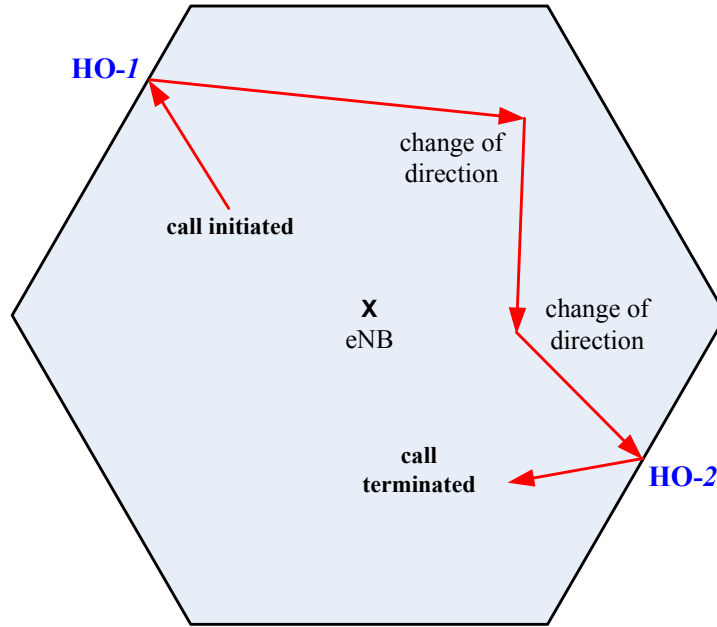


Figure 5.2: UE's path of a mobile going through two handoffs and two changes of direction before cell termination.

$$\begin{bmatrix} x_{i+1} \\ y_{i+1} \end{bmatrix} = \begin{bmatrix} x_i \\ y_i \end{bmatrix} + v \cdot \begin{bmatrix} \cos(\theta) \\ \sin(\theta) \end{bmatrix} \cdot \Delta t \quad (5.1)$$

Figure 5.3 shows the pseudo-code investigating the rate of HO for different mobility speeds, using both the random way mobility model.

- 1: *For each UE's speed*
- 2: *For each UE's call*
- 3: *Locate (x_o, y_o)*
- 4: *Define s_l , where $\sum_{l=1}^S s_l = D_m$*
- 5: *Assign each step s direction angle θ*
- 6: *Calculate boundary collision that counts for HO*
- 7: *End For*
- 8: *Rate of HO = no. of HO / no. of UEs' calls*
- 9: *End For // end of simulation*

Figure 5.3: The pseudo-code for the rate of HO for different mobility speeds.

The user mobility is managed by the network manager that every TTI updates the user position according to the selected mobility model and parameters and verifies, through the Network Manager HO Procedure function, if the handover procedure is necessary.

5.4 Handover in Wireless Systems

In a wireless networks' technologies, the term HO is defined as the process of establishing a target wireless link connection from the source to target base stations (BSs). This HO could be vertical or horizontal.

A vertical HO often occurs between different wireless technologies such as a HO for UE from LTE network to WiMAX mobile network. On the other hand, a horizontal HO occurs in the same wireless technology such as the HO of UE from one cell to other [98].

5.4.1 Handover Algorithm and Message Sequence

Figure 5.4 shows the HO algorithm. An arrow is demonstrating UE movement controlled by the same MME. In this procedure every bearer set between UE and MME will be moved to the target eNB (assuming that, the target eNB is able to handle the UE).

The presence of IP connectivity between the S-GW and the source eNB, as well as between the S-GW and the target eNB is assumed. During the simulation, each eNB maintains the list of UEs active with it, storing their ID and the latest reference signal received power (RSRP) feedbacks. Furthermore, eNBs and UEs have the information of the LTE cell they belong to. In fact, each UE keeps up to date the ID of the cell to which it belongs to and the ID of the active serving eNB.

Figure 5.5 presents the LTE HHO message sequence wherein, before the HO, the UE and the source eNB are in radio resource control (RRC) connection state. The DL and UL data are flowing between the S-GW and the UE via the source eNB. The network sets the measurement thresholds for sending measurement reports. The RRC uses the latest measurement to decide

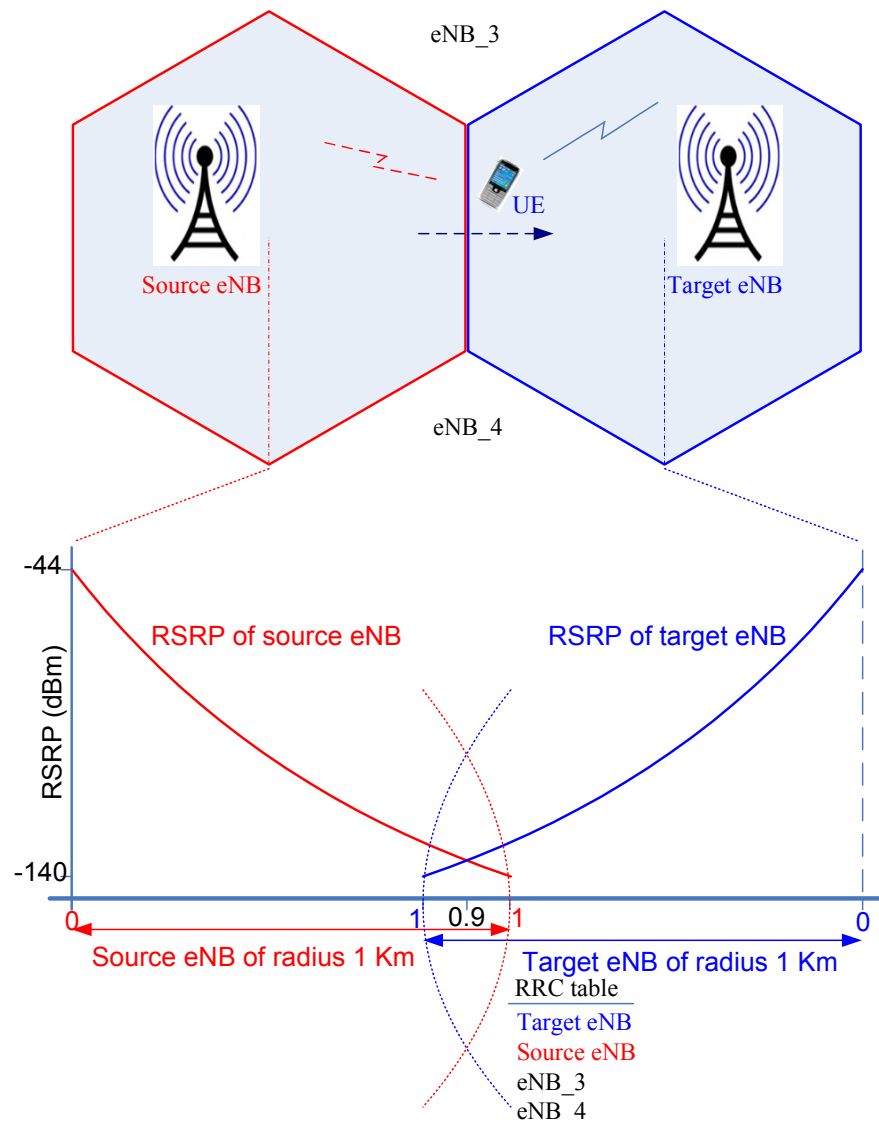


Figure 5.4: Handover algorithm.

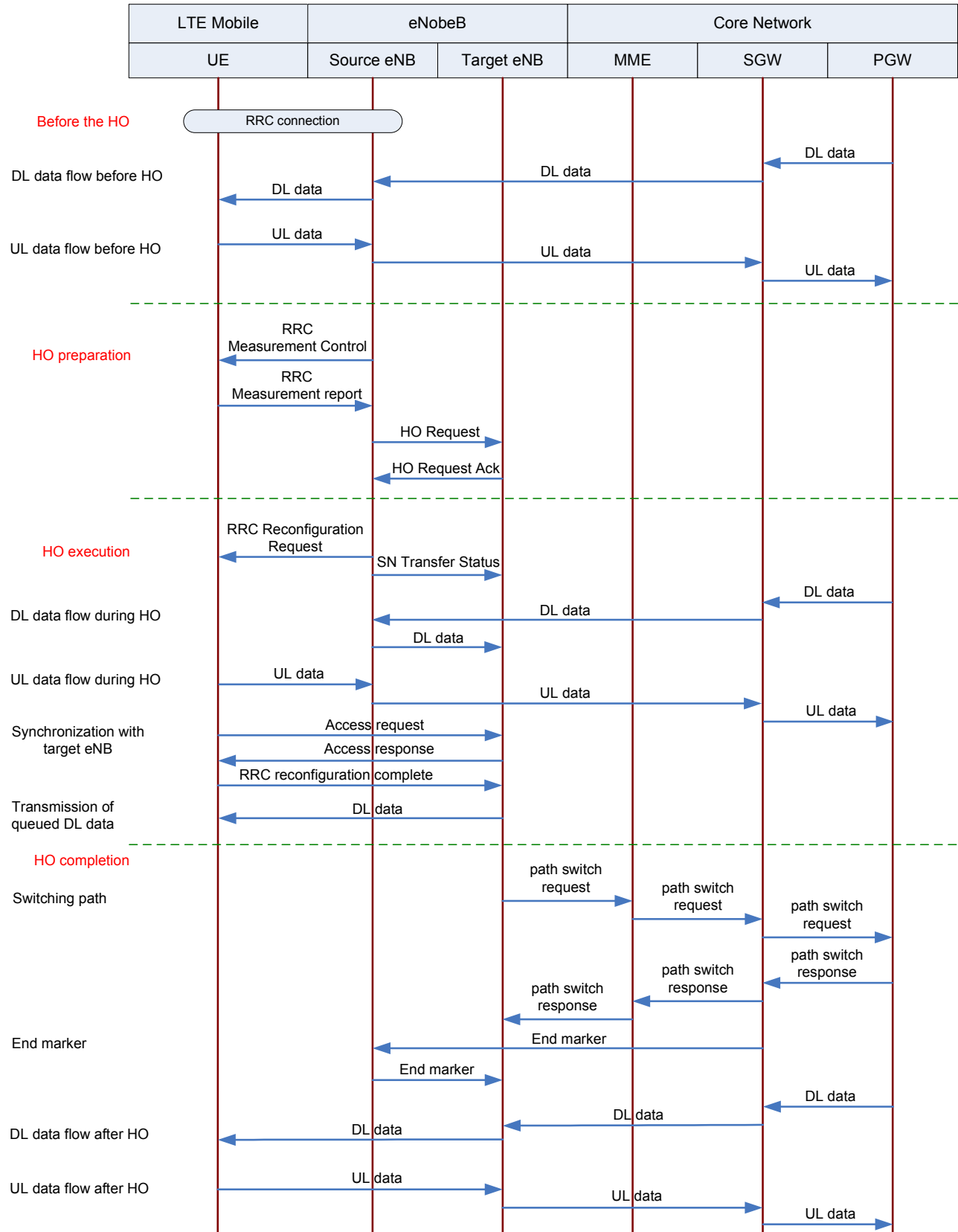


Figure 5.5: LTE handover message sequence.

if a HO is needed to another cell. The RRC measurement reports includes signal strength of serving and neighboring cells and the decision whether the HO is needed to be performed or not. If so; the target cell is selected. The eNB for the target cell is identified.

The source eNB initiates the HO with HO request message. S1 bearer is established between the target eNB and the S-GW. The target eNB allocates radio RBs for the UE that will be handed in. The target eNB responds back to the source eNB with a HO request acknowledge message. This message carries the HO command message (RRC connection reconfiguration request).

An X2 bearer is established between the source and the target eNBs. This channel will carry the UEs data during the HO. At this point, the UE is ready to buffer DL data that will be received during the HO. The source eNB sends a HO command to the UE. Meanwhile, the UE has received the HO command and it is switching to the new target cell. At this point, the UE has detached from the source eNB but is still not communicating with the target eNB. The UE is in the RRC-Idle state.

The UE sends a preamble request assigned in the HO command to start synchronizing with the target eNB. The target eNB accepts the request and responds back with a timing adjustment and an UL resource grant. The UE uses the assigned resources to transmit the HO confirm message (RRC connection reconfiguration complete).

The UE is not connected to the target eNB. Thus it transitions to the RRC-Connected state. The target eNB requests the MME to switch the path from the source eNB to the target eNB. MME requests the S-GW to switch the path to the target eNB. The S-GW asks the PGW to switch the path.

The S-GW responds back to the MME signaling the completion of the path switch. The target eNB will buffer data directly received from the SGW until all the data received via the source eNB has been transmitted. This is needed to maintain the transmission order. S-GW is now sending the data using the target eNB. MME responds back to signal the completion of the path switch. The end marker has been received at the target eNB. At this point the target

asks the source eNB to release resources for the UE.

Although the HO in LTE systems is purely based on HHO [9, 106], I would present SHO as well.

5.4.2 Hard Handover Technique

The basic idea of HHO is to break-before-make. This means that, the previous wireless connection is broken from the source eNB before a new connection is activated to the target eNB. The UE will be able to communicate with one eNB during HHO. After releasing the connection from source eNB, a new connection is established and activated with the target eNB. Whereas, after the signal strength from a target eNB exceeds the signal strength from the source eNB the HO start the execution sequence as shown in Figure 5.5.

5.4.3 Soft Handover Technique

The SHO technique in generality is to make-before-break method. In other words, a new link connection to the target eNB should be established while the old connection with source eNB is still active. The UE simultaneously receive all services data from several active eNBs. Under this technique, there are two main SHO techniques in wireless mobile communication system. The first technique is called macro diversity HO (MDHO) and the second technique is called fast base station (BS) switching (FBSS) [99].

Macro Diversity Handover

In MDHO, a list of BSs is set by the UE and BS. This set of BSs is usually called the active or diversity Set. Under this technique, UE has the ability to communicate with all BSs in the active set as shown in Figure 5.6. For DL, UE receives and performs data from all the Diversity Set BSs. In the UL, all diversity set BSs receive and perform information from UE.

The neighboring BSs can still receive the signal from the UE, but the strength is not sufficient to allow neighboring BS to be considered from the diversity set. MDHO supports fast

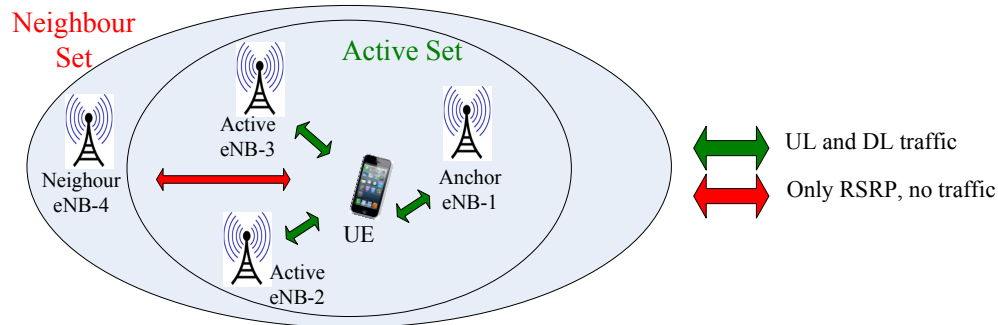


Figure 5.6: Macro Diversity Handover.

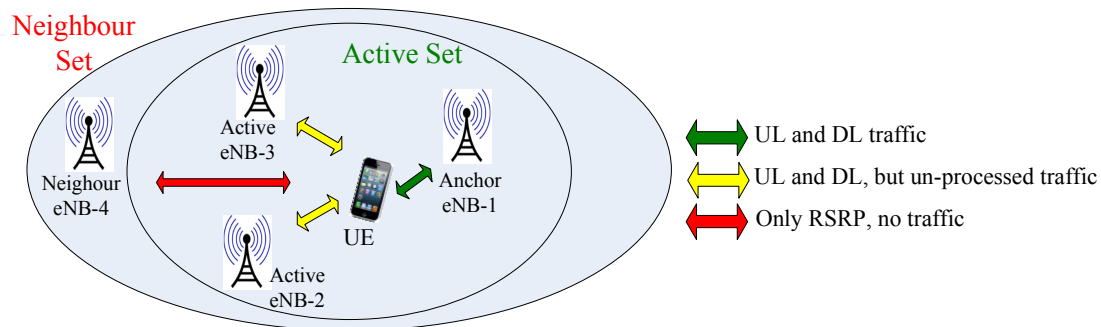


Figure 5.7: Fast Base Station Switching.

and seamless HO. In addition, MDHO is more stable and gives better performance in term of fast and seamless handover. MDHO is more complex in its design and during HO procedure than HHO. Therefore, assuming MDHO will increase system complexity and many resources will be wasted.

Fast Base Station Switching

In FBSS technique, UE and BS make a list of the available BSs called a diversity set and also communicate with BS in each frame (just like MDHO). The UE monitors the base stations in the active set and defines only one BS as an anchor BS based on the received signal strength. This anchor BS is the only BS of the diversity set that UE can communicate with for UL and DL messages with all management and traffic exchange as shown in Figure 5.7 [99].

This type of HO is much smoother in transition from the source to target eNBs and much less overhead than MDHO. In other side, FBSS has high data lost latency and outage

probability comparable to MDHO.

5.5 System Model

Consider a DL scenario, wherein, a UE belongs to SP1 is moving from a source eNB to a target eNB. The target eNB consists of multiple SPs employing different scheduling policies, such that, N SPs share an eNB.

The set of SPs is denoted as $\mathcal{N} = \{1, 2, \dots, N\}$. Each SP n is assumed to serve M_n active UEs, where $n \in \mathcal{N}$ and the set $\mathcal{M}_n = \{1, 2, \dots, M_n\}$. Denote UE_{m_n} to be the UE m belonging to SP n . Each SP has access to a number of channels (available RBs).

Intra-MME/S-GW HO using the X2 interface is considered in the HO for the UE from a source eNB to a target eNB using the X2 interface when the MME and S-GW are unchanged. This scenario is possible only when there is a direct connection exists between source eNB and target eNB with the X2 interface. Denote K_n to be the total number of available RBs in SP n . It is helpful to define some frequently used notations as shown in Table 5.1.

5.5.1 Transmission Block Size

In LTE, the subframe has a duration of 1 ms. The available spectrum is divided into RBs defined in both frequency and time domains. It consists of a contiguous set of 12 subcarriers (180 kHz with subcarrier spacing of 15 KHz) from each OFDM symbol and has a duration of 0.5 ms [51].

The overall TB size is a function of the spectral efficiency (ζ_s) of the selected MCS s and the number of allocated RBs. The total RB bandwidth is $12 \times BW$ [12, 51], where BW is the subcarrier bandwidth. The total TB size, that can be transmitted per subframe over k RBs for UE_{m_n} is given by:

$$T_{m_n,k,s}(t) = \lfloor 132 \times \zeta_s(t) \times \|k\| \rfloor, \quad (5.2)$$

Table 5.1: Frequently Used Notations

Notation	Definition
av_{RB_s}	Number of available RBs at definite TTI
k	Set of RBs allocated for UE $_{m_n}$
K_n	Total number of RBs in SP n
K_{tot}	Total number of RBs in all SPs
m	UE
m_n	UE m in SP n
M_n	Total number of UEs in SP n
M_{tot}	Total number of UEs in all SPs
n	SP
N	Total number of SPs
n_{iRB_j}	Number of RBs allocated to UE j for traffic class i
n_{ij}	Number of needed RBs to satisfy traffic i for UE j
n_{RB_j}	Number of RBs allocated to UE j
P_{tx}	eNB's transmitting power
P_{rx}	UE's received power
RB_{BW}	Size of available RB that could be allocated to UE j
s	MCS
S_i	Needed BW to satisfy traffic i (in bits) by all UEs
t	Definite TTI
T_{m_n}	TB of UE m in SP n
TTI	Transmission time interval
U_{HO}	Total number of UEs performing HO
V_{ij}	BSR size of queue i for UE j , where $i = 1$ for EF $i = 2$ for non-EF
[.]*	The new value of [.]

and thus, the number of RBs can be represented as:

$$\|k\| = \frac{T_{m_n,k,s} + \epsilon}{132 \zeta_s(t)}, \quad (5.3)$$

where $0 \leq \epsilon < 1$.

Fast HO is a network procedure with minimum HO delay without any interest in packet loss [107, 108] or interruption time. While, seamless HO are a network re-entry procedure with the capability for UE to contact with the target eNB before initiating a network re-entry control message transaction.

Generally, fast and seamless HO depends on the type of the traffic services. For example, A real-time applications require high data rate. Thus, there is degrading connection in these real-time applications (i.e. video conferencing and streaming media), that will be noted to the UEs while HO from the source to the target eNB.

However, browsing a website/transferring a file do not require a high data rate, so the UE will not notice any drop in the HO process. Thus, the most factors for fast and seamless HO are the latency and packet loss [109].

5.5.2 LTE RSRP Measurement Report

In LTE-systems technology, the measurement is done usually at two stages. One is the measurement in an idle mode, while the other is in connected mode. The idle mode is for the cell selection/re-selection process and this criteria is measured by the system information block (SIB) messages. While, the connected mode measurement is for the HO and the measurement criteria and is determined by the RRC messages for a specific UE.

In cellular networks, when a mobile moves from cell to another and performs cell selection/re-selection and HO, it needs to measure the signal strength and quality of the neighboring cells. Generally, in the LTE network, a UE measures RSRP.

The received signal strength indicator (RSSI) carrier measures the average total received

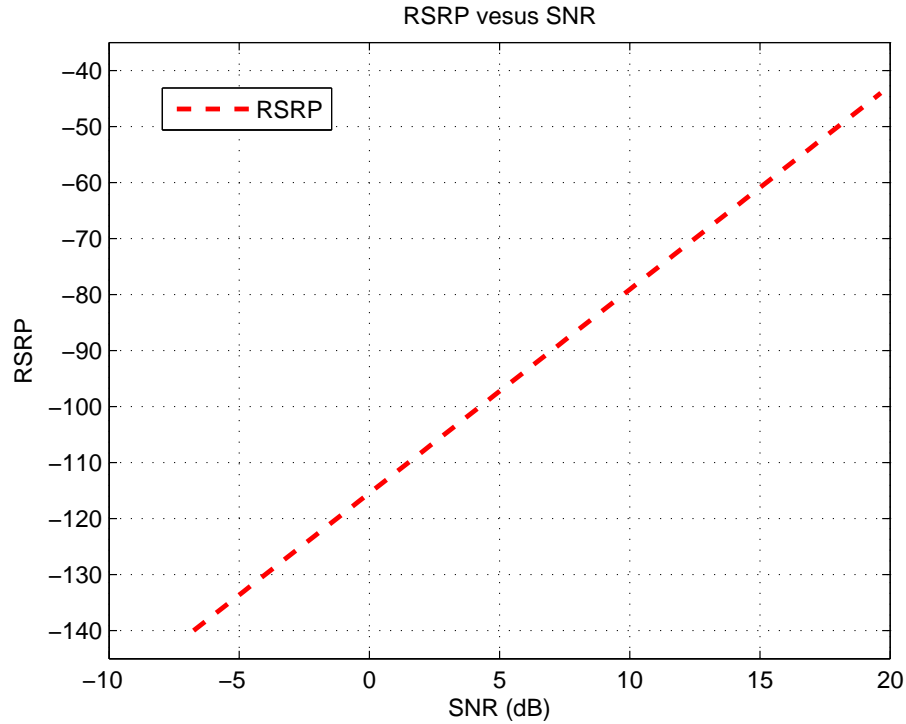


Figure 5.8: The range of RSRP reported by UE versus SNR.

power in the OFDM symbols in the channel serving and non-serving cells, adjacent channel interference, thermal noise, etc. measured over all the 12 subcarriers [4, 21].

The reference signal received quality (RSRQ) considers also RSSI and the number of used RBs k . RSRP/RSSI measured over the same BW. It indicates the quality of the received reference signal. The RSRQ measurement provides additional information when RSRP is not sufficient to make a reliable HO or cell reselection decision.

While, the RSRP is the average power received by UE from a single cell spread over the full bandwidth and narrow band. It is calculated by UE for cell selection, HO, cell reselection and for path loss calculation for power control. The power measurement is the energy of the OFDMA symbol excluding the energy of the cyclic prefix.

The range of RSRP reported by UE is between -140 dBm to -44 dBm as shown in Figure 5.8. For each 1 dBm difference from -140 dBm, UE report an integer value (ranging 0 to 97) to the eNB. For example: value 0 is reported when UE measure RSRP < -140 dBm , value 1

is reported when UE measure $-140 \text{ dBm} \leq \text{RSRP} < -139 \text{ dBm}$, and value 97 is reported when UE measure RSRP -44 dBm .

One of the most important step for Handover is Measurement Report from UE before the handover. Network make a decision on whether it will let UE HO or not, based on the measurement value from UE.

During HO, LTE uses measurement gap technique. It has the same procedure as the compressed mode in UMTS. It creates a small gap during which there is no transmission and reception. UE can then switch to the target eNB and perform the signal quality measurement and then comes back to the current cell.

Ideally, a network lets UE reports the RSRP of the serving eNB and neighbor eNBs and set the arbitrary rule for HO. The network builds up its decision on multiple consecutive measurements instead of using only a single or a couple RSRP value.

As a solution, 3GPP defines several sets of pre-defined mechanisms to be done by the UEs. These pre-defined measurements are called events.

This work usually goes seamlessly, as there should be a well established agreement between UE and network about the gap definition (e.g, starting position of the gap, gap length, number of gaps, ... etc.).

Due to the impact of large scale fading, it is possible by measuring the RSRP to determine the UE's real-time position, with the received power is being the most important criterion for HO decision [96, 110]. Received power is calculated as follows:

$$\frac{P_{rx}}{P_{tx}} dB = 10 \log_{10} X - 10 \gamma \log_{10} \frac{d}{D} - \varphi_{dB} \quad (5.4)$$

wherein, P_{rx} is the UE's received power, P_{tx} is the eNB's transmitting power, X is the path loss factor (by an average of channel attenuation, the value is generally between 0 and 1, during simulation $10 \log_{10} X = -140.72 dB$), α is a path loss exponent, D is a reference distance (usually set to 1), d is the distance between the UE and the measured eNB, φ_{dB} is a mean of 0

and standard deviation of 8 dB of lognormal shadowing value.

At first, when the UE enters the location where HO should be triggered, the UE receives the measurement volumes including: the UE terminal UE latitude and longitude information, the source eNB and the target eNB RSRP values (denoted as $RSRP_{source}$ and $RSRP_{target}$).

When the UE receives the returned measurement data, the obtained data is processed and the speed of movement of the UE is determined. If the UE's $RSRP_{source} \leq RSRP_{target}$ then the UE triggers the classic A3 event HO algorithm.

5.5.3 Traffic in Wireless System

UE's data packets are transported by dedicated radio bearers, generated with different packet jitter and delay requirements introduced as EF, AF, and BE traffic services.

Packets in dedicated bearers are generated at the application layer by 3 different traffic generators: voice traffic, trace based, and infinite buffer. The voice traffic EF application generates G.729 voice flows [55], modeled with an ON/OFF Markov chain, while the trace-based AF application sends packets based on realistic video trace files, and the BE application generates packets with CBR (as modeled in Chapter 3).

5.6 Hybrid-Handover Technique

Before HO, UE normally measures the RSRP of the target cell and report it to the eNB so that the network can make its decision whether or not to allow the UE to HO to the target cell.

SHO is possible in code division multiple access (CDMA) because adjacent cells can operate on the same frequencies as long as they use various scrambling codes. So, a UE can listen to two different cells by decoding the received signals twice, using a scrambling code from each cell on each for each decoded signal. This allows a UE to communicate with both eNBs during HO.

LTE is generally based on OFDMA, that is a frequency division technique. This means

that, a UE has to resynchronize with a different set of frequency when it hands over among cells, removing the possibility of SHO.

Just in terms of logical solution, the simplest way for inter-frequency measurement would be to implement multiple RF transceivers on UE. However, there are some issues with this solution. First is the cost issue, as it will require more cost to design and implement the additional transceiver.

Second can be the probability of interference between the current frequency and target frequency especially if the current frequency and target frequency are close. The third one would be the increase in UEs power consumption in UL and DL. These issues could be treated with by mass productivity, designing enhanced sharp RF filters, and activating the second RF transceiver only in HO operation to overcome the UL power consumption.

Also, by using HHO technique, it is hard to maintain the QoS requirement due to the delay in HO that occurs during eNB migration [111], Meanwhile, providing fast and seamless access to multimedia services and broadband internet application with minimum delay requirements is one of the main goals that should be achieved in LTE system.

The limitation of the HHO technique in LTE system in term of high data loss, disruption time, outage probability and interferences may cause un-reliable HO [99], especially for delay sensitive applications. From this point, I was motivated to highlight HY-HO technique as a solution to enhance the QoS parameters in LTE systems.

The main concept of HY-HO technique is to partially perform SHO for EF services and HHO for non-EF services. During the HO procedure, EF services are transmitted from both source and target eNBs, while non-EF services are transmitted by source or target eNBs. Figure 5.9 shows the concept of HY-HO, while Figure 5.10 shows the pseudo-code HY-HO scheduling algorithm, respectively.

From the theoretical analysis, the proposed HY-HO scheme reduces the HO latency and traffic delay compared with HHO. Furthermore, the proposed HY-HO technique enhances the QoS of EF services and improves the spectrum efficiency. Finally, the proposed HY-HO proce-

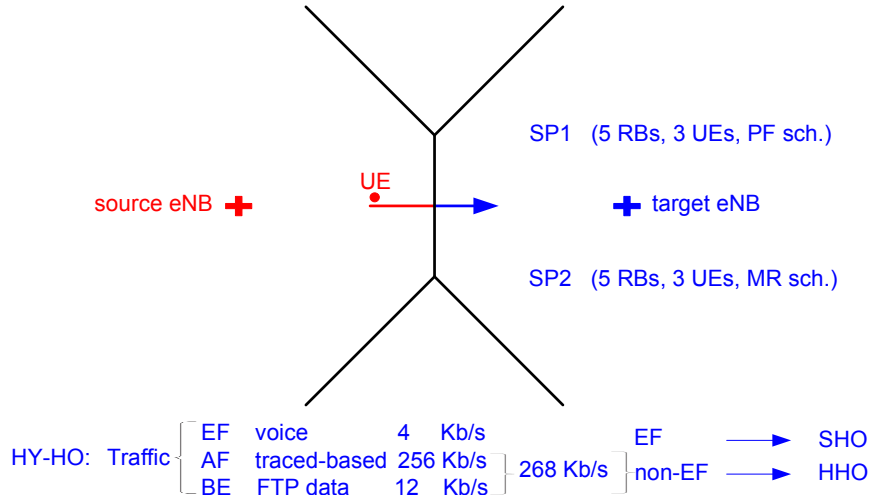


Figure 5.9: Hybrid handover scheme.

ture is backward compatible with LTE HO procedure. Therefore, HY-HO scheme can perform as a competitive choice to enhance the HO performance in LTE system.

5.7 The Allocation Scheduling Algorithms

Scheduling revenues are the charge of allocating RBs to active flows in both frequency and time domain. Many schedulers have been discussed in [11, 30, 32, 59], comparing data throughput, delay, fairness, and so on.

In this work full-buffer traffic model is considered. To foster customizable schedulers in the evolution, SPs with different utility functions (Ut) are investigated. It is assumed that SP-1 and SP-2 in the target cell foot-print share one eNB, and apply proportional fair (PF) scheduling and maximum-rate (MR) scheduling, respectively.

5.7.1 Proportional Fair Scheduling Algorithm

PF is the channel-aware scheduling algorithm that targets to increase the total throughput of the system and maintains fairness among UEs at the same time [89, 112, 113, 114]. In PF

```

1 : For each simulated TTI do
2 :    $av_{RB_s} = N$  // Total available  $RB_s$  in source and target SPs
   // phase i:  $RB_s$  allocation for traffic class  $i=1$  (EF traffic)
3 :   If  $av_{RB_s} > 0$  Then
4 :     For  $j = 1$  to  $U_{HO}$  do
5 :        $n_{ij} = \text{Ceil} \left\{ \frac{v_{ij}}{RB_{BW}} \right\}$ 
       // Needed  $RB_s$  to satisfy traffic  $i$  for  $UE_j$ 
6 :     End For
       // Needed  $RB_s$  by traffic  $i$  for UEs performing HO
7 :      $S_i = \sum_{j=1}^{U_{HO}} n_{ij}$ 
8 :     For  $j = 1$  to  $U_{HO}$  do
9 :        $n_{iRB_j} = \min \left( n_{ij}, \text{floor} \left\{ \frac{n_{ij} \times av_{RB_s}}{S_i} \right\} \right)$ 
       // Allocated  $RB_s$  for traffic class  $i$  for  $UE_j$ 
10:    End For
11:  End If
12:   $av_{RB_s} = N - \sum_{j=1}^{U_{HO}} n_{iRB_j}$  // Available  $RB_s$ 
13:  Repeat
14:    For  $j = 1$  to  $U_{HO}$  do
15:      Sort  $UE_s$  by  $\left[ \frac{n_{ij}}{n_{iRB_j}} > 1 \right]$  Descending
16:      If  $av_{RB_s} > 0$  Then
17:         $n_{iRB_j}^* = n_{iRB_j} + 1$ 
18:         $av_{RB_s}^* = av_{RB_s} - 1$ 
19:      End If
20:    End For
    // Satisfy either allocation request or vanished available  $RB_s$ 
21:  Until  $\left[ \frac{n_{ij}}{n_{iRB_j}} \leq 1 \text{ or } av_{RB_s} = 0 \right]$ 
22:  // Total available  $RB_s$  after allocation to traffic  $i$  for  $UE_j$ 
   $av_{RB_s} = N - \sum_{j=1}^U n_{iRB_j}$ 
23: End For // End of Simulation

```

Figure 5.10: The pseudo-code for HY-HO scheduling algorithm.

scheduling, data bearers are assigned the following utility function:

$$Ut_{m_n}(r) = \frac{T_{m_n}(r)}{\bar{T}_{m_n}} \quad (5.5)$$

where $T_{m_n}(r)$ is the TB size that can be transmitted by assigning the RB r to UE m in SP n , which is computed from Equation (5.2), and \bar{T}_{m_n} is the UE's historical average transmit data.

PF scheduler targets to maximize the sum of the utility functions as follows:

$$\max \sum_{r=1}^{K_n} \sum_{m_n=1}^{M_n} \frac{T_{m_n}(r)}{\bar{T}_{m_n}} \beta_{m_n,r}, \quad \forall n \quad (5.6)$$

subject to:

$$\sum_{m_n=1}^{M_n} \beta_{m_n,r} = 1, \quad \forall r \in K_n, n \quad (5.7)$$

To maximize the utility function, PF scheduler assigns RBs to UEs who have low historical average rates \bar{T}_{m_n} , which gives them more chances of using the resources and imposes fairness between UEs, or to UEs who have good channel quality $T_{m_n}(r)$ to increase the overall throughput of the system.

5.7.2 Maximum Rate Scheduling Algorithm

While, MR scheduling aims to increase the overall throughput of the system [115, 116] that can be achieved by assigning the following utility function to UEs:

$$Ut_{m_n}(r) = T_{m_n}(r), \quad \forall n \quad (5.8)$$

MR scheduler maximizes the sum of the utility functions

$$\max \sum_{r=1}^{K_n} \sum_{m_n=1}^{M_n} T_{m_n}(r) \beta_{m_n,r}, \quad \forall n \quad (5.9)$$

subject to:

$$\sum_{m_n=1}^{M_n} \beta_{m_n,r} = 1, \quad \forall r \in K_n, n \quad (5.10)$$

wherein, maximizing the objective function by assigning each RB to UEs who can transmit the largest data block over it.

To reduce control signalling overhead, the LTE standard recommends that, for each sub-frame, only one MCS should be used for all allocated UEs RBs [11, 12]. The RBs chunk and MCS that is assigned to UE determine the TB size. However, how the TB is shared between UEs' buffers is left to the UE's I.S.. In other words, distributing TB into a different UEs bearers is assumed to be handled by UE.

The I.S. distributes the received RBs grant among the different active traffic bearers, While taking into account the buffer load, priority of other UEs classes, etc.. This distribution is executed according to S.P. algorithm (discussed in Chapter 3) according to their highest flow and based on the latest buffer status information which may have changed since the buffer status was reported.

5.8 The Static and Virtualized Sharing Algorithm

The radio access network in the target cell connects multiple SPs and manages the resources allocation between them according to their SLA. Each SP owns a set of RBs K_n with no intersection between the different SPs' RBs, such that:

$$K_n \cap K_v = \phi, \quad \forall n, v \in \mathcal{N} \quad (5.11)$$

Before the HO operation, the UE performs the source SP's scheduler. During the HO; (I have three discussed cases) in case of HHO scheduling, the UE will be in Idle state (no allocation scheduling exist); in case of HY-HO scheduling, the UE perform HY-HO (HHO on the non-EF services (no allocation exist), and SHO on EF services (RBs allocated from the source

SP and target SP (SP-1)); in case of Vir. HY-HO scheduling, the UE perform Vir. HY-HO (HHO on the non-EF services (no allocation exist), and Vir. SHO on EF services (RBs allocated from the source SP and target SPs (SPs-1,2))).

While after the HO execution; in case of HHO and HY-HO scheduling; the UE performs the target SP's scheduling algorithm (SP-1); and in case of Vir. HY-HO scheduling; the UE allocates RBs from the target SPs (SPs-1,2)).

In this work, two scenarios are considered: static sharing (SS) and Vir. DS allocation scheduling. In SS, SPs are sharing only the common physical infra-structure eNB without sharing the channels among them; while in DS, LTE Vir. scheme the sharing agreement includes the SPs spectrum. Thus, SPs share their physical RBs.

5.8.1 Static Sharing Allocation

In this algorithm, each SP performs its allocation scheduling individually. Assuming an admission control scheme is applied, the resource allocation problem considering SS scenario between SPs can be expressed as:

$$\max \sum_t \sum_{n=1}^N \sum_{m_n=1}^{M_n} \sum_{r \in k} U_{t_{m_n,r}(t)} \psi_{m_n,r}(t) \quad (5.12a)$$

subject to

$$\sum_{n=1}^N \sum_{m_n=1}^{M_n} \sum_{r \in k} \psi_{m_n,r}(t) = 1, \forall t, k \in K_n \quad (5.12b)$$

$$\psi_{m_n,r}(t) \in \{0, 1\}, \forall m_n, r, t \quad (5.12c)$$

Equation (5.12a) represents the objective function that aims to maximize the overall Ut function for all UEs, where Ut and ψ are the decision variables. $Ut_{m_n,r}$ is the utility function of UE $_{m_n}$ assigned by the set of RBs k , and $\psi_{m_n,k}$ is a binary indicator used to denote whether the UE $_{m_n}$ is assigned by the set of RBs k or not.

Equation (5.12b) represents the exclusive allocation constraint [12], that ensures that at a

definite time t , only this set of RBs k is assigned to UE m_n . Equation (5.12c) shows the bounded values for the binary indicator $\psi_{m_n,k}$ that is equal 1 if RB r is assigned to UE m in SP n , and equal 0 otherwise.

5.8.2 Virtualized Dynamic Sharing Allocation

The same steps used in the SS scenario are used in the DS scenario. The only difference is that each SP assigns the best feasible RB to its UEs from the set K_{tot} that contains all RBs from all the different SPs.

In DS scheduling algorithm, a Vir. scheme is considered; wherein, the total RBs K_{tot} set is assumed to be fully pooled and accessible to the SPs [59]. RBs are assigned in accordance that SPs should be able to implement different scheduling policies. It is assumed that each UE per SP should receive at least its LBS, which it would otherwise receive in the case of a non-sharing scenario.

The resource allocation problem considering DS scenario between SPs can be expressed as:

$$\max \sum_{t=1}^{M_{tot}} \sum_{m=1}^{M_{tot}} \sum_{r \in k} U_{m,r}(t) \psi_{m,r}(t) \quad (5.13a)$$

subject to

$$\sum_{m=1}^{M_{tot}} \sum_{r \in k} \psi_{m,r}(t) = 1, \quad \forall t, k \in K_{tot} \quad (5.13b)$$

$$\psi_{m,r}(t) \in \{0, 1\}, \quad \forall m, r, t \quad (5.13c)$$

Similarly, equation (5.13a) represents the objective function that aims to maximize the overall utility function for all UEs, where $U_{m,r}$ and $\psi_{m,r}$ are the decision variables. Similarly, $\psi_{m,r}$ is a binary indicator used to denote whether the UE m is assigned the set of RBs k or not. Equations (5.13b and 5.13c) represents the exclusive allocation constraint [12], that ensures that at a definite time t , only this set of RBs k is assigned to UE m and the bounded values for the binary indicator $\psi_{m,r}$ respectively.

After the HO execution, the Vir. DS scheduling algorithm operates between the target cell SPs sharing their RBs. Wherein; M_{tot} and K_{tot} represent the total number of UEs and RBs respectively, in the target cell (SPs 1, and 2).

5.9 Simulation results

The scheme is tested using a discrete event simulator developed in MATLAB [65]. Furthermore, in order to combat the extreme uncertainty of self-similar traces and deliver conclusive results, the outcomes of multiple repeated simulation runs are averaged for each result. The solvers and the MATLAB simulator run on i7 core 3400 MHz with 12 GB of memory.

In this work, All UEs are processing EF traffic with rate 4 Kbit/s, and non-EF traffic with rate 268 Kbit/s. During the HO, the UE perform switching to a detached state for a certain time period such that there is no flows to and from the UE. This time interval is a simulator parameter (the default value is 30 ms) [64].

An urban environment is assumed with path-loss exponent of 4.5. All existing UEs are assumed to be active. Table 5.2 summarizes the list of simulation parameters and their default values.

The rate of HO versus various mobility speeds up to 350 Km/hr is plotted in Figure 5.11 investigated from the traveling pattern presented earlier in this chapter. Wherein, each mobile or UE is equipped with a single transmit antenna with 0 dB gain.

Level of 10000 calls is considered, each of uniform distribution time of average 80 s. The uniform distribution used for the spatial location of call initiations and steps' size with uniformly random distribution were chosen.

Similarly, the uniform distribution of mobiles directions over $[0, 2\pi]$ was chosen both for its simplicity and because it provides a rather general and realistic representation of real-life systems. Throughout a cellular system the relative orientation of streets and cells might vary somewhat randomly, giving on the average an approximately uniform distribution of possible

Table 5.2: Simulation Default Parameters and Values.

Parameter	Value
Spectrum allocation (UL, DL)	20 MHz
Carrier frequency	2 GHz
Number of subcarriers per RB	12 subcarriers
Neighboring subcarrier spacing	15 KHz
RB bandwidth	180 KHz
Slot duration	0.5 ms
Cell radius	1 Km
MCS	QPSK, 16QAM, 64QAM
UEs in SP1	5 UEs
UEs in SP2	5 UEs
RBs available in SP1	10 RBs
RBs available in SP2	10 RBs
SP1 scheduler	PF scheduling algorithm
SP2 scheduler	MR scheduling algorithm
Channel fading	Rayleigh
w	1
Iteration #	1e4
Mobility model	Random way model
Gap length	6 ms
Gap repetition	80 ms
gaps averaged	200 ms
eNB Tx power	46 dBm
UE Tx power	23 dBm
HO event model	A3 event model
Fading	Rayleigh
σ_n^2	1
ϵ	0
Coherence time	1 ms
Simulation time	80 s
Cells interference	Avoidance
path-loss exponent	4.5

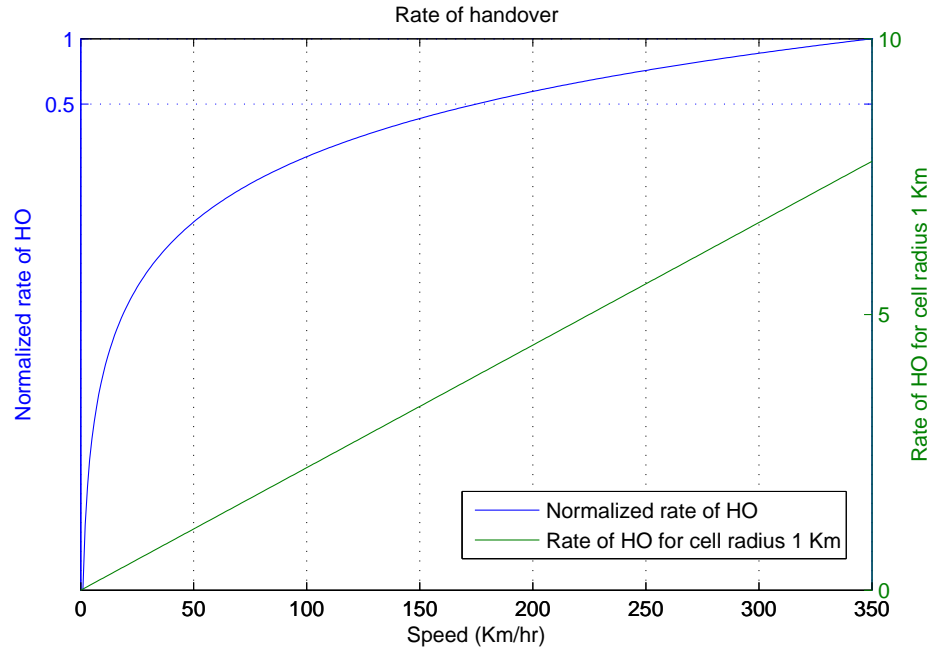


Figure 5.11: The rate of handover versus mobility speeds for cell radius of 1 Km.

directions.

The performance of high mobility UE is analyzed, that can be considered as a high mobility railway scenario with previous known information about the source and target eNBs, speed, direction of movement, and departure/arrival time of operation (disregarding the probability of ping pong effect). It is assumed that the UE moves with constant speed over the simulation, and the departure starts from the source eNB center, entering the target cell with 90° directional angle. Both eNBs have a radius of 1 Km, with 100 m overlap distance, wherein the RSRP starts to indicate the HO request.

Figures 5.12 and 5.13 show the average packets delay (EF and non-EF traffic) for mobility speed 150 Km/hr and 350 Km/hr receptively versus distance from eNB. The Vir. DS scenario ensures less average delays for EF and non-EF traffic than SS. This is due to UEs having access to a larger number of RBs, and thus they can be allocated better channels. The average packet delay for the non-EF overlaps for the HHO and HY-HO scheduling algorithm. This is because the HY-HO perform pure HHO on the non-EF traffic.

Noting that, mostly the EF class has 1 ms jitter, which is the minimum delay that could

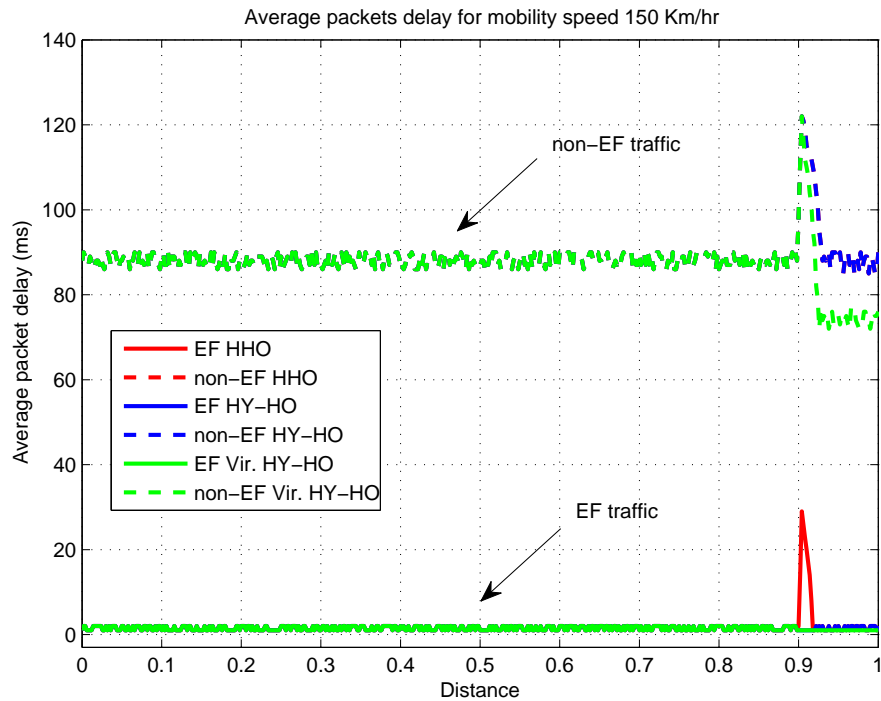


Figure 5.12: The average packets delay (EF and non-EF traffic) for mobility speed 150 Km/hr versus distance from eNB.

be satisfied (mapping time period). As in DS, the scheduler allocates more resources for the immigrant UE. Because of the higher arrival rate, the delay of the non-EF classes is noticed to be higher than EF within the entire network, moreover the I.S. gives the EF services higher priority access than non-EF.

The average packets delay (EF and non-EF traffic) for mobility speed 150 Km/hr and 350 Km/hr versus time (s) is plotted in Figure 5.14. It is clear that the UE moving with speed 350 Km/hr reaches the cell boundary and performs HO prior to the mobility speed 150 Km/hr.

The simulation results conclude that HY-HO Vir. DS scheme is capable of achieving great improvements with respect to delay when compared to the non-sharing application, improving the performances of EF during the UE's HO operation, and AF and BE traffic services after HO execution, leading to better QoS to be delivered.

In order to ensure the validity of the proposed algorithm, it is considered a mobile UE emigrant from source eNB to target eNB, exposed to high dense EF traffic with rate 40 Kbps

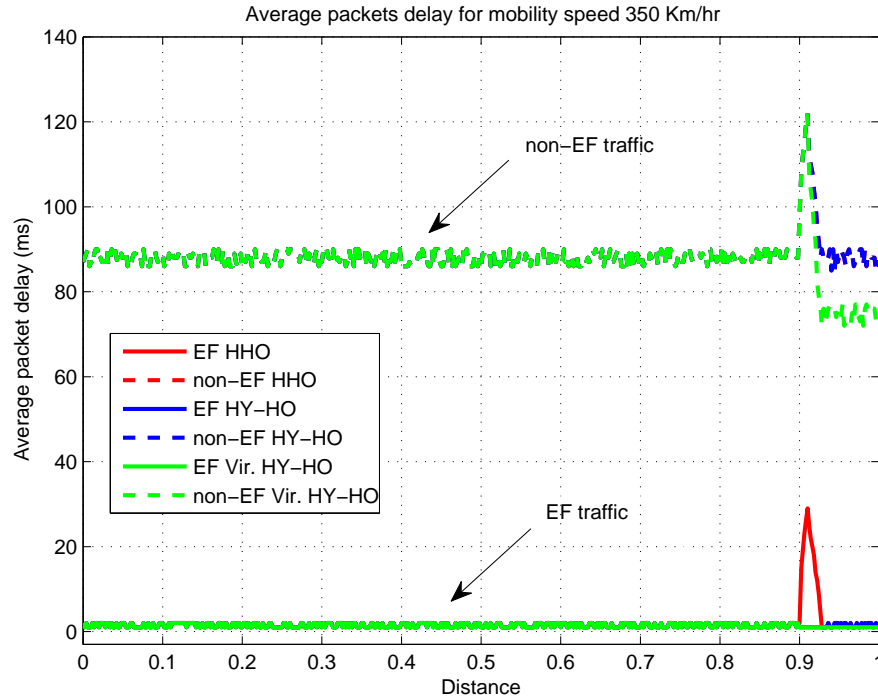


Figure 5.13: The average packets delay (EF and non-EF traffic) for mobility speed 350 Km/hr versus distance from eNB.

of CBR. Figures 5.15 and 5.16 show the average packet delay for mobility speeds 150 Km/hr and 350 Km/hr versus the distance from the source eNB. While, Figure 5.17 plots the average packet delay for mobility speeds 150 Km/hr and 350 Km/hr versus the time.

The simulation results was able to prove that HY-HO Vir. DS scheme is capable to handle the high dense EF traffic services and achieve great improvements with respect to delay when compared to the non-sharing application, improving the performances of EF during the UE's HO operation and enhance the QoS's parameters for the next wireless network generation.

5.10 Conclusion

In this chapter, the framework model represented pertains to analyze the performance of UE's HO algorithm in LTE systems. A HY-HO technique is proposed to cover the short comings of the existing approaches. The HY-HO scheme is based on the combination of SHO and

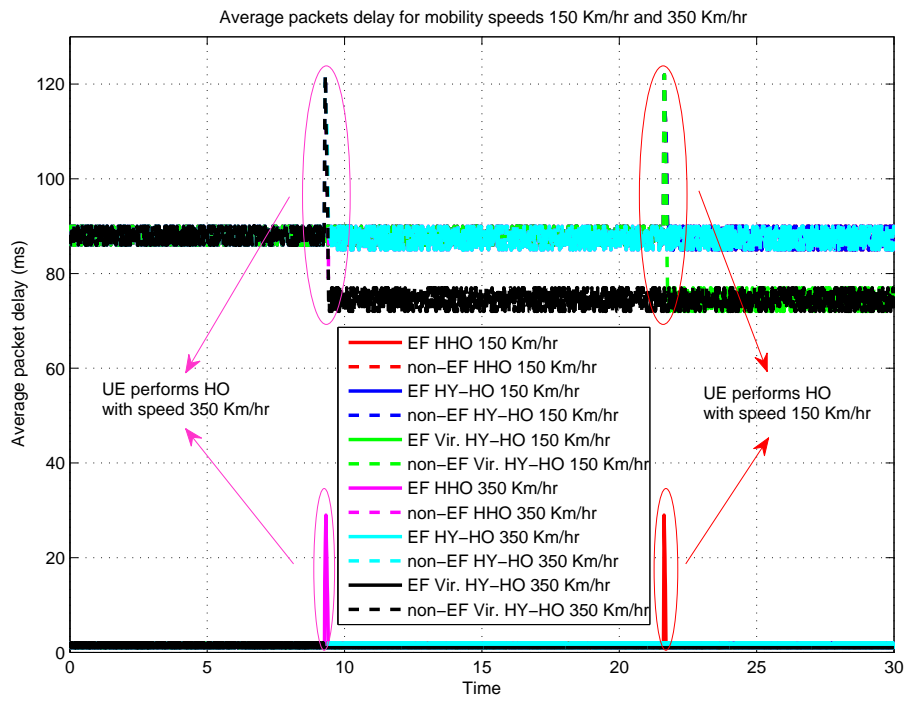


Figure 5.14: The average packets delay (EF and non-EF traffic) for mobility speeds 150 and 350 Km/hr versus time.

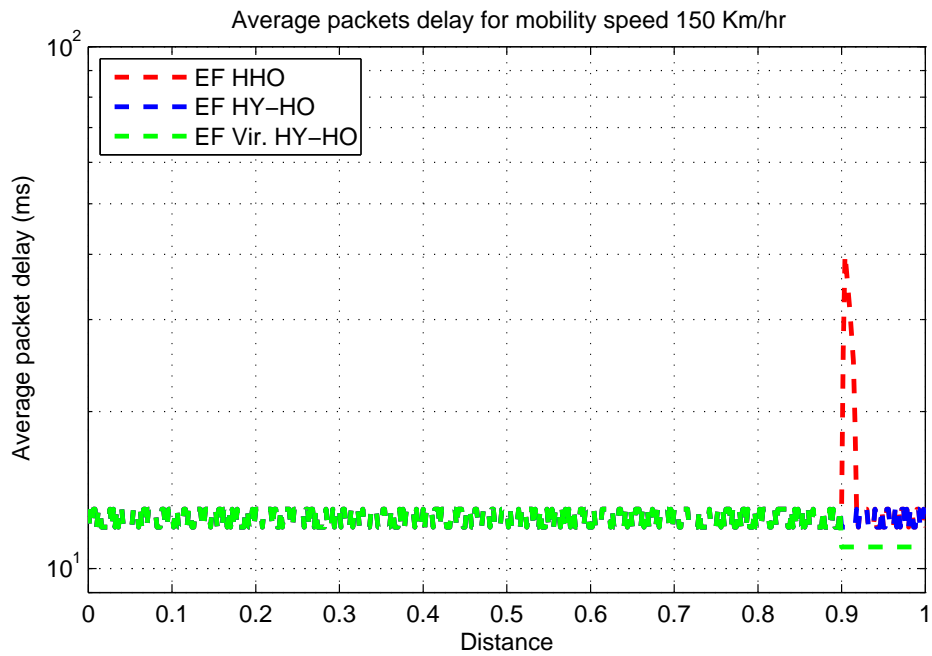


Figure 5.15: The average packets delay (high dense EF traffic) for mobility speed 150 Km/hr versus distance.

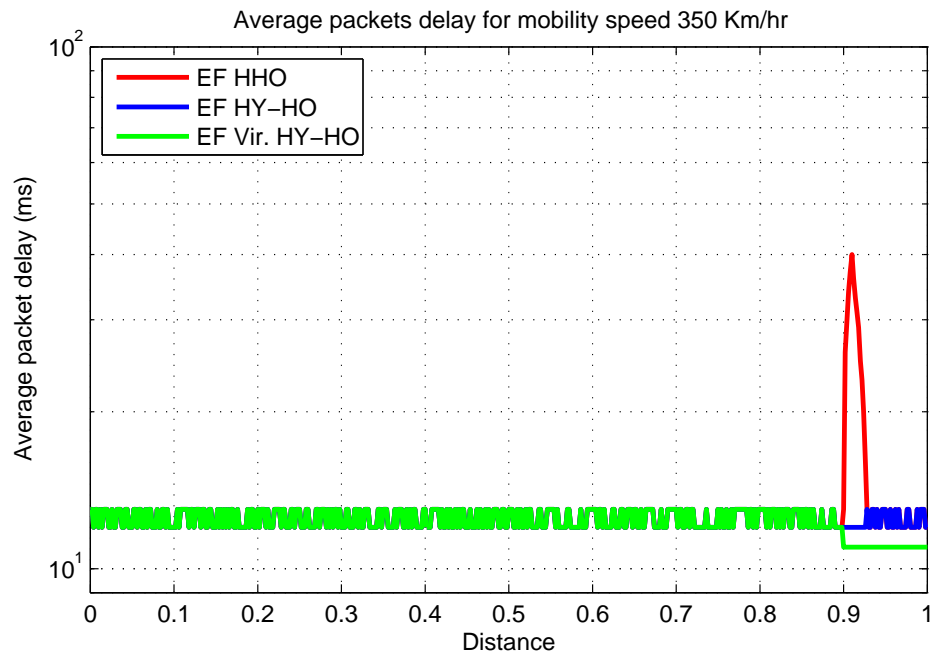


Figure 5.16: The average packets delay (high dense EF traffic) for mobility speed 350 Km/hr versus distance.

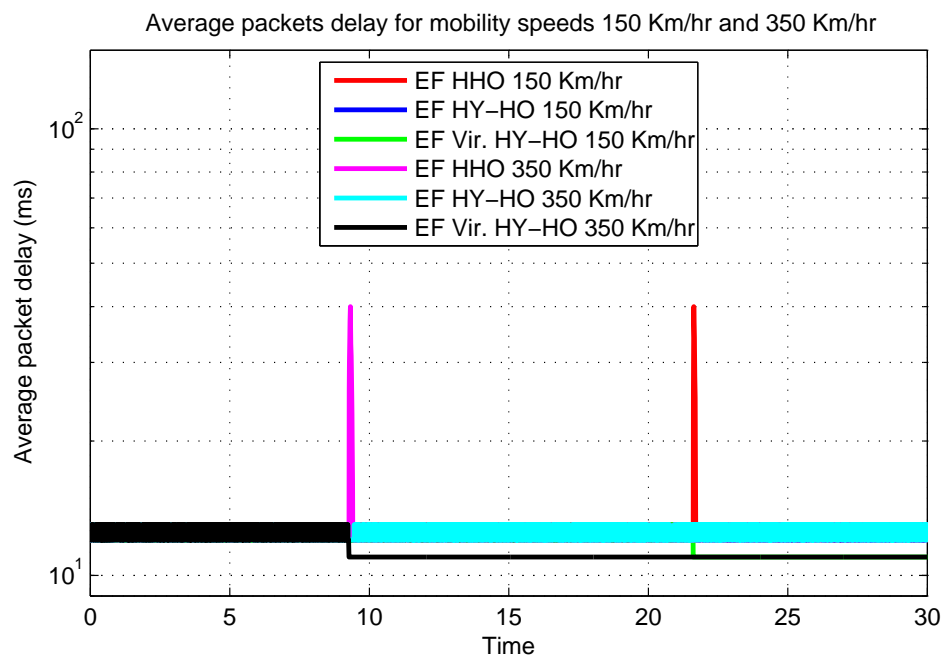


Figure 5.17: The average packets delay (high dense EF traffic) for mobility speeds 150 and 350 Km/hr versus time.

HHO. The combination was able to enhance the system performance in term of latency, interruption time and reliability during handover especially at cell boundary.

Also, the combination reduces the transmission overhead on the serving cell, which balances the traffic load within the system cells in LTE. I also evaluated the average packets delays for cases of SS and DS schemes, with the goal to close the growing gap between the capacities of backbone networks.

According to the simulation results, HY-HO virtualized DS scheme is capable of achieving great improvements with respect to delay when compared to the non-sharing application. This improvement allows SPs to customize their efforts, schedulers, and control the sharing of multi-SP resources between them.

Overall, the results confirm that the HY-HO framework yields notable improvements in average packet delay, without degrading QoS support for EF, AF, and BE services. Nonetheless, the performances of AF and BE as non-EF services are yet to be further improved, and QoS to be better delivered.

Chapter 6

Thesis Summary and Future Work

As time goes on, the need for enhancing QoSs' parameters in order to reach a future technology becomes more and more paramount. Interestingly enough, while the penetration rate for mobile users and breadth of device features continues to increase, the need for more research improvement in wireless communication networks is still of importance.

6.1 Thesis Summary

In this thesis designs are proposed for both scheduling and resource allocation methods that offer reduced complexity in multi-stream (multi-user), virtualized scenarios in both DL and UL systems.

In Chapter 3, I examined a novel design for a virtualized resources' sharing technique. This novel approach can be used to efficiently schedule traffic streams with differing QoS parameters without needing to resort to full scale optimization techniques while still guaranteeing throughput and average delay constraints.

Wherein, SPs using different scheduling algorithms are sharing their physical radio RBs in one eNB in a virtualized scheme as a promising solution for reducing operational and capital expenditures. The proposed method makes use to schedule traffic with various delay and priority requirements.

However, next in Chapters 4 and 5 this dynamic virtualization was considered. First, the main contributions in Chapter 4 resulted in a detailed study of modeling an optimized solution for the simulated sharing scheme methodology used in Chapter 3. Wherein, an optimized efficient power scheduling was proposed for a dynamic policy framework, which meets exclusive and contiguous allocation, maximum transmission power, and rate constraints restrictions while minimizing the average applied transmission power for a time-invariant channel to achieve green communication.

This dynamic virtualized scheme was used in Chapter 5 to design an extended scheduling scheme that exploited this information about the underlying channel statistics. The main contribution of this Chapter 5 was an extension of the work in Chapter 3. Wherein, the performance of UEs random-way mobility model and HO algorithms for high-mobility users was analyzed in a virtualized LTE systems. A HY-HO technique is proposed to address the shortcomings of the existing approaches and the challenges caused by the demand for high data rates. The results confirm that the HY-HO framework yields notable improvements in average packet delay, without degrading QoS.

Overall, one of the primary arguments made in this thesis is the large complexity associated with heterogenous scheduling techniques, particularly when attempting to minimize energy expended in the mobile radio. While in this thesis, methods of complexity reduction in scheduling were shown while attempting to minimize energy expenditure, it is important to note that this research area is still wide open and that there is no single solution to this complexity problems. This is particularly true as the constraints imposed by practical systems vary dramatically from system to system.

6.2 Future Work

The work in this thesis presents some investigation into the multi-stream scheduling problems, particularly with a focus on complexity issues in virtualized LTE systems. Although,

some novel techniques to reduce complexity and address this problem were proposed, there still remains numerous open issues in this area. In this section, I highlight some of these major issues that can use Virtualization in order to improve the network performance in wireless communications, enhance the QoSs' parameters, and move towards the future.

6.2.1 Optimal D2D User Allocation in Virtualized Scheduling Algorithm

The device-to-device (D2D) communication is a type of close range data transmission over a direct link and coexists with cellular networks in an underlay manner [117]. The D2D communication has advantages of enhancing network throughput, saving the power of user equipment and increasing an instantaneous data rate, which draw much attention in the recent years.

Spectrum sharing mechanism and transmission capacity are two fundamental issues of the heterogeneous system which allows secondary users sharing resource with primary users in the licensed band.

Hence, how the schedule D2D pairs working on different bands to reduce interference and improve the network capacity is an important issue that should be discussed in dynamic virtualized network environment.

6.2.2 Energy-Efficient for Green Smart Grid Communication in Virtualized Scheduling Algorithm

A smart grid is conceptualized as a combination of underlay electrical network and overlay communication network. Therefore, the communication network plays an important role for exchanging real-time information [118]. Consequently, the smart meters deployed at the customers end communicate with the SP for cost-effective and reliable energy supply to the users.

Therefore, it is necessary to establish a green wireless communication architecture that takes into account the environmental issues. Therefore, the smart meters consume huge amount of energy for real-time communication. On the other hand, plug-in hybrid vehicles (PHEVs)

play an important role to relieve the on-peak hour load from the grid, and acts as storage device as well. Intuitively, PHEVs will also communicate with the SP in order to have real-time information.

Therefore, implementation of cooperative strategies of smart meters and PHEVs can have significant impact in reducing the energy consumption in smart grids. Consequently, it is important to propose an energy-efficient technique for smart metering towards green wireless communications in the smart grid in virtualized scheduling algorithm.

6.2.3 Green Heterogeneous Networks in Virtualized Scheduling Algorithm

Despite the ever growing investment in macro-cell base stations, users still often suffer from low signal strength and poor service quality in indoor environments, especially 3G cellular networks operating in high-frequency bands [119]. To solve this problems, in UMTS LTE network, macro-cell eNB implements a significant high DL power to guarantee the QoS of associated with macro-mobile stations. However, for the edge MSs or the MSs located in a spot with their specific locations and significant interferences to the eNB, the QoS can never been guaranteed well.

More importantly, deploying femtocell underlying macrocell as a two-tier heterogeneous networks (HetNet) has been proven to greatly improve indoor coverage and system capacity. More importantly, some unique features of HetNets present more challenges in interference mitigation in the two-tier HetNets, such as random deployment for femto-cells, non-existence of macrofemto backhaul coordination and mandates forbidding to making any modifications of existing macro-cells.

Therefore, the efficient interference mitigation techniques in HetNets require resource cognition ability, which will provide more available cognitive resource opportunity of the physical RBs in space or time of macro-cell; autonomous mechanism design, where each HetNet can selfishly adjust system parameters in a self-organising way; scalability, which is perspective

required by the promising densely co-located femto-cell in the foreseeable future.

To tackle these challenges, cognitive radio HetNets to concise available resource and adapt to HetNet environments resource allocation scheme in virtualized scheduling algorithm should be considered.

Bibliography

- [1] H. Safa, and K. Tohme, “*LTE Uplink Scheduling Algorithms: Performance and Challenges*” , 19th International Conference Telecommunications (ICT), pp. 1-6, Jounieh, Apr. 2012.

- [2] R. Y. Kim, I. Jung, X. Yang, and C. Chou, “*Advanced Handover Schemes in IMT-Advanced Systems [WiMAX/LTE Update]*”, IEEE Communications Magazine, vol. 48, no. 8, pp. 78-85, Aug. 2010.

- [3] I. C. Wong and B. L. Evans, “*Optimal OFDMA Resource Allocation with Linear Complexity to Maximize Ergodic Rates*”, IEEE Transactions on Wireless Communications, vol. 7, no. 3, pp. 962-971, Mar. 2008.

- [4] 4G Americas, “*4G Mobile Broadband Evolution: 3GPP Release 11, Release 12 and Beyond*”, Feb. 2014.

- [5] H. Holma and A. Toskala, “*LTE for UMTS OFDMA and SC-FDMA Based Radio Access*”, 2009.

- [6] E. Prabhakar, B. Biyikoglu and A. El Gamal, “*Energy-Efficient Transmission over a Wireless Link via Lazy Packet Scheduling*”, in International Conference Computer Communications (INFOCOM), pp. 386-394, Anchorage, AK, Apr. 2001.

- [7] K. Elgazzar, M. Salah, A. E. M. Taha, and H. Hassanein, “*Comparing Uplink Schedulers for LTE*”, IEEE 6th International Wireless Communications and Mobile Computing Conference (IWCMC), pp. 189193, New York, USA, 2010.

- [8] A. S. AlQahtani, and M. Alhassany, “*Comparing Different LTE Scheduling Schemes*”, IEEE 12th International Symposium on Network Computing and Applications (IWCMC), pp. 264-269, Sardinia, Jul. 2013.
- [9] J. Chang, Y. Li, S. Feng, H. Wang, C. Sun, and P. Zhang, “*A Fractional Soft Handover Scheme for 3GPP LTE-Advanced System*”, in IEEE International Conference on Communications, pp. 1-5, Dresden, Jun. 2009.
- [10] M. Bechler, H. Ritter, J. H. Schiller, “*Quality of Service in Mobile and Wireless Networks: The Need for Proactive and Adaptive Applications*”, IEEE Hawaii International Conference on System Sciences (HICSS), Jan. 2000.
- [11] M. Hussein, S. Primak, and A. Shami, “*On Sharing Resources Performance Analysis in 3GPP-LTE Systems Framework*”, IEEE International Wireless Communications and Mobile Computing, pp. 302-307, Dubrovnik, Aug. 2015.
- [12] M. Hussein, A. Moubayed, S. Primak, and A. Shami, “*On Efficient Power Allocation Modeling in Virtualized Uplink 3GPP-LTE Systems*”, IEEE International Conference on Wireless and Mobile Computing, Networking and Communications (WiMob), Abu Dhabi , pp. 817-824, Oct. 2015.
- [13] M. Hussein, S. Primak, and A. Shami, “*Intra-MME/S-GW Handover Performance Analysis in Virtualized 3GPP-LTE Systems*”, in press. IEEE International Conference on Wireless and Mobile Computing (CCECE), Networking and Comm., Vancouver, Canada, May. 2016.
- [14] 3GPP.TS.36.213 11.0.0, “*LTE; Evolved Universal Terrestrial Radio Access (E-UTRA); Physical Layer Procedures*”, 2012.
- [15] 3GPP TR 36.814, “*Further Advancements for E-UTRA Physical Layer Aspects*”, 2009.
- [16] W. Rhee and J. Cioffi, “*Increase in Capacity of Multiuser OFDM System using Dynamic Subchannel Allocation*”, IEEE Vehicular Technology Conference (VTC-Spring), pp. 1085-1089, Tokyo Japan, May 2000.

- [17] E. Dahlman, S. Parkvall, J. Skold and P. Beming, “*3G Evolution HSPA and LTE for Mobile Broadband 2nd edition*”, 2008.
- [18] <http://www.4gamericas.org/index>.
- [19] A. Ghosh, and R. Ratasuk, “*Essentials of LTE and LTE-A*”, 2011.
- [20] S. Sesia, I. Toufik, and M. Baker, “*LTE-The UMTS Long Term Evolution: From Theory to Practice*”, 1st Edition, Wiley Publishing, 2009.
- [21] S. Sesia, I. Toufik, and M. Baker ”*LTE-The UMTS Long Term Evolution: From Theory to Practice*,” 2nd Edition, Wiley Publishing, Aug. 2011.
- [22] J. Wu, and P. Fan, ”*A Survey on High Mobility Wireless Communications: Challenges, Opportunities and Solutions*,” IEEE Access, vol. PP, no. 99, pp. 1-26, Jan. 2016.
- [23] 3GPP, “*Evolved Universal Terrestrial Radio Access (E-UTRA); Long Term Evolution (LTE) Physical Layer; General Description*”, TS 36.201.
- [24] 3GPP, “*Evolved Universal Terrestrial Radio Access (E-UTRA); Physical Layer Procedures*”, TS 36.213.
- [25] I. Toufik, F. Matthew, B. Philips, and S. Sesia, “*LTE The UMTS Long Term Evolution From Theory to Practice*”, ST-NXP Wireless/ETSI Research, UK, 2009.
- [26] 3GPP TS 25.814, Technical Specifications, “*Group Radio Access Network; Physical layer aspect for evolved Universal Terrestrial Radio Access (UTRA)*”, Release 7.
- [27] H. Wei, H.Jing, and W. Haiming, “*Full Uplink Performance Evaluation of FDD/TDD LTE-Advanced Networks with Type-1 Relays*”, IEEE Vehicular Technology Conference (VTC-Fall), pp. 1-5, San Francisco, USA, Sept. 2011.
- [28] “*An Introduction to LTE, LTE-Advanced, SAE and 4G Mobile Communications*”, Christopher Cox, 2012.
- [29] J. Ikuno, M. Wrulich, and M. Rupp, “*Performance and Modeling of LTE H-ARQ*”, IEEE Workshop on Smart Antennas, Berlin, Germany, pp. 1-6, Feb. 2009.

- [30] M. Kalil, A. Shami, and A. Al-Dweik, “*QoS-Aware Power-Efficient Scheduler for LTE Uplink*”, IEEE Transactions on Mobile Computing, vol. 14, no. 8, pp. 1672-1685, Aug. 2015.
- [31] H. Hawilo, A. Shami, M. Mirahmadi, and R. Asal, “*NFV: State of the Art, Challenges, and Implementation in Next Generation Mobile Networks (vEPC)*”, IEEE Network, vol. 28, no. 6, pp. 18-26, Dec. 2014.
- [32] M. Kamel, L. Bao Le, and A. Girard, “*LTE Wireless Network Virtualization: Dynamic Slicing via Flexible Scheduling*”, Vehicular Technology Conference (VTC-Fall), pp. 1-5, Vancouver, BC, Sept. 2014.
- [33] https://en.wikipedia.org/wiki/Mobile_network_operator.
- [34] J. Han, and H. Wang, “*Uplink Performance Evaluation of Wireless Self-Backhauling Relay in LTE-Advanced*”, IEEE International Conference on Wireless Communications Networking and Mobile Computing (WiCOM), pp. 1-4, Chengdu, China, Sept. 2010.
- [35] L. Zhao, M. Li, Y. Zaki, A. Timm-Giel, and C. Gorg, “*LTE virtualization: From Theoretical Gain to Practical Solution*”, in 23rd International Teletraffic Congress (ITC), pp. 71-78, Sept. 2011.
- [36] Y. Zaki, L. Zhao, C. Goerg, and A. Timm Giel, “*LTE Wireless Virtualization and Spectrum Management*”, in Wireless and Mobile Networking Conference (WMNC), pp. 1-6, Budapest, Oct. 2010.
- [37] M. Li, L. Zhao, X. Li, Y. Zaki, A. Timm-Giel, and C. Gorg, “*Investigation of Network Virtualization and Load Balancing Techniques in LTE Networks*”, in IEEE Vehicular Technology Conference (VTC-Spring), Yokohama, pp. 1-5, May 2012.
- [38] R. Kokku, R. Mahindra, H. Zhang, and S. Rangarajan, “*Cellslice: Cellular Wireless Resource Slicing for Active RAN Sharing*”, 5th International Conference on Communication Systems and Networks (COMSNETS), Bangalore, pp. 1-10, Jan. 2013.

- [39] M. Lee, and S. Keun Oh, “*On Resource Block Sharing in 3GPP-LTE System*”, 17th Asia-Pacific Conference on Communications (APCC), pp. 38-42, 2011.
- [40] O. Bulakci, A. Bou Saleh, S. Redana, B. Raaf, and J. Hamalainen, “*Resource Sharing in LTE-Advanced Relay Networks: Uplink System Performance Analysis*”, IEEE Transactions on Emerging Telecommunications Technology, vol. 24, no. 1, pp. 32-48, Jan. 2013.
- [41] M. C. Necker, “*Integrated Scheduling and Interference Coordination in Cellular OFDMA Networks*”, IEEE Broadband Communications, Networks and Systems, pp. 559-566, Raleigh, NC, USA, Sept. 2007.
- [42] S. Silverman, “*Game Theory and Software Radio Networks*”, Military Communications Conference (MILCOM), pp. 1-7, Washington, DC, Oct. 2006.
- [43] O. Bulakci, A. Bou Saleh, S. Redana, B. Raaf, and J. Hmlinen, “*Flexible Back-haul Resource Sharing and Uplink Power Control Optimization in LTE-Advanced Relay Networks*”, IEEE Vehicular Technology Conference (VTC), pp. 1-6, San Francisco, USA, Sept. 2011.
- [44] R. Kokku, R. Mahindra, H. Zhang, and S. Rangarajan, “*NVS: A Substrate for Virtualizing Wireless Resources in Cellular Networks*” IEEE/ACM Transaction Networking, vol. 20, no. 5, pp. 1333-1346, 2012.
- [45] S. Roth, J. Gan, and D. Danev, “*Subframe Allocation for Relay Networks in the LTE-Advanced Standard*”, IEEE 21st International Symposium on Personal Indoor and Mobile Radio Communications (PIMRC), pp. 1758-1763, Istanbul, Turkey, Sept. 2010.
- [46] F. Fu, and U. Kozat, “*Stochastic Game for Wireless Network Virtualization*”, IEEE Transaction on Association for Computing Machinery Networking, vol. 21, no. 1, pp. 84-97, Feb. 2013.
- [47] S. AlQahtani, and M. AlHassany, “*Performance Modeling and Evaluation of a Novel Scheduling Algorithm for LTE Networks*”, IEEE 12th International Symposium on Network Computing and Applications (NCA), pp. 101-105, Cambridge, MA, Aug. 2013.

- [48] H. Yang, F. Ren, C. Lin, and J. Zhang, “*Frequency-Domain Packet Scheduling for 3GPP LTE Uplink*”, IEEE INFOCOM, pp. 1-9, San Diego, CA, Mar. 2010.
- [49] T. Camp, J. Boleng, and V. Davies, “*A Survey of Mobility Models for Ad Hoc Network Research*”, Wireless Communications and Mobile Computing, vol. 2, no. 5, pp. 483-502, Aug. 2002.
- [50] F. Calabrese, C. Rosa, M. Anas, P. Michaelson, K. Pedersen, and P. Mogensen, “*Adaptive Transmission Bandwidth Based Packet Scheduling for LTE Uplink*”, IEEE Vehicular Technology Conference (VTC-Fall), Calgary, Canada, pp. 1-5, Sept. 2008.
- [51] D. Dechene, and A. Shami, “*Energy-Aware Resource Allocation Strategies for LTE Uplink with Synchronous HARQ Constraints*”, IEEE Transactions on Mobile Computing, vol. 13, no. 2, pp. 422-433, Feb. 2014.
- [52] M. Salah, N. A. Ali , A. E. Taha, and H. Hassanein, “*Evaluating Uplink Schedulers in LTE in Mixed Traffic Environments*”, IEEE International Conference in Communications (ICC), pp. 1-5, Kyoto, Jun. 2011.
- [53] A. Shami, X. Bai, Chadi M. Assi, and N. Ghani, “*Jitter Performance in Ethernet Passive Optical Networks*”, Journal of Light Wave Technology, vol. 23, no. 4, pp. 1745-1753, Apr. 2005.
- [54] M. Mirahmadi and A. Shami, “*Traffic-Prediction-Assisted Dynamic Bandwidth Assignment for Hybrid Optical Wireless Networks*”, El-Sevier Computer Networks Journal, 2012, vol. 56, no. 1, pp. 244-259.
- [55] C. Chuah and R. H. Katz, “*Characterizing Packet Audio Streams from Internet Multimedia Applications*”, IEEE International Conference on Communications (ICC), IEEE, vol. 2, pp. 1199-1203, 2002.
- [56] Video trace library: <http://trace.eas.asu.edu/>
- [57] G. Shen, R. Tucker, and C. J. Chae, “*Fixed Mobile Convergence Architectures for Broadband Access: Integration of EPON and WIMAX [Topics in Optical Communications]*”, IEEE Communications Magazine, vol. 45, no.8, pp. 44-50, 2007.

- [58] N. Nie and C. Comaniciu, “*Adaptive Channel Allocation Spectrum Etiquette for Cognitive Radio Networks*”, IEEE International Symposium on New Frontiers in Dynamic Spectrum Access Networks, pp. 269-278, Baltimore, MD, USA, Nov. 2005.
- [59] M. Kalil, A. Shami, and Y. Yinghua, “*Wireless Resources Virtualization in LTE Systems*”, in IEEE INFOCOM Workshop on Computer Communications, pp. 363-368, Toronto, ON, Apr. 2014.
- [60] D. J. Dechene and A. Shami, “*Energy Efficient Resource Allocation in SC-FDMA Uplink with Synchronous HARQ Constraints*”, IEEE International Conference on Communications, pp. 1-5, Kyoto, Japan, Jun. 2011.
- [61] N. Ferdosian, and M. Othman, “*Two-Level QoS-Oriented Downlink Packet Schedulers in LTE Networks: A Review*”, 1st International Conference on Advanced Data and Information Engineering (DaEng), pp. 597-604, Dec. 2013.
- [62] W. Hong, J. Han, and H. Wang, “*Full Uplink Performance Evaluation of FDD/TDD LTE-Advanced Networks with Type-1 Relays*”, IEEE Vehicular Technology Conference, San Francisco, USA, pp. 1-5, Sept. 2011.
- [63] G. Dimic and N. Sidiropoulos, “*On Downlink Beam forming with Greedy User Selection: Performance Analysis and a Simple New Algorithm*”, IEEE Transactions on Signal Processing, vol. 53, no. 10, pp. 3857-3868, Oct. 2005.
- [64] G. Piro, L. A. Grieco, G. Boggia, F. Capozzi, and P. Camarda, “*Simulating LTE Cellular Systems: An Open-Source Framework*”, IEEE Transactions on Vehicular Technology, vol. 60, no. 4, pp. 498-513, Feb. 2011.
- [65] The MathWorks Inc., “*MATLAB R2008a*”, 2008.
- [66] V. Chandrasekhar, and J. G. Andrews, “*Spectrum Allocation in Two-Tier Networks*”, IEEE 42nd Asilomar Conference on Signals, Systems and Computers, pp. 1583-1587, Pacific Grove, Oct. 2008

- [67] A. Abdelnasser, E. Hossain, and Dong In Kim, “*Clustering and Resource Allocation for Dense Femtocells in a Two-Tier Cellular OFDMA Network*”, IEEE Transactions on Wireless Communications, vol. 13, no. 3, pp. 1628-1641, Mar. 2014.
- [68] W. Li, W. Zheng, H. Zhang, T. Su, and X. Wen “*Energy-Efficient Resource Allocation with Interference Mitigation for Two-Tier OFDMA Femtocell Networks*”, IEEE 23rd International Symposium on Personal Indoor and Mobile Radio Communications (PIMRC), pp. 507-511, Sydney, Sept. 2012.
- [69] L. Gao, X. Wang, G. Sun, and Y. Xu, “*A Game Approach for Cell Selection and Resource Allocation in Heterogeneous Wireless Networks*”, IEEE 8th Annual Communications Society Conference on Sensor, Mesh and Ad Hoc Communications and Networks (SECON), pp. 530-538, Salt Lake City, Jun. 2011.
- [70] H. Marshoud, H. Otok, H. Barada, R. Estrada, A. Jarray, and Z. Dziong, “*Resource Allocation in Macrocell-Femtocell Network using Genetic Algorithm*”, IEEE 8th International Conference on Wireless and Mobile Computing, Networking and Communications (WiMob), pp. 474-479, Barcelona, Oct. 2012.
- [71] X. Chen, Y. Si, and X. Xiang, “*Delay-Bounded Priority-Driven Resource Allocation for Two-Tier Macrocell/Femtocell Downlink*”, IEEE 5th International Conference on Game Theory for Networks (GAMENETS), pp. 1-6, Beijing, Nov. 2014.
- [72] G. Miao, N. Himayat, G.Y. Li, S. Talwar, “*Low-Complexity Energy-Efficient Scheduling for Uplink OFDMA*”, IEEE Transactions on Communications, vol. 60, no. 1, pp. 112-120, Jan. 2012.
- [73] S.-H. Kuo and J. Cavers, “*Energy Optimal Scheduler for Diversity Fading Channels with Maximum Delay Constraints*”, IEEE Transactions on Wireless Communications, vol. 8, no. 11, pp. 5520-5529, Nov. 2009.
- [74] F. Meshkati, H. Poor, S. Schwartz, and R. Balan, “*Energy-Efficient Resource Allocation in Wireless Networks with Quality-of-Service Constraints*”, IEEE Transactions on Communications, vol. 57, no. 11, pp. 3406-3414, Nov. 2009.

- [75] X. Bai, A. Shami, and S. Primak, “*Power Efficient Scheduling over Fading Channel for Cross-Layer Optimization*”, Wiley Wireless Communications and Mobile Computing, vol. 12, no. 13, 2011.
- [76] S. Jungsup, G. Gye-Tae, and K. Dong-Hoi, “*Packet-Scheduling Algorithm by the Ratio of Transmit Power to the Transmission Bits in 3GPP LTE Downlink*”, EURASIP Journal on Wireless Communications and Networking (EURASIP JWCN), Jul. 2010.
- [77] A. Marques, L. Lopez-Ramos, G. Giannakis, J. Ramos, and A. Caama Ando, “*Optimal Cross-Layer Resource Allocation in Cellular Networks using Channel- and Queue-State Information*”, IEEE Transactions on Vehicular Technology, vol. 61, no. 6, pp. 2789-2807, July 2012.
- [78] B. Al-Manthari, H. Hassanein, N. Ali, and N. Nasser, “*Fair Class-based Downlink Scheduling with Revenue Considerations in Next Generation Broadband Wireless Access Systems*”, IEEE Transactions on Mobile Computing, vol. 8, no. 6, pp. 721-734, Jun. 2009.
- [79] G. Song and Y. Li, “*Utility-Based Resource Allocation and Scheduling in OFDM-Based Wireless Broadband Networks*”, IEEE Communications Magazine, vol. 43, no. 12, pp. 127-134, 2005.
- [80] T. F. Maciel and A. Klein, “*On the Performance, Complexity, and Fairness of Suboptimal Resource Allocation for Multiuser MIMO-OFDMA Systems*”, IEEE Transactions on Vehicular Technology, vol. 59, no. 1, pp. 406-419, Jan. 2010.
- [81] K. Seong, M. Mohseni, and J. Cioffi, “*Optimal Resource Allocation for OFDMA Downlink Systems*”, in Proc of IEEE International Symposium on Information Theory, pp. 1394-1398, Seattle, USA, Dec. 2006.
- [82] X. Bai, A. Shami, and S. Primak, “*Optimal Power Control over Fading Channel with Cross-Layer Performance Constraint*”, in Proc. of IEEE International Conference on Communications, pp. 2265-2269, Beijing, China, May 2008.
- [83] D. Feng, C. Jiang, G. Lim, L.J. Cimini, G. Feng, G.Y. Li, “*A Survey of Energy-Efficient*

- Wireless Communications*”, IEEE Communications Surveys & Tutorials, vol. 15, no. 1, pp. 167-178, Feb. 2013.
- [84] X. Zhu, J. Huo, X. Xu, C. Xu, and W. Ding, “*QoS-Guaranteed Scheduling and Resource Allocation Algorithm for IEEE 802.16 OFDMA System*”, in Proc of IEEE International Conference on Communications, pp. 3463-3468 Beijing, China, May 2008.
- [85] http://www.sharetechnote.com/html/Handbook_LTE_QCI.html.
- [86] N. Abu-Ali, A. M. Taha, M. Salah, and H. Hassanein, “*Uplink Scheduling in LTE and LTE-Advanced: Tutorial, Survey, and Evaluation Framework*”, IEEE Communications Surveys & Tutorials, vol. 16, no. 3, pp. 1239-1265, Dec. 2013.
- [87] G. Song and Y. Li, “*Cross-Layer Optimization for OFDM Wireless Networks-Part II: Algorithm Development*”, IEEE Transactions on Wireless Communications, vol. 4, no. 2, pp. 625-634, Mar. 2005.
- [88] H. G. Myung, J. Lim, and D. J. Goodman, “*Single Carrier FDMA for Uplink Wireless Transmission*”, IEEE Vehicular Technology Society, vol. 1, no. 3, pp. 30-38, Sept. 2006.
- [89] J. Lim, H. Myung, K. Oh, and D. Goodman, “*Proportional Fair Scheduling of Uplink Single-Carrier FDMA Systems*”, IEEE Symposium Personal Indoor Mobile Radio Communications, Helsinki, Finland, pp. 1-6, Sept. 2006.
- [90] I. Wong, O. Oteri, and W. McCoy, “*Optimal Resource Allocation in Uplink SC-FDMA Systems*,” IEEE Transactions on Wireless Communication, vol. 8, no. 5, pp. 2161-2165, May 2009.
- [91] D. J. Dechene and A. Shami, “*Energy Efficient Quality of Service Traffic Scheduler for MIMO Downlink SVD Channels*”, IEEE Transactions on Wireless Communications, vol. 9, no. 12, pp. 3750-3761, Dec. 2010.
- [92] D. J. Dechene and A. Shami, “*QoS, Channel and Energy-Aware Packet Scheduling over Multiple Channels*”, IEEE Transactions on Wireless Communications, vol. 10, no. 4, pp. 1058-1062, Apr. 2011.

- [93] Q. Liu, X. Wang, and G. Giannakis, “A *Cross-Layer Scheduling Algorithm with QoS Support in Wireless Networks*”, IEEE Transactions on Vehicular Technology, vol. 55, no. 3, p. 839-847, May 2006.
- [94] K. Wongthavarawat and A. Ganz, “*Packet Scheduling for QoS Support in IEEE 802.16 Broadband Wireless Access Systems*”, International Journal of Communication Systems, vol. 16, no. 1, pp. 81-96, Feb. 2003.
- [95] M. Neely, “*Optimal Energy and Delay Tradeoffs for Multiuser Wireless Downlinks*”, IEEE Transactions on Information Theory, vol. 53, no. 9, pp. 3095-3113, Sept. 2007.
- [96] W. Tranter, K. Shanmugan, T. Rappaport, and K. Kosbar, “*Principles of Communication Systems Simulation with Wireless Applications*”, Prentice Hall Press, 2004.
- [97] N. Prasad, H. Zhang, H. Zhu, and S. Rangarajan, “*Multiuser Scheduling in the 3GPP LTE Cellular Uplink*,” IEEE Transactions on Mobile Computing, vol. 13, no. 1, pp. 130-145, Jan. 2014.
- [98] P. Mittal, I. Darwazeh and H. Manukyan, “*Overhead Estimation During Intra eNB Handover in 4G LTE Systems*”, in IEEE Communications Systems, Networks Digital Sign Processing, pp. 960-965, Manchester, Jul. 2014.
- [99] I. Shayea, M. Ismail, and R. Nordin, “*Advanced Handover Techniques in LTE- Advanced System*”, in IEEE International Conference Computer and Communications Engineering, pp. 74-79, Kuala Lumpur, Jul. 2012.
- [100] Q. Wang, G. Ren, and J. Tu, “*A Soft Handover Algorithm for TD-LTE System in High-Speed Railway Scenario*”, in IEEE Signal Processing, Communications and Computing, pp. 1-4, Xi’an, Sept. 2011.
- [101] M. Chen, Y. Yang, and Z. Zhong, “*Location-Based Handover Decision Algorithm in LTE Networks Under High-Speed Mobility Scenario*”, in IEEE Vehicular Technology Conference, pp. 18-21, Seoul, May 2014.

- [102] G. Tomasov, M. Wu, J. Wen, and H. Liu, “*LTE Fixed-Point Handover Algorithm For High-Speed Railway Scenario*”, in IEEE Computer Science and Network Technology, pp. 919-923, Dalian, Oct. 2013.
- [103] D. Han, S. Shin, H. Cho, J. Chung, and I. Hwang, “*Measurement and Stochastic Modeling of Handover Delay and Interruption Time of Smart phone Real-Time Applications on LTE networks*”, IEEE Communications Magazine, vol. 53, no. 3, pp. 173-181, Mar. 2015.
- [104] F. Capozzi, G. Piro, L. Grieco, G. Boggia, and P. Camarda, “*Downlink Packet Scheduling in LTE Cellular Networks: Key Design Issues and a Survey*”, IEEE Communication Surveys Tutorials, vol. 15, no. 2, pp. 678-700, 2013.
- [105] R. A. Guerin, “*Channel Occupancy Time Distribution in a Cellular Radio System*”, IEEE Transactions on Vehicular technology, vol. 36, no. 3, Aug. 1987.
- [106] Z. Naizheng, and J. Wigard, “*On the Performance of Integrator Handover Algorithm in LTE Networks*”, IEEE in Vehicular Technology Conference (VTC-Fall), pp. 1-5, Calgary, BC, Sept. 2008.
- [107] P. Legg, G. Hui, J. Johansson, “*A Simulation Study of LTE Intra-Frequency Handover Performance*”, IEEE Vehicular Technology Conference Fall (VTC-Fall), pp. 1-5, Ottawa, ON, Sept. 2010.
- [108] J. Han, and B. Wu, “*Handover in the 3GPP Long Term Evolution (LTE) Systems*”, Global Mobile Congress (GMC), pp. 1-6, Shanghai, 2010.
- [109] D. Aziz, R. Sigle, “*Improvement of LTE Handover Performance through Interference Coordination*”, IEEE 69th Vehicular Technology Conference (VTC-Spring), pp. 1-5, Barcelona, Apr. 2009.
- [110] S. Sun, T. S. Rappaport, S. Rangan, T. A. Thomas, A. Ghosh, I. Z. Kovacs, I. Rodriguez, O. Koymen, A. Partyka, and J. Jarvelainen, “*Propagation Path Loss Models for 5G Urban Micro- and Macro-Cellular Scenarios*”, in press. IEEE 83rd Vehicular Technology Conference (VTC), Nanjing, China, May 2016.

- [111] Y. Yuan, Z. Chen, "A Study of Algorithm for LTE Intra-Frequency Handover", International Conference on Computer Science and Service System (CSSS), pp. 1986-1989, Nanjing, Jun. 2011.
- [112] M. Ergen, S. Coleri, and P. Varaiya, "QoS Aware Adaptive Resource Allocation Techniques for Fair Scheduling in OFDMA Based Broadband Wireless Access Systems", IEEE Transactions on Broadcasting, vol. 49, no. 4, pp. 362-370, Dec. 2003.
- [113] Y. Barayan, and I. Kostanic, "Performance Evaluation of Proportional Fairness Scheduling in LTE", the World Congress on Engineering and Computer Science (WCECS), vol. 2, San Francisco, USA, Jul. 2013.
- [114] A. Leith, M. Slim, D. Kim, X. Shen, "Flexible Proportional-Rate Scheduling for OFDMA System", IEEE Transaction on Mobile Computing, vol. 12, no. 10, pp. 1907-1919, Oct. 2013.
- [115] M. Kobayashi and G. Caire, "An Iterative Water-Filling Algorithm for Maximum Weighted Sum-Rate of Gaussian MIMO-BC", IEEE Journal on Selected Areas in Communications, vol. 24, no. 8, pp. 1640-1646, Aug. 2006.
- [116] R. H. Y. Louie, M. R. McKay, and I. B. Collings, "Maximum Sum-Rate of MIMO Multiuser Scheduling with Linear Receivers", IEEE Transactions on Communications, vol. 57, no. 11, pp. 3500-3510, Nov. 2009.
- [117] Z. Liu, T. Peng, H. Chen, and W. Wang, "Optimal D2D User Allocation over Multi-Bands under Heterogeneous Networks", IEEE Global Communications Conference (GLOBECOM), pp. 1339-1344, Anaheim, Dec. 2012.
- [118] S. Bera, S. Misra, and M. S. Obaidat, "Energy-Efficient Smart Metering for Green Smart Grid Communication", IEEE Global Communications Conference (GLOBECOM), pp. 2466-2471, Austin, Dec. 2014.
- [119] C. Yang, J. Li, M. Sheng, and Q. Liu, "Green Heterogeneous Networks: A Cognitive Radio Idea", IEEE in Communications, Institution of Engineering and Technology (IET), vol. 6, no. 13, pp. 1952-1959, Sept. 2012.

Curriculum Vitae

Name: Mohamed Hussein Abdelwahab Ahmed

Post-Secondary Education and Degrees: 2013-2016 Ph.D.
Communications and Data Networking
The University of Western Ontario
London, Ontario, Canada

2009 - 2013 TA/RA
Electrical and Computer Engineering
Military Technical College
Cairo, Egypt

2007 - 2009 M.E.Sc.
Electrical and Computer Engineering
Military Technical College
Cairo, Egypt

2002 - 2007 TA/RA
Electrical and Computer Engineering
Military Technical College
Cairo, Egypt

1997 - 2002 B.Eng.
Electrical and Computer Engineering
Military Technical College
Cairo, Egypt

Publications:

1. Mohamed Hussein, K. Elbarbary, and M. Medhat, “*Design and Implementation of Digital-Up/-Down Frequency Converters*”, 6th International Conference on Electrical Engineering (ICEENG), Cairo, Egypt, May 2008.
2. A. Maklad, M. ALSanabawy, M. Bakr, and Mohamed Hussein, “*Performing Low Thrust Maneuvers for Low Earth Orbit Missions*”, 13th International Conference on Aerospace Sciences and Aviation Technology (ASAT), Cairo, Egypt, May 2009.
3. A. Amein, M. Hussein, and H. Alarsh, “*Enhanced Digital Up/Down Frequency Converter*”, IEEE International Geoscience and Remote Sensing Symposium (IGRSS), Hawaii, Jul. 2010.
4. M. Hussein, S. Primak, and A. Shami, “*On Sharing Resources Performance Analysis in 3GPP-LTE Systems Framework*”, IEEE International Wireless Communications and Mobile Computing (IWCMC), pp. 302-307, Dubrovnik, Aug. 2015.
5. M. Hussein, A. Moubayed, S. Primak, and A. Shami, “*On Efficient Power Allocation Modeling in Virtualized Uplink 3GPP-LTE Systems*”, IEEE International Conference on Wireless and Mobile Computing, Networking and Communications (WiMob), pp. 817-824, Abu Dhabi, United Arab Emirates, Oct. 2015.
6. M. Hussein, S. Primak, and A. Shami, “*Intra-MME/S-GW Handover Performance Analysis in Virtualized 3GPP-LTE Systems*”, in press. IEEE Canadian Conference on Electric and Computer Engineering (CCECE), Vancouver, May 2016.
7. M. Hussein, A. Moubayed, S. Primak, and A. Shami, “*Virtualized Allocation Performance Analysis in 5G Two-Tier Cellular Networks*”, in press. IEEE Canadian Conference on Electric and Computer Engineering (CCECE), Vancouver, May 2016.

Teaching Assistantships:

In the Military Technical College:

1. Communication Theory.
2. Digital Communication.
3. Telecommunication Engineering I.
4. Telecommunication Engineering II.
5. Radio Communication Engineering.
6. Computer communication Networks I.
7. Computer communication Networks II.
8. Fiber Optic Communications.
9. Communication Techniques.
10. Theory of Reliability.
11. Data Communications.
12. Circuit Theory I.
13. Electrical Measurements.
14. Television Video Processing.
15. Ground Electrical Equipments.

In the University of Western Ontario:

1. ECE 2208, Electrical Measurement and Instrumentation.
2. ECE 3374, Introduction to Electronics for Mechanical Engineering.

Awards:

1. Award for outstanding presentation in ECE graduate symposium 2015 (Communications and Data Networking).